

Understanding and quantifying clogging and its management during re- injection of CSG water permeates, brines and blends

Final Report

S. Torkzaban, J. Vanderzalm, S. Treumann, T. Amiriashoja
November 2015

Land and Water

ISBN (print) 978-1-4863-0632-9

ISBN (online) 978-1-4863-0633-6

Citation

Torkzaban S., Vanderzalm, J, Treumann, S., Amirianshoja T. (2015). Understanding and quantifying clogging and its management during re-injection of CSG water permeates, brines and blends, Final Report. CSIRO, Australia.

Copyright and disclaimer

© 2015 CSIRO To the extent permitted by law, all rights are reserved and no part of this publication covered by copyright may be reproduced or copied in any form or by any means except with the written permission of CSIRO.

Important disclaimer

CSIRO advises that the information contained in this publication comprises general statements based on scientific research. The reader is advised and needs to be aware that such information may be incomplete or unable to be used in any specific situation. No reliance or actions must therefore be made on that information without seeking prior expert professional, scientific and technical advice. To the extent permitted by law, CSIRO (including its employees and consultants) excludes all liability to any person for any consequences, including but not limited to all losses, damages, costs, expenses and any other compensation, arising directly or indirectly from using this publication (in part or in whole) and any information or material contained in it.

Contents

Acknowledgments	x
Executive summary	xi
1 Introduction and literature review	1
1.1 Clogging Processes	2
1.1.1 Air and gas binding	2
1.1.2 Biological clogging	2
1.1.3 Geochemical clogging	5
1.1.4 Physical clogging	5
1.2 Mobilization, transport and deposition	7
1.3 Aquifer mineralogy	8
1.3.1 Quartz.....	8
1.3.2 Clay minerals	8
1.3.3 Cation exchange of clay minerals.....	10
1.4 Clogging induced by clay	11
1.4.1 Clay swelling	11
1.4.2 Clay mobilization.....	11
1.5 Factors affecting DLVO interaction energies	12
1.5.1 Electrostatic interactions.....	12
1.5.2 Van der Waals energy	13
1.5.3 Ionic strength and ion type.....	13
1.5.4 pH	14
1.5.5 Redox	14
1.5.6 Hydrodynamic forces	15
1.6 Colloid deposition	16
1.6.1 Surface filtration and size exclusion	16
1.6.2 Bridging.....	16
1.6.3 Attachment	17
1.7 Modelling clogging process in aquifers	20
1.7.1 Classical deep bed filtration theory	20
1.7.2 Filtration theory for injection wells	21
1.7.3 Pressure changes due to clogging	22
1.8 Physical clogging assessment	22
1.9 Clogging control and remediation	23
1.9.1 Stabilization of clay particles	23
1.9.2 Selection of treatment fluids	23
1.9.3 Clay stabilization.....	24
1.9.4 Inorganic cations (IC).....	24

1.9.5	Cationic inorganic polymers	25
1.9.6	Cationic organic polymers	25
1.9.7	Oligomers	25
1.9.8	pH–buffer solutions	26
1.9.9	Chemical alteration of clay with KOH	26

2 An experimental and modelling investigation of clogging potential 27

2.1	Anticipated Clogging processes	27
2.2	Materials and Methods	28
2.2.1	Aquifer Materials	28
2.2.2	Characteristics of aquifer materials	29
2.2.3	Groundwater chemistry	30
2.2.4	Aqueous solution used in the core-flooding experiments	31
2.2.5	Description of the experimental setup	31
2.2.6	Experimental procedure	32
2.2.7	Core-flooding tests	33
2.2.8	Determination of Critical Salt Concentration (CSC) in a single salt system.....	34
2.2.9	Effect of Flow Reversal.....	34
2.2.10	Influence of flow velocity on CSC	34
2.2.11	Determination of Critical Ionic Strength in a mixed salt system	34
2.2.12	Effect of pH	35
2.3	Mathematical modelling of clogging due to colloid release and transport	35
2.3.1	Modelling the release process	36
2.3.2	Transport of suspended clay	37
2.3.3	Clay retention at the pore constrictions	37
2.3.4	Permeability reduction.....	37
2.4	Results	39
2.4.1	Clogging potential of Precipice sandstone	39
2.4.2	Simulations	43
2.4.3	Critical Salt Concentration (CSC) in a single salt system	43
2.4.4	Effect of flow velocity on the CSC.....	45
2.4.5	CSC for a divalent cation solution.....	47
2.4.6	The Critical Ionic Strength (CIS) in a mixed solution.....	49
2.4.7	Effect of pH	51
2.4.8	Effect of flow reversal	52
2.5	Discussion	52
2.5.1	Clogging Mechanisms	52
2.5.2	Salinity Effect	53
2.5.3	Effect of pH	55
2.5.4	Cation Exchange Effect	55
2.5.5	Hydrodynamic effect.....	57

2.5.6	Water-compatibility criteria for injection-water salinity	57
2.6	Conclusions	58

3	Preventing Well Clogging Using Chitosan as a Clay Stabilizer	61
----------	---	-----------

3.1	Introduction	61
3.2	Chitosan Chemistry	63
3.3	Materials and methods	63
3.3.1	Sandstone cores	63
3.3.2	Chitosan solution	64
3.3.3	Core-flooding experiments	64
3.3.4	Zeta potential	65
3.4	Results and discussion	65
3.4.1	Water Sensitivity of Sandstones	65
3.4.2	Effectiveness of Chitosan Treatment	68
3.4.3	Effect of Chitosan Concentration	69
3.4.4	Effect of pH	69
3.4.5	Effect of core length	70
3.4.6	Effect of flow rate	71
3.4.7	Characterizing chitosan–clay composites	71
3.5	Conclusion	71

4	Conclusions and Recommendations	72
----------	--	-----------

5	References	74
----------	-------------------	-----------

Appendix A 79

Appendix B 82

Figures

Figure 1.1. Deposition mechanisms of particle suspension injected in porous media (after McDowell-Boyer et al. 1986).....	16
Figure 1.2. A representation of pore bridging (from de Zwart, 2007)	17
Figure 1.3. Three basic particle transport mechanisms of suspended particle transport to a collector surface (Yao et al., 1971).....	18
Figure 1.4. Basal spacing of smectite clays vs concentration of various brines (after Himes et al., 1991).....	24
Figure 1.5. Polymer coating of pore surface for clay migration prevention (after Zaitoun and Berton, 1996)	26
Figure 2.1. Typical SEM Micrographs and EDX spectrum of sand grains of the Precipice sandstone showing the Morphology of the clay and chemical composition on sand grains indicating that the major mineral was quartz.....	30
Figure 2.2. Experimental set-up for colloid release and clogging experiments	32
Figure 2.3. Calibration curve for the absorbance against colloid concentration.....	33
Figure 2.4. A conceptual illustration of pore body and throats in porous media. (a) shows that at equilibrium all the colloidal particles are attached to the pore surface. (b) shows that a fraction of the colloids are released and trapped at the pore constrictions following the release of colloids	36
Figure 2.5. Observed breakthrough concentrations of colloids with changes of salt concentration. The core samples were initially preconditioned with 0.5M NaCl, then the IS of influent water was decreased to that of RO water at time zero. Note that one pore volume (PV) corresponds to ~20 mL	40
Figure 2.6. Experimental data (symbols) and model calculations (solid lines) of colloid release and permeability loss (K/K_0) upon RO water injection into core sample E (a) and F (b) from Precipice sandstone	41
Figure 2.7. Typical SEM Micrograph and EDX spectrum of the released colloids from BSF core samples showing the majority of the released colloids was Kaolinite	42
Figure 2.8. Representative plots of the effluent colloid concentration for two core samples from BSF as a function of pore volumes (PV) for transient ionic strength (IS) experiments. The sequence of the transient experiments was as follows: Preconditioning of the core with 0.5M NaCl solution and then influent solution IS was lowered in several steps indicated in the figure. Note that no noticeable permeability change was observed for these cores during the entire experiment.	44
Figure 2.9. Representative plots of the effluent colloid concentration for two core samples from BSF as a function of pore volumes (PV) when the IS decreased in stepwise manner for two different flow velocity	46
Figure 2.10. Representative plots of the effluent colloid concentration for two core samples from BSF as a function of pore volumes (PV) when the concentration of Ca^{2+} decreased in stepwise manner. The sequence of the transient experiments was as follows: Preconditioning of the core with 0.1M $CaCl_2$ solution and then influent solution IS was lowered in several steps.	48
Figure 2.11. Representative plots of the effluent colloid concentration and relative permeability for a core sample from Reedy Creek (RC_64_15) as a function of pore volumes (PV) when the pH of the 30 mM Na^+ solution increased in stepwise manner	52

Figure 2.12. Salinity criteria for the injection water at various values of groundwater ionic strength.....	58
Figure 3.1. Permeability decline of core samples of Buff Berea (a), Berea (b), and Precipice (c) upon RO water injection.....	66
Figure 3.2. Clay release in Buff Berea (a), Berea (b), and Precipice (c) core samples upon RO water injection.....	67
Figure 3.3. Permeability decline of core samples Buff Berea (a) and Precipice (b) initially saturated and flushed with 0.1 M CaCl ₂	68
Figure 3.4. Representative plots of the relative permeability for two core sample from Buff Berea (a) and Precipice (b) as a function of pore volumes (PV) when the core was treated with chitosan at 20 ppm.....	68
Figure 3.5. Representative plots of the relative permeability for two core samples from Precipice as a function of pore volume (PV) when the core was treated with chitosan at 10 ppm (a) and 5 ppm (b).....	69
Figure 3.6 Representative plots of the relative permeability for a core sample from Precipice as a function of pore volumes (PV) when the core was treated with 10 ppm chitosan at pH=6.5 ..	70
Figure 3.7. Representative plots of the relative permeability for two core samples with different length, 5 cm (a), and 10 cm (b) from Buff Berea sandstone when the core was treated with 10 ppm chitosan at pH=4.....	70

Tables

Table 1.1. Microbially mediated redox reactions in recharge systems involving the degradation of organic matter represented by the model compound CH ₂ O (data from Baveye et al., 1998) ...	5
Table 1.2. Cation exchange Capacities (CEC) of clay minerals (from Grim, 1968)	10
Table 1.3. Overview of dimensionless numbers used in the correlation equations, from Tufenkji and Elimelech (2004) (where v the fluid approach velocity, D the bulk diffusion coefficient (described by the Stokes-Einstein equation), A the Hamaker constant, k the Boltzmann constant, T the absolute temperature, $d_{particle}$ and $d_{collector}$ the particle and collector diameter respectively, $\rho_{particle}$ and ρ_{fluid} the particle and fluid density, $r_{particle}$ the particle radius, and g the gravitational acceleration)	19
Table 2.1. Mean percentage of clay content of the cores sent to CSIRO Adelaide for clogging assessment.	28
Table 2.2 XRD analyses	29
Table 2.3. A summary of water quality for groundwater from the Precipice aquifer at Reedy Creek and Condabri, RO feed (untreated CSG associated water), and RO permeate (treated CSG associated water).....	31
Table 2.4. Summary of the values of the parameters of the best fit for modelling of the core samples a and b from the Precipice sandstone	43
Table 2.5. Values of CSC for various core samples initially in equilibrium with 0.5 M NaCl. The average pore water velocity was maintained 5 m/day during the course of experiment	45
Table 2.6. Values of CSC for various core samples initially in equilibrium with 0.5 M NaCl. The average pore water velocity was maintained at 5 m/day during the course of experiment ..	47
Table 2.7. Values of CSC for various core samples initially in equilibrium with 0.1 M CaCl ₂ . The average pore water velocity was maintained at 5 m/day during the course of experiment ..	48
Table 2.8. Summary of the values of the CIS for several core samples from Reedy Creek at various IS and calcium percentages	49
Table 2.9. Summary of the values of the CIS for several core samples from Condabri at various IS and calcium percentages	50

Acknowledgments

This project has been funded by GISERA with contributions coming from Australia Pacific LNG and CSIRO. We would like to thank Ryan Morris and Lauren Helm from Origin for providing sandstone samples and their comments that helped strengthen this report.

We gratefully acknowledge the staff of CSIRO Land and Water Analytical Services Unit (Waite Campus) in particular John Gouzos, for prompt delivery of analytical data; Toney Hirnyk (CSIRO) for work on core-flooding setup and; Salini Sasidharan (CSIRO) for assistance with SEM analysis.

Executive summary

The coal seam gas (CSG) industry has been rapidly developing in Australia over the past decade. CSG extraction results in the co-production of water to decrease pressure in the coal bed and permit desorption of methane gas from the coal surface. Management of produced water is a challenge for the CSG industry and re-injection of this water, which may be treated to various extents, into overlying aquifers, underlying aquifers, and to the coal seams themselves on completion of mining, is a valuable approach allowing new and expanded beneficial use of water resources for the wider community. The re-injection technique may require water treatment in order to ensure compatibility of injected water with the aquifer so as (a) not to clog injection wells and (b) to prevent adverse changes in water quality in the storage zone. The latter issue is addressed by a related project. Clogging of injection wells has been found to be the single biggest cause of failure in aquifer recharge operations. Well clogging is defined as a reduction in permeability of the formation immediately surrounding the injection well. Clogging assessment, control, and remediation are among the most important issues to be resolved for efficient managed aquifer recharge operation. Well clogging may be caused by physical, chemical, hydrodynamic, mechanical, and biological processes. The rate and extent of clogging is strongly dependent on properties of the aquifer sediment and native groundwater quality, and characteristics of the injected water.

The intended source water for re-injection water into aquifers is a blend of reverse osmosis (RO) treated CSG associated water with micro filtered-CSG associated water (the pore size of the filter is 0.03 micron). Based on an understanding that the potential for biological and physical clogging due to nutrients and colloids present in the source water will be minimised by micro-filtration prior and/or reverse osmosis to injection, the predominant clogging mechanism associated with the use of low salinity treated CSG-associated water is the potential for in situ clay release. Therefore, the objective of this study was to undertake a literature review, extensive series of laboratory experiments and mathematical modelling to assess clogging potential due to dispersion of in situ clay colloids during reinjection of low salinity treated CSG-associated water into the Precipice Sandstone aquifers at Reedy Creek and Condabri in the Surat Basin, Queensland.

Initially a literature review was conducted to establish a conceptual framework to investigate the clogging mechanisms near injection wells, modelling approaches and methods to control and remediate clogging, including the strengths and drawbacks of existing approaches. The literature review aim was to identify various clogging processes in injection wells including entrained air and gas binding, deposition of colloidal particles present in the injectate, biological growth, geochemical reactions, and in situ colloid rearrangement, release, and recapture in the porous media. A verified clogging model based on a series of planned laboratory tests was developed to provide scientific guidance and help develop strategies to avoid or minimize clogging.

Key findings of this report include:

- 1) In-situ clay particles were rapidly released from grain surfaces when core samples were flushed with high salinity water (CSG brine) followed by reverse osmosis (RO) treated water (i.e CSG water permeates) or low salinity water (<20 mM). This mobilisation resulted in a high concentration zone of clay which moved through the core and caused a severe permeability reduction. The critical concentration of NaCl solution which initiated rapid clay release in sandstone samples was found to be in the region of 20 mM at neutral pH.

- 2) Cation exchange processes between clay and the aqueous solution were responsible for inducing the release (dispersion) of in situ clay particles. The rate of cation exchange was dependent on the salt concentration and pH of the native groundwater and injected water.
- 3) Hydrodynamic shear forces alone at typical groundwater conditions were not effective to induce the release of attached clay particles. A weakening of the adhesive forces between the colloids (e.g. clays) and colloid-grain was a precursor for the release. This weakening allowed an electrostatic double layer expansion to occur when RO water or low ionic strength solution came into contact with clays. The hydrodynamic shear force then became an important factor to induce the clay release and subsequent clogging.
- 4) The underlying mechanism of permeability reduction (clogging) in sandstone cores, where clay mobilisation occurred, was due to a hydrodynamic bridging mechanism resulting in rapid blockage of pore constrictions in the cores. The probability of hydrodynamic bridging was directly dependent on the concentration of clay in the aqueous phase. The bridged clay particles could be liberated by flow reversal depending on their deposited condition.
- 5) The treatment of sandstone with divalent cations significantly minimised the rate of clay release. An effective reduction of clay mobilization was observed with maintaining a relatively low concentrations (~0.1 mM) of calcium cation in solution. However, these cations are effectively exchanged with monovalent cations upon introduction of a sufficiently concentrated monovalent electrolyte. When only 10% of the cations in the injection water were divalent (calcium or magnesium), the permeability of the core was unaffected during the injection with varying water velocities.
- 6) The laboratory findings are in agreement with the observations made during injection trials where no noticeable clogging due to clay release was observed. During the trials, the salinity of injected water was maintained above 95% of the salinity of the native groundwater (>1300 $\mu\text{S}/\text{cm}$) and pH within 0.5 unit of the native groundwater (~8).
- 7) Chitosan, a biodegradable biopolymer, was found to effectively prevent clay mobilisation and permeability reduction. Negligible clay release and clogging was observed when core samples were subjected to RO water injection following chitosan treatment at a concentration of 20 ppm.

A guideline for the quality of injected water was developed in order to minimize problems of compatibility between water and aquifer materials. The critical concentration of divalent cations was combined into a generalized stability diagram for various values of groundwater ionic strength. At any given ionic strength of the native groundwater, when injection water chemistry (i.e. total salinity and calcium percentage) is located above and to the right of the critical salinity line, the injection water can be considered compatible and clay release will be unlikely to occur. Below and to the left of the critical line, injection water would have insufficient total and/or divalent cation concentration to prevent clay release and the potential for clogging will be high. The lower the ionic strength or divalent cation, the greater the clogging potential. It should be mentioned that the critical salinity line strongly depends on the cation composition of the native groundwater and clay type. Prevention of clay dispersion and mobilisation can be achieved through chemical amendment and/or blending with raw micro-filtered CSG water to a target salinity and sodium adsorption ratio given in the guideline.

1 Introduction and literature review

Aquifers are porous sediments where water is held and transmitted. Aquifers are commonly found in sedimentary sandstone and limestone or unconsolidated sediment. The coal seam gas (CSG) industry has been rapidly developing in Australia over the past decade. CSG has developed to such an extent that Australia is now the second largest producing country after the USA (Freij-Ayoub, 2012). CSG extraction results in the co-production of water to decrease pressure in the coal bed and permit desorption of methane gas from the coal surface. Management of produced water is a challenge for the CSG industry and re-injection of this water, which may be treated to various extents, into overlying aquifers, underlying aquifers, and to the coal seams themselves on completion of mining, is a valuable approach. This water management strategy will neutralise impacts of mining on water resources, protect springs and riverine ecosystems, and allow new and expanded beneficial use of water resources for the wider community. Re-injection of brine into deep formations or the coal seams may be used to reduce environmental risks on the surface.

Origin Energy, on behalf of Australia Pacific LNG (APLNG), is evaluating the feasibility of injection of CSG associated water (reverse-osmosis permeate, brine or blends) into aquifers. The re-injection technique requires water treatment in order to ensure compatibility of injected water with the aquifer so as (a) not to clog injection wells and (b) to prevent adverse changes in water quality in the storage zone. The latter issue is addressed by a related project (Prommer et al., 2015).

Clogging is a generic terminology referring to permeability reduction of porous media by various adverse processes. Clogging of injection wells has been found to be the single biggest cause of failure in aquifer recharge operations (Page et al., 2014). Well clogging is defined as a reduction in permeability of the formation immediately surrounding the injection well. Clogging may result in decreasing injection flow rate (injectivity) or the need to continually increase the well pressure head to maintain a constant injection rate. Therefore, this will limit the quantity of water that is stored within the aquifer and/or may necessitate costly pre-treatment and maintenance procedures, or even project abandonment of wells in extreme cases. Clogging assessment, control, and remediation are among the most important issues to be resolved for efficient groundwater recharge operation. Well clogging may be caused by many factors such as physical, chemical, hydrodynamic, mechanical, and biological. The rate and extent of the clogging is strongly dependent on the properties of the aquifer sediment and native groundwater quality, and the characteristics of the injected water.

The focus of this study is on Precipice Sandstone aquifers at Reedy Creek and Condabri in the Surat Basin, Queensland, where the intended source water for re-injection water into aquifers is a blend of reverse osmosis (RO) treated CSG associated water with micro filtered-CSG associated water (the pore size of the filter is 0.03 micron).

Sreekanth and Moore (2015) assessed the regional scale impacts of CSG reinjection in the Surat Basin. An important consideration of assessing regional scale impacts is the pressure head that develops and how this impacts on nearby groundwater uses and they reported a maximum groundwater head increase in a domestic bore 15 km from the well field was approximately 4 m (Sreekanth and Moore, 2015). When considering impacts on a localised scale, it is important to consider the influence clogging on pressure head or injection rate.

In the following sections of Chapter 1, an extensive literature review is presented, covering the subject areas of: clogging processes; colloidal transport; mineralogy of aquifer colloidal particles, with particular attention on clays; the principle of porous media flow and modelling; colloid filtration theory to provide a better understanding of hydrodynamic forces and colloid-surface

interactions; and clogging control and remediation. The experimental methodology, results and discussion of the experimental work and a model formulated for colloid release and capture in pore constrictions during well injection in sandstone aquifers are presented in Chapter 2. A verified clogging model based on the mechanistic understanding gained through laboratory experiments can provide scientific guidance and help develop strategies to avoid or minimize clogging in a field operation. Chapter 3 presents an evaluation of chitosan as a management strategy to minimize clogging impacts. The conclusions of the study are presented in Chapter 4 with some practical recommendations.

1.1 Clogging Processes

Processes that are primarily responsible for clogging in injection wells include entrained air and gas binding, deposition of colloidal particles present in the injectant, biological growth, geochemical reactions, and in situ colloid rearrangement, release, and recapture in the porous media (Khilar and Fogler, 1998; Reed, 1974). Properties of the porous media, groundwater, well construction, injection facilities design, and injection rate determine the influence of these processes on well clogging. Each clogging process and the relevant parameters are briefly described below.

1.1.1 Air and gas binding

Two main sources of air contribute to well clogging: firstly, bubbling due to the free fall of water inside a recharge well (cascading) and, secondly, air entrance into the well if negative pressure occurs (Olsthoorn, 1982). Entrained air bubbles can move downward and get into the aquifer formation, increasing the resistance to water flow. Such a build-up of resistance is usually quite rapid, although it levels off within hours because bubbles redissolve into the flowing water which equalizes with the rate of bubble formation. Typically, the possibility of air entrapment is prevented by proper design and operation to maintain a positive pressure in the injection tube.

Release of dissolved gases is another problem. Dissolved oxygen (DO) is an indicator of the concentration of gases in the solution. Generally, gas dissolution is not a concern unless DO concentration exceeds 10 mg/L (Pyne, 2005). Dissolved gases may be released due to an increase in temperature or a decrease in pressure. However, a decrease in pressure is unlikely to occur during injection operations as an increase in pressure head tends to occur as the water moves down the well and into the storage zone. This pressure increase tends to keep dissolved gases in solution in spite of increased temperature. Microbial activity may also increase gases as a metabolic by-product, which may result in reduced permeability. However, no evidence of clogging due to release of gases from microbial activity has been reported in ASR wells to date (Pyne, 2005).

1.1.2 Biological clogging

Microbial growth, defined as the collective increase in the number of bacterial cells and the extracellular polymeric materials that they secrete, plays a major role in the biological clogging of recharge wells. This has been shown by numerous studies including those of Rebhun and Schwarz (1968), Vecchioli (1970), Ehrlich *et al.*, (1973) and Okubo and Matsumoto (1983) that have studied biological clogging using highly treated effluent in infiltration experiments. The microflora involved in the biological clogging processes consists primarily of bacteria (Shaw *et al.*, 1985), although fungi (Okubo and Matsumoto, 1983) and protozoa have also been identified. Microorganisms are present in the subsurface environment in two forms, namely sessile, attached to the solid phase, and mobile, moving freely in the groundwater (van Beek and van der Kooij, 1982). Microbial clogging develops over time-scales of days to weeks (Rinck-Pfeiffer *et al.*, 2000;

Marsden, 2001, Page et al., 2014). Clogging that occurs due to microbial growth during recharge is not well understood. In the absence of microbial inhibitors such as chemical disinfectants, the degree of microbial growth is related to the amount of labile carbon and nutrient present.

A great deal of research has been devoted to quantify the effect of biomass accumulation on the reduction in permeability in porous media. Bacteria can cause well clogging if they are able to grow and multiply in the well and in the aquifer. This means that bacteria can only be a cause of severe clogging if the nutrient status in the well is suitable. Bacterial growth is dependent on the availability of external electron acceptors and assimilable organic carbon. A single bacterial cell can in theory, under the right conditions, with a doubling time of 8 hours, produce 10^{16} progeny, enough to form a 1 cm thick layer of biomass and slime to cover a 1 m² borehole surface in about 12 days (Olsthoorn, 1982).

Most of the bacterial clogging usually occurs at the screen slots and in the first few centimetres of the gravel pack, or in the perimeter of an open hole completion (Sniegocki and Brown, 1970). Some bacteria are introduced with the injectant or are introduced into the formation during well construction. The native bacteria in the aquifer are also encouraged to grow when oxygen is introduced during injection periods (Rinck-Pfeiffer et al., 2000). Increasing the concentration and forms of organic carbon will increase the diversity and numbers of organisms that can be supported.

A common method of controlling biological growth during recharge is to maintain a chlorine residual of 1 to 5 mg/L in the source water (Pyne, 2005). However, a drawback of chlorination during recharge is potential formation of disinfection by-products (DBPs). Pre-treatment to reduce total organic carbon (TOC) is sometimes practiced to control bacterial activity in the well. While this is effective, it is also expensive. It may be more cost-effective to control bacterial activity in the well and near-well formation with chlorine rather than with TOC removal treatment processes. It has been shown that DBPs may be reduced or eliminated by natural processes occurring in anoxic aquifers over time (Pyne, 2005; Pavelic et al., 2006).

The potential of the injectant to lead to microbial clogging can be determined by examining source water parameters including organic carbon, nitrogen and phosphorus. Biodegradable organic carbon (BDOC) provides an indicator of the bio-availability of the organic carbon in water samples that may be analogous to microbial clogging of injection wells (Hijnen and van der Kooij, 1992; Pavelic et al., 2007; Page et al., 2014). The data would suggest whether the injectant offers an opportunity for growth of microbial slimes.

Several authors have tried to correlate bacterial numbers with the extent of clogging and resulting hydraulic conductivity losses through sand columns. Gupta and Schwartzendruber (1962) observed up to 100 fold decrease in the hydraulic conductivity (K) in sand columns having bacterial densities higher than 1.3×10^6 colony forming units (CFU) g⁻¹. Vandevivere and Baveye (1992a) determined that in sand columns inoculated with *Arthrobacter sp.*, no significant K reductions were detected for biomass densities less than 4 mg wet weight cm⁻³, while large K reductions occurred above that value. K was found to be reduced by one, two and three orders of magnitude as the biomass density reached 10, 20, and 35 mg wet weight cm⁻³ respectively. When expressed as the percentage of the pore volume occupied by bacterial cells, these densities amounted to 2.4%, 4.8%, and 8.5% respectively (Baveye *et al.*, 1998). The first study involving the research on the relationship between water quality and biological clogging was undertaken by Okubo and Matsumoto (1983), who found that a high infiltration rate can be maintained at dissolved organic carbon (DOC) concentrations of < 10 mg/L in the recharge water, in this case an artificial wastewater.

Polysaccharide Production

The mechanisms most often associated with biological clogging involve the production of extracellular polymers often referred to as polysaccharides (Allison, 1947; Shaw *et al.*, 1985).

Bacteria attach to surfaces by proteinaceous appendages referred to as fimbriae. Once a number of fimbriae have "glued" the cell to the surface, it makes detachment of the organism very difficult. One reason bacteria prefer to attach to surfaces is the organic molecules adsorbed there provide nutrients. Once attached, the organisms begin to produce polysaccharides. The amount of polysaccharides produced can exceed the mass of the bacterial cells by a factor of 100 or more. The extracellular polymer produced may tend to provide a more suitable protective environment for the survival of the organism.

Polysaccharide production is dependent upon a variety of environmental factors such as the presence of surfaces, the soil type, moisture conditions, temperature, redox potential, the availability and nature of the organic substrate, nitrogen availability, oxygen concentration, and the physiological status of microorganisms (Baveye *et al.*, 1998). The polysaccharides produced vary depending on the species but are typically made up of repeating oligosaccharides (sugars), such as glucose, mannose, galactose, xylose, and others. Polysaccharides can form either a gel structure or a highly viscous solution. They are often termed 'slime', are hydrophilic in nature and contain about 99% water (Rittman and McCarthy, 1980). This is why polysaccharides are potential clogging agents as they reduce the saturated hydraulic conductivity either by increasing the viscosity of the fluid or decreasing the volume and size of fluid-conducting pores (Baveye *et al.*, 1998). Vandevivere and Baveye (1992a), De Lozada *et al.*, (1994) and Ragusa *et al.*, (1994) showed that the production of polysaccharides within the inlet section of sand columns had an important impact on the hydraulic conductivity of the sand.

Hoyle (1994) observed a decrease in the hydraulic conductivity at the inlet end of his columns by four orders of magnitude after inoculating a sand column with two slime producing *Pseudomonas* strains. The cause of clogging was found to be due to a gelatinous deposit filling the column inlet region.

Effect of Iron Bacteria

The clogging of wells due to accumulation of iron oxyhydroxides by iron bacteria has been described widely but not completely explored. Microbial-induced clogging may also occur due to the precipitation of iron hydroxides (Forward, 1994) or aluminium hydroxides (James-Smith *et al.*, 2005). Iron precipitates can occur if iron-bearing minerals such as pyrite present within the aquifer are oxidized by oxygen and nitrate. Soluble Fe^{2+} from the native anaerobic groundwater can react with oxygen present in the recharge water (injectant), to form insoluble ferric oxyhydroxides around the injection well and predominantly in the area of the screen (Ralph and Stevenson, 1995). The oxidation of Fe^{2+} and the reduction of oxygen are coupled and deposition of Fe^{3+} oxyhydroxides occurs. A number of iron bacteria catalyse the oxidation of Fe^{2+} to Fe^{3+} which in turn contributes significantly to injection well clogging. In most cases the microbial oxidation of Fe^{2+} in groundwater at neutral pH is associated with the activity of iron bacteria such as *Gallionella* and the *Sphaerotilus-Leptothrix* group (Ehrlich, 1996). The minimum ferrous ion concentrations that can stimulate iron deposition are between 0.15 and 0.22 mg/L (Ford, 1982), when redox conditions are prevalent. However, iron precipitating bacteria must be present for extensive clogging to occur, even though conditions are suitable for iron precipitation to take place. Clogging due to iron precipitation is due to a combination of both bacterial biomass and sticky polysaccharides incorporating the precipitated iron into the slime. The most effective iron precipitating bacteria have been found to belong to the *Gallionella*, *Leptothrix* and *Sphaerotilus* species. These species consist of long filaments and can grow quite rapidly and clog up pores. There are certain bacteria such as *Pseudomonads* and *Enterobacter* which can precipitate iron as well.

The potential for biological clogging to impact on CSG reinjection in the Surat Basin is low as the source water is low in biodegradable dissolved organic carbon, nitrogen, phosphorus and oxygen following pre-treatment by micro-filtration, reverse osmosis and deoxygenation (Morris, personal communication).

1.1.3 Geochemical clogging

During injection, geochemical reactions can occur that adversely affect aquifer permeability. These chemical changes are a function of injection water quality, native groundwater quality, aquifer mineralogy, and changes in temperature and pressure that occur during injection. The most notable of the possible adverse geochemical reactions are precipitation of calcium carbonate (calcite), iron and manganese oxide hydrates, and the swelling, or dispersion of clay particles (Pavelic et al 2007). The injectant (highly saturated with oxygen) is usually very different in chemical composition than the native groundwater (often devoid of oxygen) and mixing of the two waters can lead to an array of geochemical reactions such as precipitation of calcite, precipitation of iron and manganese, dissolution reactions (e.g. of calcite), redox reactions including sulphate reduction, methanogenesis and denitrification (Pyne *et al.*, 1992). Some reactions are microbially mediated by a range of microorganisms some of which are listed in Table 1.1.

Table 1.1. Microbially mediated redox reactions in recharge systems involving the degradation of organic matter represented by the model compound CH₂O (data from Baveye et al., 1998)

Reaction	Equation	Bacteria associated with this reaction
Aerobic respiration	$\text{CH}_2\text{O} + \text{O}_2 \rightarrow \text{CO}_2 + \text{H}_2\text{O}$	Various
Denitrification	$\text{CH}_2\text{O} + (4/5)\text{NO}_3^- + (4/5)\text{H}^+ \rightarrow \text{CO}_2 + (2/5)\text{N}_2 + (7/5)\text{H}_2\text{O}$	<i>Bacillus</i> , <i>Pseudomonas</i> , <i>Alcaligenes</i> , <i>Thiobacillus</i>
Mn (IV) reduction	$\text{CH}_2\text{O} + 2\text{MnO}_2 + 4\text{H}^+ \rightarrow 2\text{Mn}^{2+} + 3\text{H}_2\text{O} + \text{CO}_2$	<i>Bacillus</i> , <i>Clostridia</i>
Fe(III) reduction	$\text{CH}_2\text{O} + 8\text{H}^+ + 4\text{Fe}(\text{OH})_3 \rightarrow 4\text{Fe}^{2+} + 11\text{H}_2\text{O} + \text{CO}_2$	<i>Bacillus</i> , <i>Aerobacter</i> , <i>Pseudomonas</i> , <i>Clostridia</i> , <i>Staphylococcus</i>
Sulfate reduction	$\text{CH}_2\text{O} + (1/2)\text{SO}_4^{2-} + (1/2)\text{H}^+ \rightarrow (1/2)\text{HS}^- + \text{H}_2\text{O} + \text{CO}_2$	<i>Desulfovibrio</i> sp.
Methane fermentation	$\text{CH}_2\text{O} \rightarrow (1/2)\text{CH}_4 + (1/2)\text{CO}_2$	Methanogenic bacteria ie. <i>Methanospirillum</i> sp., <i>Methanosaeta</i> sp.

Chemoorganotrophic bacteria are those that oxidise organic molecules to obtain energy (Baveye et al., 1998). They can use a wide range of oxidants to oxidise the organic matter (CH₂O) present in the recharge water and in the aquifer matrix. Some of these oxidants are O₂, NO₃²⁻, Mn⁴⁺, Fe³⁺ and SO₄²⁻.

The potential for geochemical reactions resulting from the injection of CSG water into the formation has been assessed in a related project (Prommer et al., 2015). In this sister project, groundwater and core samples from the target sites for injection were used in PHREEQC to determine the nature of the reactive mineral phases in the storage zone. Electron activity (pe), calculated from Eh measurements, was used to describe the redox state of all solutions, according to Eh=0.059pe (Prommer et al., 2015).

1.1.4 Physical clogging

The presence of colloidal particles in groundwater is well-known in many engineering disciplines. An important issue related to transport of colloids through porous media is the effect on permeability of the medium. In injection wells, this phenomenon is very common. The injected water often contains suspended particles or it may cause release of some of the attached colloids

originally present in the aquifer. As the water travel farther in the aquifer, the flow velocity decreases resulting in colloid re-deposition. This reduces the permeability of the aquifer near the well bore formation and as a result the injection efficiency decreases (Al-Abduwani, 2005). Pore blocking due to colloids occur through a number of processes. These processes are based on transport of colloids through pores and retention due to hydrodynamic or physicochemical mechanisms. Before discussing the different particle mobilization, transport and capture processes, it is useful to explain what it is defined as a particle.

The diameter of mobile particles with clogging potential in a natural porous media ranges from 0.11 to 100 μm (Ryan and Elimelech, 1996). Particles with size below this range are too small to cause noticeable clogging and particles above this range will not be in suspension under normal conditions. Particles of size between 0.01 to 10 μm are classified as colloids. Particles at the top range, from 10 to 100 μm , are referred to as suspended particles (Ryan and Elimelech, 1996).

Colloids may comprise the following phases:

- Silicate particles: clays, highly polymerised silica
- Carbonates (e.g., CaCO_3)
- Humic substances: macromolecular humic acids, biological detritus
- Iron (III) and manganese (III, IV)-oxihydroxides
- Aluminium hydroxides
- Sulphides and polysulphide (under anoxic conditions)
- Micro-organisms, viruses, bacteria, fungi

Besides colloid properties, the porous media and aqueous phase properties also affect clogging. The ratio of colloid size and porous media grain size is a key parameter for different clogging processes. Particles much larger than the average pore throat diameter will not be transported in the porous medium, simply because of size exclusion. In addition to the difference in colloid size the colloid concentration too varies in different aquifers and conditions. The concentration is related to changes in water quality and hydrodynamic conditions (Ouyang et al. 1996; Ryan and Elimelech 1996). The capture and release of colloids is related to a number of processes of which the most relevant are discussed in the following sections.

The sandstone matrix often contains substantial amounts of colloidal particles, such as, quartz fragments and a range of clay minerals. These particles are either present as flocculated material in the pore space or are attached to the pore surfaces in single or multilayer clusters. During well injection, permeability losses are often observed in many aquifers. The reaction or water-sensitivity of colloidal particles in aquifer sediments to changes in physicochemical conditions is considered to be a primary cause of well clogging. Early research suggested that the swelling of specific types of clay as the principal cause while, more recently, dispersion and release of clays and pore plugging has been found to be significant (Khilar and Fogler, 1998). Even aquifers containing only small quantities of clay minerals would be likely to suffer permeability loss during water injection. Therefore, a thorough understanding on why water sensitivity occurs is valuable in the prevention of clogging problems during water injection into an aquifer.

The water sensitivity of sandstone is a common cause of clogging in injection wells (Khilar and Fogler, 1998). Normally, it happens when a low salinity water is injected into a brackish groundwater, as proposed for CSG-reinjection in the Surat Basin. This process can induce release and transport of clay particles through the porous media, which may cause plugging of down-gradient pores. The damage, often most severe in the vicinity of injection wells, may also occur deep inside an aquifer where it is more difficult to remedy (Civan, 2007). The underlying factors for water sensitivity have not been fully understood in the reported literature (Civan, 2007). It is believed that coupled chemical, physical, and hydrodynamic effects are responsible for the

permeability losses of a given porous medium. For example, colloid release and transport could be due to fluid flow conditions alone. It has been observed that the water velocity was critical for particle release and clogging effects (Torkzaban et al., 2014). The chemical effects attribute greater significance to the interactions between sediments, water, and the clay particles contained in the pore space. In the pore surfaces and constrictions, the interaction between the clay particles and grain surfaces is generally considered to have a great influence on the clay release and re-deposition.

The main sites of clogging are at the injection well-face and the formation immediately surrounding the well. Normally, the colloidal particles (e.g. clay) attached to the pore walls in porous media are at equilibrium in the presence of the native groundwater. However, various disturbances such as physical, chemical, and hydrodynamic changes may induce the salinity, velocity, and thermal shock phenomena causing colloid release or mineral precipitation (Civan, 2007). Once colloids are introduced into the pore space, they become mobile and may re-deposit down gradient (especially in pore constrictions) resulting in a drastic and rapid permeability loss. To mitigate clogging, a pre-treatment of injectate is required to increase its compatibility with the fluid and solid phase of the aquifer so as not to clog injection wells. It is imperative to obtain insights on the factors affecting the clogging process. With an increased understanding of the clogging mechanisms, predictive tools can be used during the planning stages to estimate treatment and redevelopment requirements. Moreover, an increased understanding of clogging will be useful during operations in diagnosing the magnitude and origin of clogging, and in developing operations and maintenance guidelines.

Despite the considerable research done in the field of particle detachment, transport and re-deposition, the understanding of the coupled effects of physicochemical factors on these phenomena is still limited. Much of this uncertainty is due to the fact that aquifers contain a wide range of colloidal particles, differing in shape, size and surface properties, making their characterisation a difficult task. It is often assumed that all clay particles behave in the same way under injection conditions.

1.2 Mobilization, transport and deposition

The state in which colloids are present in the subsurface depends on several conditions, such as water chemistry, mineralogy of the matrix, pore size distribution and hydrodynamic conditions. In the literature, the discussion about generation of colloids is in most cases has focused on mobilization of existing colloids, which are a major source of colloids in groundwater. Small minerals from the aquifer matrix can be mobilized by changes in chemistry, physical, and hydrodynamic conditions (Ryan and Elimelech 1996). The relevance of these different conditions can be determined from the analysis of hydrodynamic, physicochemical forces (Torkzaban *et al.*, 2007). Besides the release of existing colloidal particles, a smaller source of colloids is in situ precipitation of supersaturated mineral phases and natural degradation. Under normal conditions, these processes appear to be uncommon, but near injection wells it may have a significant contribution to the generation of colloids.

The most important properties of an aquifer from the production and injection point of view, are porosity and permeability. Porosity of a porous medium, the ratio of pore to total volume, provides storage capacity for water while permeability is a measure of the movement of water in the aquifer or from the aquifer to a well. Therefore, permeability or hydraulic conductivity is a measure of the water transmitting capacity of the aquifer. It depends on the porosity, the pore size distribution, the degree of interconnection of pores. All these factors are determined by the geological history of the aquifer.

Permeability is typically defined by Darcy equation as:

$$k = \frac{\mu QL}{A\Delta P} \quad (2.1)$$

where K is permeability (Darcy), μ is water viscosity (poise), L is the length of porous media (m), A is the cross-section of porous media (m^2), ΔP is the pressure loss across porous media (bar), and Q is the flowrate (m^3/s).

Aquifer sediments possess permeability from a few milli-darcys to several darcys. The degree of pore interconnection in a porous medium has a significant effect on its permeability. Therefore, a sediment can have a high porosity while displaying a low permeability. As a result, effective porosity as opposed to total porosity is a more useful parameter for characterisation of permeability. Aquifers typically have porosities in the range from 10% to 40%. The coarser-grained sedimentary aquifer such as sandstones, are the most typical aquifer, having relatively high porosities. Limestone ('carbonate') aquifers have generally variable porosity. However, they can have reasonably high permeability when they possess fractures.

1.3 Aquifer mineralogy

This section describes the properties of quartz, clay, and, other minerals of sandstone aquifers. Sandstones often contain significant quantities of inorganic colloidal particles. Typically, fragments-of-quartz, feldspar, and a wide spectrum of clay minerals can be found in the pore spaces, the single particle ranging in size from the sub-micron to a few tens of microns. During re-injection, these colloids can be mobilised by changes in the ionic strength or chemical constitution of the injectant. Even areas of high permeability can be permanently affected by such mobilised colloids. It is considered that clays make a significant contribution to clogging based on their complex surface charges.

1.3.1 Quartz

Usually greater than 90% by weight of sandstones are composed of quartz, which is a highly crystalline silica. This mineral forms the basic porous structure through fusion at high temperatures and pressures. The porous nature of sandstone can be attributed to the relative hardness of quartz.

1.3.2 Clay minerals

Clay are crystalline alumino-silicate particles with the size of smaller than 2 microns. However, larger clay particles exist, which are important in terms of clogging problems (Sposito, 1998).

The silica and alumina take the form of alternating layers, which are integrated into one another to varying degrees, depending on the number of layers required to form the repeating unit structure. The silica layer comprises a silicon atom surrounded by four oxygen, atoms or hydroxyl ions, forming a tetrahedral sheet (Sposito, 2008). The alumina forms an octahedral sheet with one aluminium atom at the centre of six hydroxyl ions. Two-layered, three-layered, mixed-layer and amorphous clays all exist in nature (Sposito, 2001). The clay minerals in the pores of an aquifer porous material may be affected by the ionic environment resulting in swelling or mobilization effects. Other colloidal particles like silica materials may also be mobilised and therefore contribute to the pore clogging.

The structure and composition of the clay minerals provide them with unique physical and electrochemical properties. The three-layered clays such as montmorillonite exhibit swelling when in contact with low-salinity water (Sposito, 2008). These clays possess very reactive surfaces due to charge imbalances within their structures. This factor is the cause of their ion exchange, chemical adsorption and double layer characteristics. Ion exchange reaction is the exchange of ions in solution for those on the solid surfaces, the exchange ions in the subsurface environment are typically Na^+ , K^+ , Mg^{2+} , Ca^{2+} . These ions are held between the layers as well as on the outer surfaces of the structural unit, without any alteration to the basic clay structure (Sposito, 2008).

Kaolinite

The chemical formula of kaolinite is $\text{Al}_2\text{Si}_2\text{O}_5(\text{OH})_4$. Its structure consists of one tetrahedral silicon-oxygen sheet and one aluminium-hydroxyl layer. This type of structure is usually referred to as a 1:1 lattice. No expansion of the lattice occurs when kaolinite comes into contact with aqueous solutions (i.e. non-swelling clay) (Sposito, 2008). The replacement of aluminium by iron or magnesium within the structure of this clay mineral has not been reported. X-ray diffraction patterns of a typical kaolinite result in a spacing between the alumina and silica sheets of about 7.2 Angstroms. Kaolinite has been reported to exist in various states of crystallinity which can usually be quantified by differential thermal analysis. Kaolinite is primarily a product of the weathering of feldspathic minerals. Particles of kaolinite are recognised by their characteristic hexagonal platelet form in the 0.1-5 micron size range. Individual platelets often are found clumped together as "card-pack" structures. The surface and ion-exchange properties of kaolinite clays are lower compared to other types of clay minerals (Sposito, 2008).

Montmorillonite

This mineral is a three-layered clay with the unit cell consisting of a sheet of alumina sandwiched between two layers of silica molecules. Particles of montmorillonite are usually very small (less than 1 micron). They are very susceptible to swelling when in contact with water, which can penetrate the loose layer structure. Potassium, sodium, calcium and magnesium ions are readily exchanged which have the highest cation exchange capacities of the clay mineral group, from ten to fifty times greater than crystalline kaolinite (Sposito, 2008).

Illite

This is also a three-layered clay mineral. However it does not display swelling characteristics due to the presence of potassium ions situated between the unit layers. The presence of potassium balances the charge deficiency inherent in the structure and reduces the cation exchange capacity. Particles of illite are generally irregularly shaped and, less, than 2 microns in their characteristic dimension. It is interesting to note that illite may be degraded when potassium is removed from the structure by the leaching action of slightly acidic water. Degraded illite is susceptible to expansion when water enters between the unit layers as the ion exchange process takes place. In general, illite has a lower ion exchange capacity than the montmorillonites (Sposito, 2008).

Chlorite

Although it is not strictly a clay, chlorite is commonly found in a clay fraction. Particles are small, generally sub-micron, and of a structure is similar to that of the three layered clays but with the addition of a layer of magnesium hydroxide in between the alumina and silica unit layers.

Mica

The group of lamellar minerals collectively termed 'mica' are commonly associated with clays in nature, but are found over a much wider size range. They consist of aluminosilicates with weak interlayer forces. Mica has been found often to be closely associated with kaolinite (Sposito, 2008).

Feldspar

Feldspar is probably the most abundant mineral in sandstones after quartz; and is widely-regarded as the base material for the formation of clay minerals. The potassium form consisting of the block-like crystals is very common in nature.

1.3.3 Cation exchange of clay minerals

The cation exchange capacity of clay minerals arises from a combination of sources as follows (Van Olphen, 1977):

- a) Isomorphic substitution within the crystal structure. This is the process where one ion is replaced by another of similar size without altering the physical structure. Normally, aluminium ions substitute for silicon ions creating a charge deficit at the surface.
- b) Preferential adsorption of potential-determining ions, caused by the presence of lattice imperfections and broken bonds.
- c) Exposed hydroxyl groups.

The cation exchange capacities of a number of clay minerals are given in Table 1.2. The ion exchange capacity of clay is higher when there are a large number of broken bonds and surface imperfections present on the particles and when a clay mass is poorly crystallised (Grim, 1968).

Table 1.2. Cation exchange Capacities (CEC) of clay minerals (from Grim, 1968)

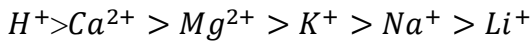
Clay mineral	CEC in meq/100g
Illite	20-40
Kaolinite	1-10
Montmorillonite	80-100
Chlorite	10-40
Mica	20-50

In general, clay particles are negatively charged in aqueous solution due to the deficiency of charge of the mineral structure. The magnitude of the charge varies with pH and water salinity. Broken bonds around the edges of the clay units give rise to excess charges which are balanced by adsorbed ions. Broken bonds tend to occur on the non-cleavage vertical surfaces of clay particles, in the case of kaolinite, on the edges of individual plates. The number of broken bonds per unit surface area-increases when the particles become smaller hence the exchange capacity is expected to increase. It is known that with rising pH the negative charge of clays increases due to increased ionization of the acid groups (silicon) and the positive charge decreases due to lower proton addition to the basic groups. In the low exchange capacity clays such as kaolinite, illite, and chlorite, broken bonds at the edges of particles are regarded a major cause of exchange capacity.

The substitution of aluminium (Al^{3+}) for silicon (Si^{4+}) in the tetrahedral sheet and of lower valence ions such as magnesium for aluminium in the octahedral sheet produces net charge deficiencies in clay particles. Such substitutions may either be balanced by intra-lattice changes or by cation adsorption. The hydrogen of exposed hydroxyl groups could be replaced by an exchangeable cation even though it is comparatively tightly held. In kaolinite, the presence of the hydroxyl sheet on one side of the cleavage plane suggests that this cause of ion exchange may be significant (Grim, 1968). An interesting property of kaolinite is that the exchangeable cations occur only on the basal oxygen surface of the silica tetrahedral units and that the cation exchange capacity depends on the thickness of kaolinite platelets (Spisito, 2001).

It has been observed that as the amount of exchangeable Ca^{2+} ions on a clay surface decreases, the more difficult is the removable of further ions (Spisito, 2008). However, sodium ions show the

reverse relationship. Both replacing power and the strength with which the exchange cation is held increase by a higher valency of the ion. The relative replacing power of one cation by another are given by the following series:



The exception to the above replacement rule is the hydrogen ion. Also the series is not valid for all clay minerals due to clay-specific structural differences.

1.4 Clogging induced by clay

Most sandstones contain significant amount of colloidal particles within their pore spaces, which can be mobilised during water injection. Most research on this topic is more qualitative largely due to difficulties in characterising the behaviour of colloids under different water injection conditions. However, with more sophisticated analytical techniques, better characterisation of aquifer materials has enabled detailed study of the underlying mechanisms of colloid mobilization problems.

1.4.1 Clay swelling

Several early studies attributed clogging to a reduction of pore volume from the swelling of the montmorillonite type of clays present in the formation (Khilar and Fogler, 1998). In one study, core samples containing on average 8% swelling clays flushed with fresh water exhibited an average 92% reduction in the permeability (Goldenberg et al., 1984). Montmorillonite has been found most active in cation exchange reactions and most susceptible to swelling, while illite and kaolinite affected to a lesser degree (Goldenberg et al., 1984). It is known that monovalent cations could be much more easily removed from clays than divalent cations and that the forces keeping particles aggregated in high salinity water could break down allowing dispersion and swelling to occur.

1.4.2 Clay mobilization

It is now recognised that non-swelling clays such as illite and kaolinite may also participate in the pore clogging due to dispersion mechanism (Khilar and Fogler, 1998). When a strongly water sensitive sandstone is permeability tested, the evidence of mobile clay behaviour is typically found. A severe clogging due to dispersion and clay mobilization was observed when only the clay fraction was 5-8% of the core (Khilar and Fogler, 1998). Calcium ions were thought to prevent dispersion and permeability loss. Permeability tests were conducted by Gray and Rex on Berea sandstone cores containing little or no swelling clays (Goldenberg et al., 1984). Fresh water permeabilities were on average less than 33% of connate water permeability. The clogging phenomenon was explained by clay particle plugging action.

Khilar and his co-workers studied the water sensitivity phenomenon in the well-characterized Berea sandstone containing 8% colloidal particles, mainly quartz, kaolinite and illite (Khilar and Fogler, 1998). The concept of salinity change was demonstrated to be critical in causing clogging. Below a critical salinity, the rate particle release and pore-plugging effects were observed. Increased salinity gradients produced higher concentrations of colloids in the core effluent. Fast particle release induced by double layer expansion in the clays was suggested as the mechanism of permeability reduction. Critical salt and clay concentration levels were suggested as the governing criteria for the release and clogging process.

Sharma and his co-workers examined the conditions under which deposition and release of clays takes place in sandstones (Sharma et al., 1985). Constant charge clay surfaces were assumed, in

their double layer analysis. In conducting electrophoretic mobility measurements for the estimation of the zeta potentials, the surface charge properties of the sandstone were assured to be largely unaffected by crushing. Particle deposition and release were expressed in terms of the surface potential interaction of the clays with sandstone surfaces. In this way, regions of capture and release were determined. The transition between an equilibrium state and particle deposition was found to be extremely narrow. This was also found to be true for the transition to particle release from a state of particle attachment. It was proposed that inside the deposition or release regimes, the respective rates are a function of the fluid interstitial velocity. The theoretical-analysis also showed that smaller particles would be more difficult to deposit and easier to release, pointing out that experimental work has, not yet shown this to be true.

In the work by Kia et al. (2001), the electrophoretic mobilities of kaolinite clay and crushed sandstone were measured. In the initial stage of a fresh water core flood, the pH was observed to rise before attaining the pH of the water injected. This effect was attributed to the replacement of sodium ions on clay surfaces by hydrogen ions from the water. The authors concluded that as the pH is lowered, permeability loss is reduced and that at pH values less than 4.8 no permeability reduction occurs when fresh or low salinity water is contacted with sandstone cores.

Two conditions must be satisfied in order to mobilize colloids in an aquifer. First, a source of colloids has to be present. Second, the local conditions must be such that colloids become detached from the matrix and remain in suspension. The first condition is strongly influenced by the lithological composition of the aquifer material. A typical source of colloids in an aquifer is clay, silt and other fine particles. The second condition is related to changes in chemical and hydrodynamic conditions (Ryan and Elimelech 1996).

Where a colloid source is present in porous media, water chemistry is important for the mobilization of the colloids. The physicochemical conditions determine whether colloids will be released from a potential source or not. This depends on the forces between the colloids and the surfaces of mineral grains. These forces include electrostatic double layer attraction or repulsion, London-van-der-Waals attraction and other short-range forces such as hydrophobic, acid-base, born forces (Bradford and Torkzaban 2008). The electrostatic and van der Waals forces are commonly described by Derjaguin–Landau–Verwey–Overbeek (DLVO) theory (Derjaguin and Landau, 1941; Verwey and Overbeek, 1947). Changes in pH, ion type, and ionic strength promote colloid mobilization mainly by altering the double layer potential energy (Torkzaban et al., 2007; Ryan and Elimelech 1996).

1.5 Factors affecting DLVO interaction energies

1.5.1 Electrostatic interactions

The electrostatic repulsions between the particles create an energy barrier that prevents the coalescence of the particles. However, the electrostatic interaction between charged colloidal particles involves not only the interactions between the colloidal particles, but also the interactions between colloidal particles and the sea of ions surrounding the particles. As every particle has a finite surface charge there should be an excess of ions of opposite charge in the solution to maintain overall electric neutrality of the system (DLVO theory 1942). Oppositely charged ions (anions) in the system are attracted towards the ions present on the surface of particles. But the thermal motion of the ions counteracts this attraction. Therefore, the ions take an equilibrium position to balance the electrostatic interaction energy with the thermal energy.

This results in a diffuse double layer of ions surrounding the particle: one layer formed from the charge on the surface of the particles and other layer form from excess of oppositely charged ions present in the solution. One of the governing equations in the electrical double-layer region is Poisson's equation, which can be derived from Coulomb's law of electrostatics (Jackson, 1975):

$$\frac{d^2\psi}{dz^2} = -4\pi \frac{\rho_\varepsilon}{\varepsilon} \quad (1.2)$$

For the case where the thickness of an electric double layer is much smaller than the radius of the particle the repulsive electrostatic energy, Φ^{el} [ML²T⁻²], is determined using the constant surface potential interaction expression of Hogg et al., (1966) for a sphere-plate interaction as:

$$\Phi^{el}(h) = \pi\varepsilon\varepsilon_0r_c \left\{ 2\zeta_1\zeta_2 \ln \left[\frac{1+\exp(-\kappa h)}{1-\exp(-\kappa h)} \right] + (\zeta_1^2 + \zeta_2^2) \ln[1 - \exp(-2\kappa h)] \right\} \quad (1.3)$$

where ε (dimensionless) is the dielectric constant of the medium, ε_0 [M⁻¹L⁻³T⁴A⁻², where A denotes ampere] is the permittivity in a vacuum, r_c [L] is the radius of a colloid, ζ_1 is the zeta potential of the colloid, ζ_2 is the zeta potential of the collector, and κ [L⁻¹] is the Debye-Huckel parameter.

1.5.2 Van der Waals energy

Van der Waals attractive forces (or London dispersion forces) are weak forces that exist between uncharged molecules as a result of polarity. These forces become significant when sizes of the particles are very small and the distances are in nano level. It is important to remember that van der Waals' forces are forces that exist between molecules of the same substance. They are quite different from the forces that make up the molecule. For example, a water molecule is made up of hydrogen and oxygen, which are bonded together by the sharing of electrons. These electrostatic forces that keep a molecule intact are existent in covalent and ionic bonding but they are not van der Waals' forces.

The origin of the van der Waals attractions may be related to the fluctuations in the charge distribution of atoms. It is important to note that electrons are constantly moving within a bond. There are moments that electrons are crowded in one side. This gives a temporary polarity to the atom. This induces polarity to the adjacent atom by repelling the electron cloud. However, this temporary charge disappears as quickly as it appeared because the electrons are moving so fast. According to the theory of London [1930], the attractive forces between atoms are additive in nature. Because of this nature, the attractive interaction between two colloidal particles containing many atoms is appreciable. The retarded van der Waals interaction energy, Φ^{vdW} , for a sphere-plate interaction was determined using the expression by Gregory (1981) as:

$$\Phi^{vdW}(h) = -\frac{A_{123}r_c}{6h} \left[1 + \frac{14h}{\lambda} \right]^{-1} \quad (1.4)$$

where A_{123} [ML²T⁻²] is the Hamaker constant, and λ is a characteristic wavelength of the dielectric, taken as 100 nm (Gregory, 1981). All interaction energies were made dimensionless by dividing by the product of the Boltzmann constant ($k_B = 1.38 \times 10^{-23}$ J K⁻¹) and the absolute temperature (T_K).

1.5.3 Ionic strength and ion type

The most common chemical perturbation that causes mobilization of colloids is a decrease in ionic strength (IS) of the groundwater. The electrolyte concentration influences the double layer thickness and the stability of the suspension. A change in IS is caused by injection of water with a different IS than that of the native groundwater. Reduction of IS may cause clay minerals to swell

and/or disperse, because their diffusive double-layers are expanded (Ryan and Elimelech 1996). The swelling of clays may lead to pore clogging. The amount of swelling also depends on the type of clay, for example montmorillonite swells more than illite or kaolinite. Clogging by clay dispersion, where mobilized particles are deposited in narrow pore throats, is irreversible without a change in flow direction.

Closely related to the IS is the ratio or proportion of multivalent to monovalent cations in the electrolyte, often expressed as the sodium adsorption ration (SAR). This ratio is an important indicator for mobilization of clay particles. When Na dominates the ion balance with respect to Ca, the release of colloids may increase due to disaggregation (McCarthy 1989). Ion exchange between the fluid and the grain surface can change the IS of the fluid. Ion exchange also influences the zeta potential, because it influences the electrostatic charge and therefore the resulting electrostatic repulsion between colloidal particles and the collector surfaces (Ryan and Elimelech 1996). Examples of ion exchange processes are the exchange of Na-H and Na-Ca.

1.5.4 pH

A change in pH of groundwater influences the release of colloids by clay dispersion and by dissolution of cementing agents, such as calcite and oxide minerals. Clay dispersion occurs when the isoelectrical point of the clay involved is exceeded due to an increase of the pH. The isoelectrical point depends on the mineralogy and crystal structure of clays (Tchistiakov 2000). In this case colloid– grain surface interactions play an important role. For example, coating of grains by iron oxides changes these interactions. Again these coatings can also be a source of colloids. The solubility of the iron oxides is dependent on the pH. If the pH in these sediments exceeds a critical value of about 8, colloids attached to the iron oxide coatings can be rapidly released (Ryan and Elimelech 1996).

Calcite and other carbonate cements will dissolve when the pH is lowered. Below the critical value pH=5, these mineral materials may become released as colloids. Under natural conditions, the changes in pH will not be very large. Therefore, the effect on colloid release will probably be limited. It is expected that fast changes in water chemistry occur when water is injected into a confining layer. This water usually has a different chemical composition and changes the conditions within the aquifer affecting the stability of colloids (Tchistiakov 2000).

1.5.5 Redox

Redox reactions can change the water chemistry and generate *in situ* particles. A common example is the dissolution of pyrite and the corresponding products (Sposito, 2008). Pyrite can react with dissolved nitrate and thereby create iron hydroxides. The decomposition of the pyrite also releases organic matter, which is captured onto pyrite, usually in small amounts. The reaction products can also cause a coating on mineral grains. Coatings of oxide minerals can attach passing colloids to the surface of the grains. Sediments that are rich in oxide minerals can therefore decrease the colloid concentration in the groundwater. These sediments act as collectors for the mobile colloids. In turn the oxide rich layers can be sources of colloids, when the groundwater chemistry is changed, i.e., when the hydroxides are reduced by an anoxic plume (Ouyang et al. 1996).

1.5.6 Hydrodynamic forces

Other important conditions, which can affect the colloid concentration and its distribution in groundwater, are the groundwater velocity and the direction of the flow. The velocity is important because of the hydrodynamic forces (drag forces) on colloid mobilization and re-deposition (Torkzaban et al. 2007). In the vicinity of injection wells, groundwater has high flow velocities. The further from the well, the lower the velocity will be, due to the divergence of the streamlines from the well. After colloids have been mobilized by hydrodynamic or physical-chemical perturbations, they are transported through the medium and can be deposited again. Deposition of suspended colloids is caused by various processes. Again changes in hydrodynamic conditions and chemistry influence the deposition of colloids. Additionally, aquifer properties such as the pore size distribution and physical and chemical heterogeneity play an important role. In the following sections different deposition processes are discussed.

1.6 Colloid deposition

As described in the previous sections colloids can be in suspension due to a number of processes. The deposition of these particles occurs through different processes such as surface filtration, size exclusion, bridging, and attachment. Bradford and Torkezaban (2008) and McDowell-Boyer et al. (1986) identified various particle deposition mechanisms, based on injection of a fluid in a porous medium (Figure 1.1). The classification of these processes is related to the ratio of particle sizes (in suspension) and the pore size distribution of the porous medium.

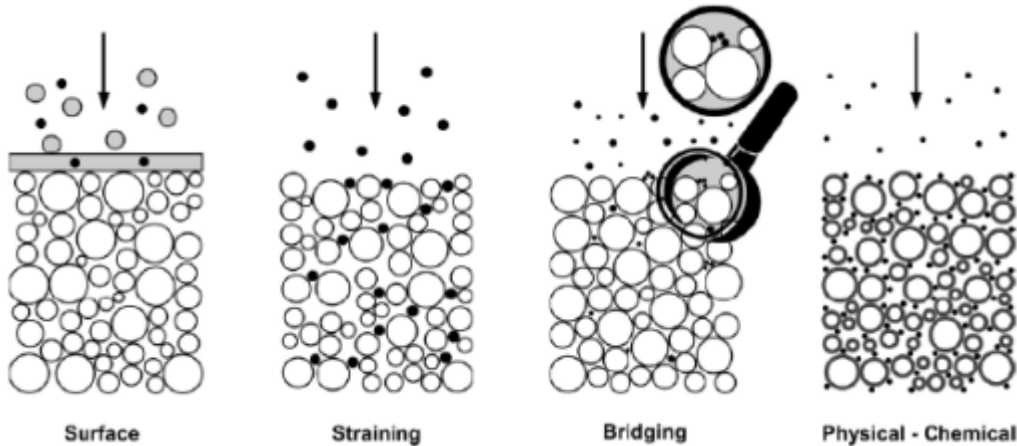


Figure 1.1. Deposition mechanisms of particle suspension injected in porous media (after McDowell-Boyer et al. 1986)

1.6.1 Surface filtration and size exclusion

The first deposition mechanism is surface or cake filtration. Cake filtration occurs when a solution containing particles with sizes larger than the pore size of the porous medium is injected. Particles are immediately captured at the surface because particles are too large to pass through the pores (McDowell-Boyer et al., 1986). Therefore, the particles will accumulate on top of the porous medium forming a layer, called the filter cake. When a thick filter cake has been formed the permeability of porous medium is substantially decreased. However, if the average suspended particle size is smaller than the average pore size, particles will flow through the porous medium. Depending on pore size and particle size distribution, larger particles will be trapped in smaller pores, because these particles are too large to pass through. This mechanism is known as straining or size exclusion. A number of papers report different criteria on straining depending on particle and grain size distributions (Bradford et al., 2002; Herzig et al., 1970; Sen and Khilar, 2006).

1.6.2 Bridging

Another possible colloid capture process near the vicinity of the borehole wall is hydrodynamic bridging. Bridging may cause clogging even when the size of the individual particles is sufficiently small to pass the filter. Bridging occurs when several particles arrive at a pore constriction at the same time and wedge together (de Zwart, 2007). A bridge consisting of multiple particles is formed and blocks the pore constriction while the rest of the pore space remains open (Figure 1.2). When the majority of colloids are smaller than the average size of pore throats, straining is not expected to play an important role as a primary process.

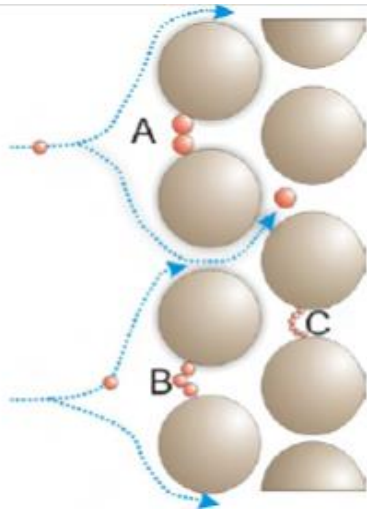


Figure 1.2. A representation of pore bridging (from de Zwart, 2007)

Particle bridging occurs under specific subsurface conditions. It is in particular dominant at high flow velocities, since this increases the probability that several particles enter the pore throat at the same time (Ramachandran and Fogler, 1999). This is related to force balance between hydrodynamic forces and the repulsive particle-grain forces. At higher flow rates the hydrodynamic forces overcome the repulsive forces, which is favourable for bridging. In case of physical well clogging it is expected that bridging occurs close to the well where the particle flux and flow velocity is highest. Colloid deposition due to bridging depends upon a number of parameters. It depends on pore size distribution of the aquifer, the colloid size and concentration, and colloid-grain surface interaction forces (Ramachandran and Fogler, 1999). Among these the ratio between the grain size and particle size is one of the most important parameters influencing bridging. This ratio is known as the aspect ratio in the literature concerning colloid filtration. For large aspect ratios, i.e., large pores, more particles are needed to form a bridge. Therefore for large aspect ratios the probability of bridge formation is low (Sen and Khilar 2006). Another aspect affecting bridging is the colloid concentration suspended in groundwater. Higher concentration increases the colloid flux and therefore leads to an increase of the likelihood of bridge formation. Based on the literature, it is expected that the most important parameters for bridging are 1) Particle concentration, 2) Flow velocity as higher flow velocity mobilizes more particles and also overcomes the repulsive particle-grain surface forces which may result in bridging, 3) Aspect ratio; the ratio between pore size and particle size influences the number of particles required to form a bridge. Small ratios are favourable for bridging, 4) Colloid properties; shape, surface charge and roughness.

1.6.3 Attachment

The aquifer functions as a source of colloids as well as a filter. Attachment of suspended colloids can be affected by changes in the hydrodynamic conditions and chemistry of groundwater. Colloid attachment depends on the attractive and repulsive forces between the colloid and matrix, and between colloids. Pore and colloid diameters, physical and chemical properties of the matrix, colloids, and solution affect the attachment processes. Electrostatic and London-Van der Waals forces mainly determine the attractive or repulsive conditions. The physical-chemical attachment processes are commonly described by the classical filtration theory based on the Yao-Habibian model. The filtration theory given by the following equation has three capture processes: interception, diffusion, and sedimentation (Yao et al., 1971, see Figure 1.3).

$$\lambda = \frac{3(1-n)}{2d_g} \alpha \eta \quad (1.5)$$

In the model the attachment coefficient (λ) is related to porosity n , grain diameter d_g , and two empirical coefficients called sticking (attachment) efficiency (α) and the collision probability or collector contact efficiency (η). Interception occurs when a colloid collides with a collector surface (grain surface) because of its finite size, and is a function of the aspect ratio (ratio of the pore diameter to the particle diameter). Sedimentation occurs when colloids settle on the collector surface when the density difference between the colloid and liquid phase is significant. Small colloids undergo Brownian motion (diffusion) which can then collide with the collector.

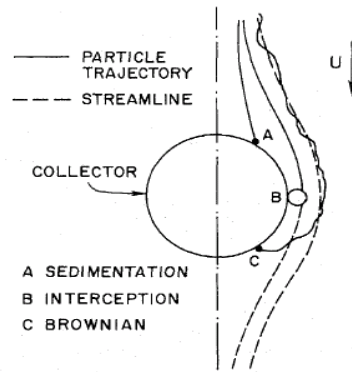


Figure 1.3. Three basic particle transport mechanisms of suspended particle transport to a collector surface (Yao et al., 1971)

The classical filtration model of Yao et al. (1971) however does not include hydrodynamic interactions and the universal van der Waals attractive forces. Hydrodynamic interactions play an important role in the filtration behaviour of colloidal particles (Torkzaban et al., 2007; Tufenkji and Elimelech, 2004). Below we will briefly explain the single collector efficiency equation of Tufenkji and Elimelech (2004). The collision probability (collector contact efficiency, η) is given by the ratio of the number of particles colliding with the collector surface to the number of particles approaching the collector. The collision efficiency (α) gives an indication of the conditions of the aquifer and is defined as the ratio of the number of particles deposited onto the collector surface to the number of particles colliding with the collector. When the sticking efficiency is equal to 1 the conditions are favourable for deposition and all colliding colloids are deposited. When the sticking efficiency is less than one, the conditions are unfavourable.

Tufenkji and Elimelech (2004) have found a new equation for predicting the single-collector contact efficiency (η) in physiochemical particle filtration in saturated porous media. The new equation is based on a rigorous numerical solution of the advection-diffusion equation with the assumption that the overall collision probability can be calculated by the sum of the contribution of each individual transport mechanisms: interception, gravitational sedimentation, and Brownian diffusion.

$$\eta = \eta_I + \eta_G + \eta_D \quad (1.6)$$

Where η_I , η_G , η_D are the collision efficiencies contributed by interception, gravity, and diffusion induced transport respectively. A separate correlation is determined for each mechanism.

Interception occurs when a particle moving along a streamline hits the collector surface due to its finite size. The collision efficiency due to interception is given by

$$\eta_I = 0.55 A_s N_R^{1.55} N_{Pe}^{-0.125} N_{vdw}^{0.125} \quad (1.7)$$

Where A_s is Happel's correction factor, N_R is the aspect ratio, N_{Pe} is the Peclet number, N_{vdw} is the van der Waals number (see Table 1.3).

The Happel correction factor A_s is defined as

$$A_s = \frac{2(1 - g^5)}{2 - 3g + 3g^5 - 2g^6} \quad (1.8)$$

where $g=(1-n)^{1/3}$ and n is porosity. The streamline model of Happel is used to account for the flow restrictions within a porous medium. The model describes the flow around a sphere and corrects for the packing of a medium built out of spheres. When using the Happel correction factor the flow velocity in the model should be the pore velocity.

Gravitational sedimentation occurs when particles start settling due to density differences. Particles with larger densities than the groundwater start settling on the collector surface. The collision efficiency due to gravitational sedimentation is given by

$$\eta_G = 0.475 N_R^{-1.35} N_{Pe}^{-1.11} N_{vdw}^{0.053} N_{gr}^{1.11} \quad (1.9)$$

where N_{gr} is the gravitational number, see Table 1.3.

Small particles undergo Brownian diffusion which can result in particles coming into contact with the collector grain. The collision efficiency due to Brownian diffusion is given by

$$\eta_D = 2.4 A_s^{0.33} N_R^{-0.081} N_{Pe}^{-0.715} N_{vdw}^{0.052} \quad (1.10)$$

The overall single-collector collision probability (contact efficiency) for deposition in a saturated porous media can be written as the sum of the individual transport contributions as:

$$\eta = 0.55 A_s N_R^{1.55} N_{Pe}^{-0.125} N_{vdw}^{0.125} + 0.475 N_R^{-1.35} N_{Pe}^{-1.11} N_{vdw}^{0.053} N_{gr}^{1.11} + 2.4 A_s^{0.33} N_R^{-0.081} N_{Pe}^{-0.715} N_{vdw}^{0.052} \quad (1.11)$$

Table 1.3. Overview of dimensionless numbers used in the correlation equations, from Tufenkji and Elimelech (2004) (where v the fluid approach velocity, D the bulk diffusion coefficient (described by the Stokes-Einstein equation), A the Hamaker constant, k the Boltzmann constant, T the absolute temperature, $d_{particle}$ and $d_{collector}$ the particle and collector diameter respectively, $\rho_{particle}$ and ρ_{fluid} the particle and fluid density, $r_{particle}$ the particle radius, and g the gravitational acceleration)

Parameter	Definition	Physical interpretation
N_R	$d_{particle} / d_{collector}$	Aspect ratio
N_{Pe}	$vd_{collector} / D$	Peclet number characterizing ratio of convective transport to diffusive transport
N_{vdw}	A / kT	Van der Waals number characterizing ratio of van der Waals interaction energy to the particle's thermal energy
N_{gr}	$4\pi r_{particle}^4 (\rho_{particle} - \rho_{fluid}) g / 3k$	Gravitational number; ratio of particle's gravitational potential when located one particle radius from collector to particle's thermal energy

The sticking efficiency, α , represents the fraction of the particles colliding with the solid grains that remain attached to the collector (Torkzaban et al., 2007). The sticking efficiency reflects the net effect of repulsive and attractive forces between the surfaces of the particles and the solid grains and depends on the surface characteristics of the colloids and porous media. Therefore, it depends on pH, organic carbon content, and ionic strength. It is believed that α is also dependent

on hydrodynamic forces. Commonly, α is derived from experimental values of attachment coefficient (λ) and calculated values of the collision efficiency η using Equation 7.

1.7 Modelling clogging process in aquifers

As described in detail in previous sections, one of main clogging processes in water injection wells is physical particle deposition processes. A number of factors such as physicochemical conditions, water velocity, colloid and pore size influence clogging. In this section the modelling approach based on the classical deep bed filtration theory to quantitatively describe the clogging of injection wells due to colloid deposition is presented. First, the basics of deep bed filtration are given, followed by the increase in pressure drop related to the colloid deposition and the clogging function.

1.7.1 Classical deep bed filtration theory

Due to the dynamic behaviour of clogging processes, it is a challenge to model this phenomenon. A large number of clogging models is available. Most of the models originate from the classical deep bed filtration theory (Yao et al., 1971), which is summarized here, the detailed derivation and assumption can be found in the literature (Yao et al., 1971).

The one-dimensional particle mass balance equation is given by

$$\frac{\partial}{\partial t}(\rho_b S + nC) + \frac{\partial}{\partial x}(uC) - Dn \frac{\partial^2 C}{\partial x^2} = 0 \quad (1.12)$$

where u is the specific flow velocity of the particles (L/T), C is the colloid concentration in the aqueous phase (M/L³), x is the distance along the flow direction (L), S is the concentration of deposited colloids (M/L³), n is the porosity, ρ_b is the bulk density (M/L³), and D is the dispersion coefficient (L²/T).

It is well-known that the deposition rate depends on the flow velocity u , the concentration of suspended colloids and the so-called filtration coefficient λ (as mentioned before Yao et al. (1971) presented equation 1 for λ):

$$\frac{\rho_b \partial S}{\partial t} = \lambda u C \quad (1.13)$$

This filtration coefficient can be determined experimentally and ranges from 0.001 to 0.1 m⁻¹ (Herzig et al., 1970). The filtration is known to depend on many factors. Detailed overviews of such processes can be found in the literature (Herzig et al., 1970; Kretzschmar et al., 1999; McDowell-Boyer et al., 1986; Rajagopalan 1976; Ryan and Elimelech, 1996; Sen and Khilar, 2006). The filtration coefficient λ may be estimated using the classical filtration theory based on the Yao-Habibian model. However, this coefficient has been shown to be a function of the deposition concentration S , pore size d_p , suspended colloid concentration C , zeta potential ζ and other parameters (Alvarez, 2005; Bedrikovetsky et al., 2001). As a result it may vary in time and space:

$$\lambda = f(S, C, d_p, \zeta, \dots) \quad (1.14)$$

Equations (8) and (9) require initial and boundary conditions for C and S . The following initial condition represents an initially clean bed of length L :

$$C = 0, S = 0 \text{ for } 0 \leq x \leq L \text{ and } t=0 \quad (1.15)$$

The boundary condition representing constant inlet particle concentration at a constant flow rate are given by

$$C = C_{in} \quad \text{at } x = 0 \quad (1.16)$$

In the special case where λ and u are constant, the analytical solution can be easily obtained from (8) through (12) yielding

$$C = C_{in} e^{-\lambda x} \quad (1.17)$$

$$S = \frac{u \lambda t}{\rho_b} C_{in} e^{-\lambda x} \quad (1.18)$$

From equation (13) it follows that the colloid concentration in the liquid phase is a function of the distance only, i.e., it is independent of time assuming changes in porosity are negligible. The model given by (8) and (9) is most often used to fit experimental data. The effluent (outlet) concentrations in sandbox or column experiments are measured and used to determine the filtration function. From this, the deposition profile can be calculated. The expression to calculate the constant filtration coefficient λ can be obtained from (13), using the length of the core L and the known effluent concentrations C .

$$\lambda = -\frac{1}{L} \ln \frac{C}{C_{in}} \quad (1.19)$$

Different forms for $\lambda(S)$ have been proposed (Alvarez, 2005; Bedrikovetsky et al., 2001; Herzig et al., 1970). For complex filtration functions, numerical procedures have been developed to solve equation (8) with initial and boundary conditions (11) and (12). Such procedures can be applied for both diffusive and non-diffusive cases, i.e., require less restrictive model assumptions.

1.7.2 Filtration theory for injection wells

To model colloid deposition in the vicinity of water injection wells, the colloid transport model where the dispersion is ignored has to be cast into cylindrical coordinates (Wennberg and Sharma 1997). If porosity changes due to colloid retention are negligible, i.e., $n = \text{constant}$, this becomes this equation does not incorporate the dynamic behaviour of the porous medium, i.e., the changes in porosity due to particle retention. It is assumed that the effects of changes in porosity are relatively small compared to the effects of loss of permeability due to particle retention.

$$n \frac{\partial C}{\partial t} + u(r) \frac{\partial C}{\partial r} = -\frac{\partial S}{\partial t} \quad (1.20)$$

$$\frac{\rho_b \partial S}{\partial t} = \lambda(S, u(r)) |u(r)| C \quad (1.21)$$

$$u(r) = \frac{Q}{2\pi r D} \quad (1.22)$$

where r is the one-dimensional cylindrical space coordinate, $u(r)$ is the Darcy flow velocity as a function of r , Q is the recharge rate and D is the thickness of aquifer. For simplicity, the flow rate $Q(t)$ is assumed for now to be a constant Q . For linear flow, the flow velocity is constant in r . In the case when the flow velocity varies in a given flow geometry, i.e., injection wells, the velocity changes with the radial distance. Here the deposition is related to the flow velocity and therefore also to r . This dependence has been observed in laboratory experiments with radial flow geometry (de Zwart 2007; Ramachandran and Fogler, 1999).

$$\lambda = \lambda_0 (u(r))^\delta \quad (1.23)$$

where λ_0 is the filtration coefficient of the medium and the δ power expresses the nonlinearity of the velocity dependence. Note that, for $\delta = 0$, the filtration coefficient λ reduces to a constant λ_0 as in the classical literature. For arbitrary filtration functions, where λ depends on σ and u , the equation has to be solved numerically. An analytical solution has been derived for the case of a constant filtration coefficient using the method of characteristics (Bedrikovetsky et al., 2001).

1.7.3 Pressure changes due to clogging

Due to deposition of particles, the permeability of the porous medium is affected. The related pressure changes in the system can be obtained from Darcy's law.

$$\frac{\partial p}{\partial r} = -u \frac{\mu}{k_0 k(s)} \quad (1.24)$$

where u depends on r according to (18), p is the pressure, μ is the viscosity, k_0 is the initial permeability of the porous medium prior to particle retention and $k(s)$ is a function describing the permeability reduction due to deposition of colloids. In the literature, different functions for $k(s)$ have been proposed (Civan, 2007). A large class of functions can be approximated by an expression given by McDowell-Boyer et al. (1986):

$$k(s) = \frac{1}{1 + \beta_1 s + \beta_2 s^2 + \dots + \beta_n s^n} \quad (1.25)$$

In a first order approximation, this reduces to

$$k(s) = \frac{1}{1 + \beta s} \quad (1.26)$$

This function is often referred to as the formation damage function, where β is the so-called formation damage coefficient (Civan, 2007).

1.8 Physical clogging assessment

The potential for the injection water to lead to physical clogging can be evaluated to some extent from examining the levels of indicator parameters such as Membrane Filtration Index (MFI), total suspended solids (TSS), volatile suspended solids (VSS) and turbidity. Levels of particulate matter in injectant characterized by the levels of turbidity may be used as an indicator for physical clogging. MFI is an index of physical clogging potential that better accounts for the effect of particle size and composition than TSS or turbidity. MFI is a laboratory-based measure of the potential for physical clogging of a 0.45 μm membrane filter (Dillon et al., 2001). The greater the retention of particles on the filter, the greater the MFI value (reported in units of sec/L^2) and hence also the rate of physical clogging. Note that chemically and biologically forms of clogging are not accounted for due to the nature and brevity of the test procedure. The values generally accepted as an upper limit by Dutch water utilities for injection into fine-textured dune sands are the range of 3-5 sec/L^2 (Olsthoorn, 1982). However, values of MFI as high as 400 to 4200 sec/L^2 were estimated to have been successfully injected into a sandy limestone aquifer with significant secondary porosity in the near-well zone during four successive years with routine backwash redevelopment every 40 ML (Pavelic et al., 2006). These two examples illustrate that: a) the clogging potential of any given source water is highly dependent on the hydraulic characteristics of the target formation; and b) there is a trade-off between the source water quality and the extent of clogging and hence the degree of redevelopment needed to sustain injection rates.

1.9 Clogging control and remediation

Control and remediation of clogging are among the most important issues to be resolved for efficient exploitation and cost management of aquifer recharge. The development of technologies and strategies for cost-effective clogging control and remediation is an immature field of science. There are no proven technologies that are a universal remedy for all problems (Civan, 2005). Creative approaches, supported by science and laboratory and field tests yield the best solution. An examination of the reported studies reveals that numerous recipes and/or recommended procedures have been developed. However, their applicability and/or effectiveness have been validated for certain specific rock and fluid systems and, therefore generalization of these approaches is questionable (Civan, 2005).

In the last few decades, a great effort has been made in the field of petroleum industry to control and minimize the damage related to clay release and transport. As a result, numerous chemicals often called clay stabilizers have been developed. Clay stabilizers have evolved from simple inorganic chemicals to inorganic polymers, and to complex organic polymers (Zhou et al., 1995). Many of them are used in drilling, completion, fracturing, water flooding, and steam injection. The economic aspect of applying clay stabilizers depends on the choice of clay stabilizer(s). To efficiently use clay stabilizers, it is important to evaluate the applicability and limitations of the clay stabilizers available.

In the following sections, some of the more common treatment methods are reviewed. However, their applicability in specific fields should be investigated and adapted by laboratory core testing.

1.9.1 Stabilization of clay particles

Both clay release and swelling occur by the negative surface charge on clay surfaces. Therefore, most of clay stabilizers are designed to neutralize or reverse the negative charge of clay particles. They can be multivalent cations or complex cationic polymers. Cations like Ca^{2+} , Mg^{2+} , and Al^{3+} at sufficient concentration, can prevent swelling and dispersion of clay minerals. However, their stabilizing effect is temporary or reversible because they can be exchanged or displaced by monovalent cations (e.g. Na^+) with higher concentration. The swelling clays like smectites stabilized by simple multivalent cations are prone to fresh water sensitivity. Conversely, cationic polymers can stabilize clay particles permanently or irreversibly because the cationic polymers cannot be displaced by monovalent cations. Organic polymers can control clay release by "bridging" and "encapsulating" clays.

1.9.2 Selection of treatment fluids

As expressed by Thomas et al. (1998), the type and location of the clogging must be determined to select the proper treating fluids. Additionally, precautions should be taken to avoid further damage. Damage can be from wettability changes, scale, organic deposits, silt and clay, and bacterial deposits. In most cases, the type or types of clogging cannot be precisely identified. However, the most probable type or types can be determined; therefore, most matrix treatments incorporate treating fluids to remove more than one type of damage.

The selection of the treatment fluids depends on the specific applications and purposes. The treatment fluid volumes are usually determined by means of laboratory core tests and mathematical models. Treatment fluids contain various additives for various purposes.

The major treating fluid is designed to remove the clogging effectively. Additives are used to prevent excessive corrosion and prevent precipitation of reaction products. Additionally, additives are used in pre-flushes and over-flushes to stabilize clays, inhibit scale and organic deposition.

Additive selection is primarily dependent upon the treating fluid, the type of well, bottom-hole conditions, and the placement technique.

1.9.3 Clay stabilization

When clay is exposed to lower salinity solutions, two mechanisms may cause clogging (Himes et al., 1991). Swelling clays imbibe water into their crystalline structure and enlarge in size and plug the pore space. Mobilization, migration, and deposition of clays can plug the pore throats. Himes et al. (1991) describe the desirable features of effective clay stabilizers, especially for applications in tight formation as following:

1. The product should have a low, uniform molecular weight to prevent bridging and plugging of pore channels.
2. The chemical should be non-wetting on sandstone surfaces to reduce water saturation.
3. It should have a strong affinity for clay surfaces
4. The molecule must have a suitable cationic charge to neutralize the surface anionic charges of the clay effectively.

The various approaches utilized for clay stabilization are described in the following sections.

1.9.4 Inorganic cations (IC)

Clay stabilization can be accomplished by maintaining the aqueous solution salinity above that of the native water (Himes et al., 1991). Figure 1.4 by Himes et al. (1991) shows the clay stabilizing effectiveness of various brines. The basal spacing vs. the salt concentrations are shown as an indication of clay swelling, measured by X-ray diffraction (XRD). The clay will disperse when the basal spacing is greater than 21Å (Himes et al., 1991). In this respect, Figure 1.4 indicates that the clays are stable even at very low concentrations of K^+ and NH_4^+ cations, whereas a sufficiently high concentration of Na^+ cation is necessary to maintain clay stability. Therefore, K^+ and NH_4^+ are natural clay stabilizers, but are not permanent because they can be exchanged with Na^+ (Himes et al., 1991). Figure 1.4 shows that calcium ion can maintain clay stability, but it is not preferred as a clay-stabilizing agent because it may react with the formation and chemical additives (Himes et al., 1991). Clogging resulting from clay swelling and mobilization, migration, and redeposition can be prevented by adding certain ions in injection fluids to stabilize the clays (Keelan and Koepf, 1977).

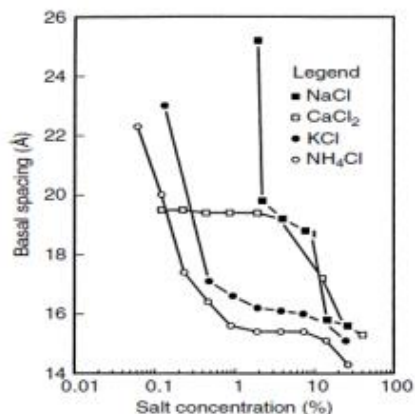


Figure 1.4. Basal spacing of smectite clays vs concentration of various brines (after Himes et al., 1991)

1.9.5 Cationic inorganic polymers

In order to provide somewhat permanent clay stabilization, cationic inorganic polymers (CIP) such as hydroxyl aluminum and zirconium oxychloride have been introduced (Reed, 1974; Himes et al., 1991). These agents provide resistance to cation exchange, but they are applicable for clay stabilization in noncarbonate-containing sandstones and the formation should be retreated after acidizing (Himes et al., 1991).

CIP such as OH-Al are relatively cheap and easy to apply in the field. It is effective for preventing both clay swelling and release. Because it is inexpensive, a large volume of reservoir can be treated. The disadvantage of CIPs is that they are applied only on a limited pH range. For Al, the polymerization pH is 3.5-6. In very acidic solution ($\text{pH} < 3.5$), Al will not polymerize. In neutral and alkaline solutions ($\text{pH} > 6$), Al will precipitate as hydroxide. Thus the application of CIPs is limited in the near well region, especially as a post-acid treatment. The carrier solution has to be strongly buffered in order for CIPs to penetrate further into a reservoir Zhou et al., (1995).

1.9.6 Cationic organic polymers

Quaternary cationic organic polymers (COP) are used for effective and permanent stabilization of clays (especially smectite clays), and for controlling fines and sand in sandstone as well as carbonate formations (Himes et al., 1991). They are applicable in acidizing and fracturing treatments. They provide permanent protection because of the availability of multiple cationic sites of attachment. However, their applicability in tight formations is limited to low concentrations (Himes et al., 1991). They can cause permeability damage by pore plugging because these high molecular weight and long-chain polymers have molecular sizes comparable with the some pore size fractions in porous rock.

1.9.7 Oligomers

Oligomers are low molecular weight, cationic, organic molecules having an average of $0.017 \mu\text{m}$ length (Penny et al., 1983; Himes et al., 1991). Oligomers offer many potential advantages over the cationic organic polymers for clay stabilization (Himes et al., 1991). Because of their smaller size compared to pore size, the treatment-imposed permeability damage is significantly reduced. Because they are only slightly water-wetting (contact angle is 72°), the irreducible water content is also reduced. Zaitoun and Berton (1996) examined the effectiveness of cationic polyacrylamides (CPAM) and nonionic polyacrylamides (PAM) for stabilization of montmorillonite clay by means of the critical salinity concentration method (CSC). As schematically depicted in Figure 1.5 by Zaitoun and Berton (1996), the polymers prevent fines migration by coating over the pore surface and blocking the clay particles. They determined that low molecular weight polymers have comparable stabilizing capability to high molecular weight polymers and are more advantageous because they cause less treatment-induced permeability damage.

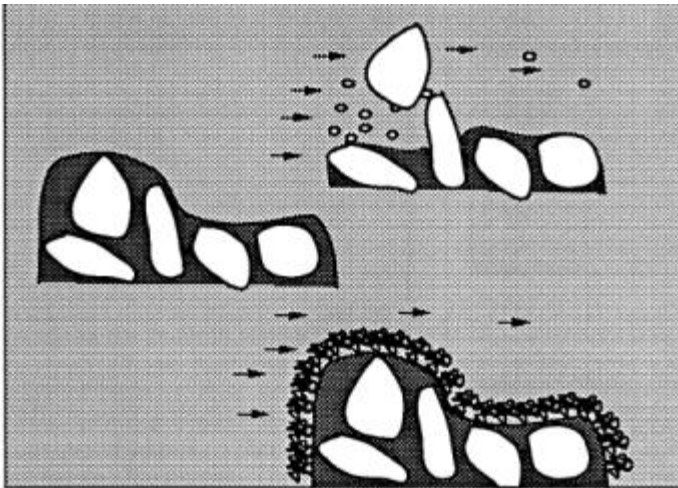


Figure 1.5. Polymer coating of pore surface for clay migration prevention (after Zaitoun and Berton, 1996)

1.9.8 pH–buffer solutions

Buffering is an effective means of pH control by maintaining the hydrogen concentration constant in spite of the changing conditions. Buffer capacity expresses the sensitivity of pH of an aqueous solution to adding a strong base (Gustafsson et al., 1995). Hayatdavoudi (1998) hypothesizes that alteration of kaolinite to dickite, nacrite, and halloysite, through chemical oxidation may be responsible for fines generation, at high pH in the presence of alkali hydroxides. Therefore, Hayatdavoudi (1998) recommends buffering the pH of injectant to 8 or below and avoid aeration of injected fluids to prevent kaolinite comminution-induced clogging.

1.9.9 Chemical alteration of clay with KOH

Norman and Smith (2000) explain that the chemical structure of the clay minerals can be permanently transformed to non-water sensitive types by reaction with potassium hydroxide (KOH). The formation surrounding the wellbore should be treated up to a sufficiently long distance to avoid particle mobilization owing to the interstitial fluid velocity exceeding the critical velocity required for particle detachment. Norman and Smith (2000) caution that KOH causes the divalent ions Ca^{2+} and Mg^{2+} to form damaging precipitates and therefore the divalent ions should be removed from the region considered for KOH treatment. This can be accomplished by pre-flush using a 2–3% (weight) KCl solution, free of such divalent ions, to push away the formation brine from the treatment zone, which may contain some divalent ions. Then, a divalent ions free concentrated (15–30% weight) KOH slug is applied, considering that it will be diluted by mixing with the pre-flush solution placed in the treatment zone. Finally, a fresh water post-flush is applied. Norman and Smith (2000) warn that KOH treatment should be only considered when the well material and conditions are suitable because KOH is very corrosive and damaging.

2 An experimental and modelling investigation of clogging potential

2.1 Anticipated Clogging processes

Processes which are primarily responsible for clogging in injection wells include entrained air and gas binding, deposition of colloidal particles present in the source water, biological growth, geochemical reactions, and in situ colloid rearrangement, release, and re-deposition in the porous media (Khilar and Fogler, 1998). Properties of the porous media, groundwater, source water, well construction, injection facilities design, and injection rate determine the influence of these processes on well clogging.

The intended source water for the re-injection water into aquifers is a blend of RO water with micro filtered-CSG associated water (the pore size of the filter is 0.03 micron). Based on an understanding that the potential for biological and physical clogging due to external colloids will be minimised by micro-filtration prior to injection, the predominant clogging concern associated with the use of treated CSG-associated water is the potential for in situ clay release and subsequent clogging. Therefore, the objective of this chapter is to provide a summary of the findings of an extensive laboratory and modelling study undertaken to assess the clogging potential due to dispersion of in situ clay colloids during reinjection of CSG associated water into the Precipice Sandstone aquifers at Reedy Creek and Condabri.

Based on the mineralogy of the Precipice Sandstone aquifer at Reedy Creek and Condabri, which is presented later on in this chapter, it is expected that dispersion of in situ colloidal particles (e.g. clay) upon injection of water with a lower salinity than that of groundwater has the potential to be a dominant clogging process. Normally, the colloidal particles attached to the sediment grains of the porous media are at equilibrium in the native groundwater conditions. However, various disturbances such as physical, chemical, and hydrodynamic changes may induce the salinity, velocity, and thermal shock phenomena causing colloid release (Civan, 2007). Once colloids are introduced into the pore space, they become mobile and may re-deposit down gradient (especially in pore constrictions) resulting in a drastic and rapid permeability loss. To mitigate clogging, a pre-treatment of injectant is required to increase its compatibility with the fluid and solid phase of the aquifer so as not to clog injection wells. It is imperative to obtain insights on the factors affecting this type of clogging process. With an increased understanding of the clogging mechanisms, predictive tools can be used during the planning stages to estimate treatment and redevelopment requirements.

This experimental and modelling study was specifically aimed at providing a better understanding of the mechanisms of well clogging due to colloid release and the effects of flow velocity, chemical conditions, and the properties of porous media on clogging propensity. The investigation included laboratory core-flooding experiments with core material collected from different depths in the Precipice Sandstone aquifers at Reedy Creek and Condabri and numerical simulations to develop the understanding of processes leading to clogging. The clogging mechanisms assessed were colloidally- and hydrodynamically- induced colloid release and entrapment at pore constrictions which may occur during injection of RO-water or blends.

2.2 Materials and Methods

2.2.1 Aquifer Materials

Aquifer materials collected from the Precipice Sandstone aquifer at Reedy Creek and Condabri were employed in this study to examine the effects of injection water with various flow rates and chemical compositions on the kinetic of clay release and clogging potentials. APLNG/Origin Energy provided more than 70 samples from the Precipice Sandstone aquifer at Reedy Creek and Condabri to the CSIRO Land and Water Waite Laboratories in Adelaide for their use in core-flooding experiments. These are APLNG's trial sites for reinjecting coproduced waters. Available core samples from the Reedy Creek trial injection site included three bores providing (1) 17 samples from the Westbourne Formation at Reedy Creek SC1-Wb, (2) three samples from the Springbok Sandstone at RCMB2-S, and (3) 26 cores spanning the Precipice Sandstone, Evergreen Formation, and Hutton Sandstone from the bore Reedy Creek MB3-H. Samples from the Condabri trial injection site include 27 samples spanning the Precipice Sandstone, Evergreen Formation, Hutton Sandstone, and Eurombah Formation. Samples from Talinga and Strathblane were not assessed in this study as their initial permeability was very low (<0.1 m/day). At selected depths in representative target aquifers, aquifer cores (63 mm i.d.) were collected for the clogging assessment. These cores (~80 cm lengths) were transferred and stored in aluminium tubes with "cam-lock" caps and flushed with nitrogen gas to limit potential oxidation of sediment material during transport and storage. Core material at selected depths was sub-sampled for geochemical analysis (Table 2.1). More than 90 core plugs from Precipice sandstone aquifers at Reedy Creek and Condabri were cut at Challenger Geological Services in Adelaide for use in core-flooding experiments. Details of these core samples are given in Appendix A.

Table 2.1. Mean percentage of clay content of the cores sent to CSIRO Adelaide for clogging assessment.

Location	Tube ID	Sample No.	Depth below ground (m)	Kaolinite (%)	Illite (%)
Condabri	MB94-A	63	1458	13	4.2
Condabri	MB94-A	70	1490.98	17	4.5
Condabri	MB94-A	65	1498.99	13	2.3
Condabri	MB94-A	69	1512.09	9.6	2.4
Condabri	MB9-H	71	1538.56	7.4	1.3
Condabri	MB9-H	74	1547.93	0.8	<0.1
Reedy Creek	MB3-H	064A	1301.24	12	2.7
Reedy Creek	MB3-H	067A	1309.3	13	2.5
Reedy Creek	MB3-H	070A	1316.06	9	0.5
Reedy Creek	MB3-H	076A	1347.25	4	2.3

2.2.2 Characteristics of aquifer materials

The Precipice Sandstone is generally white to grey in colour and predominantly consist of quartz, with minor clay, feldspar and mica. Selected core samples from the Precipice Sandstone were analysed by X-ray diffraction (XRD) (performed for Origin Energy by Weatherford Laboratories) to determine proportions of constituent minerals (see Tabl 3.2). Detailed information on XRD analyses can be found in Australia Pacific LNG (2013). In summary, quantitative XRD analysis showed that the Precipice Sandstone comprises quartz (60 to 92 %), clay minerals (5 to 38%), calcite (0 to 25%) and K-feldspar (0 to 10 %), with minor siderite (<3 %) and anatase (<1%). In the BSF (the Braided Stream Facies), the percentage of quartz is greater (>83 %), at the expense of the other minerals. Clay mineral fractions are dominated by kaolinite (80 to 95 %), with some illite/mica (<10 %) and mixed-layer illite/smectite (<5 %). As kaolinite is the dominant clay mineral and is a non-swelling clay, it is expected that clay release will be a more important clogging mechanism than swelling. The effective porosity of the selected sandstone cores from the Precipice and BSF aquifers was estimated to range between 14 to 23%. Due to the low clay content of BSF, the effective porosity of the cores from BSF was higher (19 – 23%). The Precipice Sandstone, which is finer grained and contains a higher clay mineral content, showed more varying results, with effective porosity typically within the range 14 to 21% (see Appendix A).

Table 2.2 XRD analyses

SITE	FORMATION	STATISTIC	QUARTZ (%)	KAOLINITE (%)	ILLITE & ILLITE/SMECTITE (%)	FELDSPAR (ALB) (%)	FELDSPAR (MIC) (%)	CALCITE (%)
Reedy Ck MB3-H	Precipice	Mean (σ)	74.9 (13.2)	11.6 (5.9)	4.1 (3.5)	0.8 (0.7)	4.3 (2.5)	2.9 (5.6)
		Min	61.1	3.9	1	0	1.1	0
		Max	92.7	17.1	1	1.5	7.3	11.3
Condabri MB9-H	Precipice	Mean (σ)	68.0 (28.0)	16.0 (12.9)	5.4 (6.0)	0.3 (0.3)	2.9 (3.9)	4.3 (10.1)
		Min	38.8	3.7	0	0	0	0
		Max	96.3	38.1	14.8	5.2	10.1	25

Source: Origin Energy

Core-flooding experiments were conducted with selected core samples from different depths of the Precipice and BSF sandstones. Prior to experiments, each core plug was vacuum saturated with an electrolyte solution, encompassing a range of ionic strengths and ionic compositions (Appendix A). Scanning electron microscopy (SEM) with energy dispersive X-ray microbeam (EDX) analysis of representative core sample (MB9H_71_8) showed that larger quartz grains were covered with smaller clay particles (Figure 2.1). Colloidal particles showed morphologies of kaolinite clay particles.

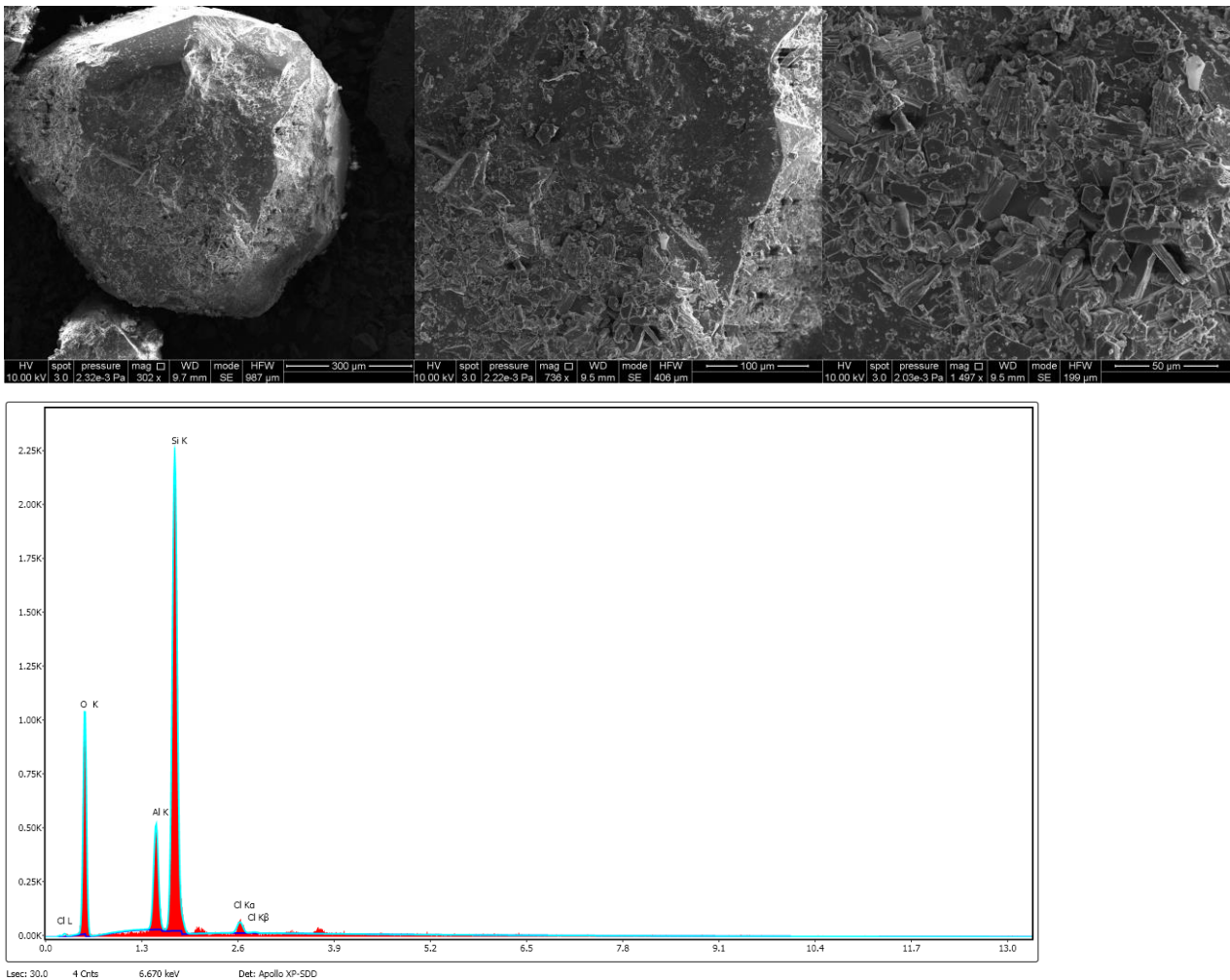


Figure 2.1. Typical SEM Micrographs and EDX spectrum of sand grains of the Precipice sandstone showing the Morphology of the clay and chemical composition on sand grains indicating that the major mineral was quartz

2.2.3 Groundwater chemistry

Analyses of groundwater quality samples collected from the Precipice Sandstone aquifer at Reedy Creek and Condabri was used to establish baseline conditions for potential clogging assessment. The data indicates that the mean total dissolved solids (TDS) of groundwater from the Precipice Sandstone aquifer is about 900 and 1950 mg/L at Reedy Creek and Condabri, respectively (APLNG, 2014). The pH measurements of the water ranged from 7.09 to 8.90, with a mean pH of 8.35. The ion compositions indicate that sodium is the strongly dominant cation in groundwater samples tested, which results in a high SAR value. A summary of water quality for groundwater from the Precipice aquifer at Reedy Creek and Condabri, in comparison to RO feed (untreated CSG associated water), and RO permeate (treated CSG associated water) is given in Table 2.3.

Table 2.3. A summary of water quality for groundwater from the Precipice aquifer at Reedy Creek and Condabri, RO feed (untreated CSG associated water), and RO permeate (treated CSG associated water)

Parameter	unit	Groundwater (Reedy Creek- Precipice)	Groundwater (Condabri- Precipice)	RO- Feed	RO- permeate
pH	-	8.77	8.03	9.2	7.8
Sodium Adsorption Ratio (SAR)	-	59	119	177	8.5
Electrical Conductivity	$\mu\text{S}/\text{cm}$	1380	2650	6500	250
Total Dissolved Solids	mg/L	897	1950	3950	152
Ionic Strength	mM	22	42	104	4
Total Suspended Solids	mg/L	NM	NM	20	<1
Total Alkalinity as CaCO_3	mg/L	626	1750	3000	80
Calcium	mg/L	2	2.3	3	<1
Sodium	mg/L	349	786	1600	40
Magnesium	Mg/L	<0.5	0.6	1.9	<0.5
Total Iron	mg/L	0.19	0.18	0.2	<0.1
DOC	mg/L	2	5	17	1.1

NM: Not measured

2.2.4 Aqueous solution used in the core-flooding experiments

The aqueous solutions used in the experiments were electrolyte solutions with varying cation concentrations prepared by adding NaCl and CaCl_2 in water from a double reverse-osmosis filter, hereafter denoted as RO-water. The electrical conductivity (EC) of the RO-water was less than 0.05 mS/m, sodium and calcium concentrations were below 1 mg/L and its pH was 5.8. Mixed solutions of NaCl and CaCl_2 were prepared to examine the effect of salinity concentrations and ion compositions on the release of clay from the grain surfaces and subsequent clogging of the porous media.

2.2.5 Description of the experimental setup

The experimental setup included a core holder, water reservoir, pump, effluent sample collector, pressure transmitter, and a data acquisition system. Figure 2.2 shows the schematic drawing of the system that operates at ambient laboratory temperature ($\sim 21^\circ\text{C}$). The system allows for applying an overburden pressure over the rubber sleeve containing the core plug. The dimensions of the core plugs can be between 2.5–5 cm in diameter and 3–11 cm in length. The differential-pressure transmitters are used to measure the pressure values across the core plug. The system is equipped with a computer-aided data acquisition system. The pressure differences across the cores are recorded over the course of the experiment at specified time intervals. This system has the capability of testing about 100 bar overall pressure difference across the core sample. An

overburden pressure of at least 30 bar over the injection fluid pressure is applied during the core tests. The injection flow rate in the experiments ranges between 0.1 to 100 mL/min.

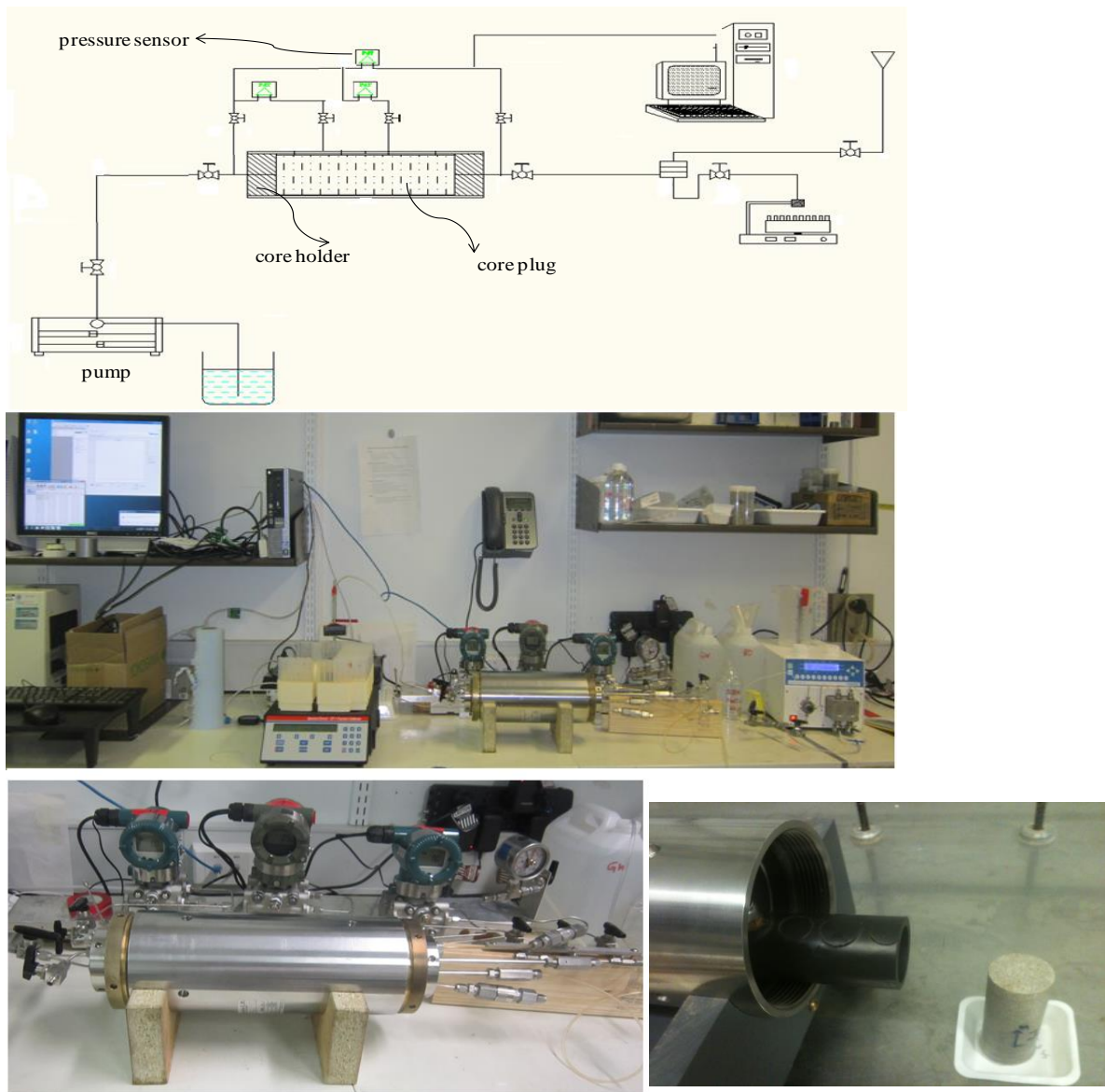


Figure 2.2. Experimental set-up for colloid release and clogging experiments

2.2.6 Experimental procedure

The core plugs were cut in a cylindrical shape with the diameter of 4 cm and length of 5 or 8 cm. Prior to each experiment, the core samples were initially vacuum saturated with a desired aqueous solution. Then, the core plug was inserted into the cylindrical rubber tube with an inner diameter of 4 cm. The core was then placed in a Hassler core-holder under a confining pressure of 130 bar, corresponding to a depth of 1300 m. The pressure difference across the core plug was measured with a pressure transducer. The outlet pressure was always atmospheric.

At the core holder outlet, the effluent was collected by a fraction collector and analysed for clay concentration using a UV/vis spectrophotometer at an optical density of 600 nm (OD600). Colloid size distribution in the suspension was measured using a dynamic light scattering (DLS) method. A linear correlation was established between OD600 and the clay concentration that was determined after drying effluent samples (Figure 2.3). This correlation was verified employing

different series of samples to be independent of the solution chemistry and flow rates for our experimental conditions.

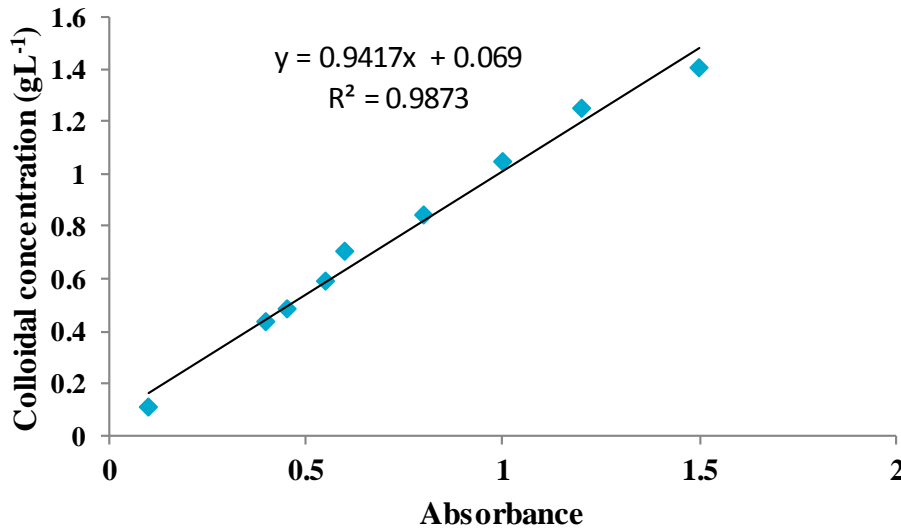


Figure 2.3. Calibration curve for the absorbance against colloid concentration

Selected effluent samples of the effluent breakthrough curve (BTC) were also analysed for electric conductivity (EC), pH and major cation concentration using an inductively coupled plasma atomic emission spectrograph at CSIRO Land and Water Analytical Services Unit (Waite Campus). The values of EC of the effluent were utilised as a tracer to determine the porosity and hydrodynamic dispersion of each core. Breakthrough concentrations for the conservative tracer are well described by the classical advection-dispersion equation (ADE). The value of dispersivity coefficient was obtained by fitting the experimental data with the HYDRUS-1D model (Simunek et al., 2008). For selected water samples (BTC), the clay material in the effluent suspension was deposited on a filter paper for SEM and EDX analysis.

The pressure drops across the core plug were measured as a function of pore volumes of the water injected into the core. The pressure data was used to calculate the hydraulic conductivity by employing Darcy's law for one dimensional laminar fluid flow through a porous media. Darcy's law is given by

$$u = -\frac{k}{\mu} \frac{\partial p}{\partial x} \quad (3.1)$$

Where u is Darcy velocity (L/T), ∂p is pressure drop across the core (pa), L is the length of the core plug (L), k is permeability of the core (L²) which is related to the hydraulic conductivity as $\kappa = K \frac{\mu}{\rho g}$ where K is the hydraulic conductivity, (L/T), μ is the dynamic viscosity of the fluid, (M/(L·T)), ρ is the density of the fluid, M/L³, g is the acceleration due to gravity, L/T².

2.2.7 Core-flooding tests

The core-flooding laboratory tests were performed to assess the effects of solution chemistry (e.g. ionic strength, ion type, pH) and flow velocity on release and migration of the colloidal particles, mainly clay minerals, within the aquifer sediments and subsequent clogging potential. The core-flooding tests were conducted at Waite Laboratories of the CSIRO Land and Water. The initial

hydraulic conductivity of the core samples employed in the core-flooding experiments is given in Appendix A.

Initially the clogging potential of core samples due to clay dispersion was assessed by changing the solution chemistry from 0.5M NaCl to RO-water. Low salinity water is expected to have the greatest potential for clay dispersion and therefore the 'worst-case' scenario for clogging potential was tested with RO-water.

2.2.8 Determination of Critical Salt Concentration (CSC) in a single salt system

A series of experiments using single salt system (NaCl, CaCl₂) were undertaken to examine the concept of critical salt concentration (CSC) for colloid release and clogging potentials in Precipice Sandstone. In a typical experiment, the core sample was vacuum saturated for 2 to 3 days in a 0.5 M NaCl (3 wt %) or 0.1 M CaCl₂ solution. The saturated core was then placed inside the core holder and a 0.5 M NaCl or 0.1 M CaCl₂ solution was injected through the core, at a given flow velocity. These high salt concentrations were employed to prevent any possible initial clay dispersion and permeability damage. The salt concentration was then decreased in small steps, until an increase in colloid concentration at the effluent or a drop in core permeability was observed. The experiments were performed with different monovalent and divalent solutions. The pH of the solution in all cases was maintained around neutral (pH 7).

The ionic strength of the solution is decreased in a stepwise manner, and this technique has been used successfully (Khilar, 1981; Khilar and Fogler, 1984) to determine the CSC of various single salt systems. The critical ionic strength is defined as the ionic strength at which there is a sharp decline in the relative permeability (K/K_0) and/or an increase in colloid release at the core effluent is observed.

2.2.9 Effect of Flow Reversal

In practice a flow reversal, or back flushing, is often practiced when the well exhibits injectivity decline due to clogging, as an operational measure to restore injection rates. Usually the effect is beneficial in the short term. In a set of experiments, core samples in which clay release was already underway through salinity shock, the water flow was stopped and the flow of solution continued in reverse mode.

2.2.10 Influence of flow velocity on CSC

A series of experiments was conducted to evaluate the impact of flow velocity on clay mobilization and subsequent clogging and also to identify the critical flow velocity at a given chemical condition. After the core was saturated and equilibrated with 0.5 M NaCl solution, NaCl solutions with various concentrations were injected into the core at different flow velocities, ranging from 1 to 100 m/day. At a given solution ionic strength, the flow velocity at which clay particles started to appear in the outflow was identified as the critical water velocity.

2.2.11 Determination of Critical Ionic Strength in a mixed salt system

A set of experiments were conducted to examine the processes of clay release and clogging in a mixed salt system of NaCl and CaCl₂. These experiments were specifically aimed at delineating the importance of divalent cations in the solution and cation exchange process on the clay release and clogging. We expected that the critical ionic strength below which clay release occurs would be dependent on the mole percentage of calcium in the solution and the ionic strength. The ionic

strength at which the pressure drop across the core begins to increase or the clay particles appear in the effluent determines the critical ionic strength.

A similar experimental procedure was used in this series of experiment. In a typical experiment, a sandstone core was vacuum saturated with a mixed NaCl/CaCl₂ salt solution of 0.1 M ionic strength (IS) and at a particular mole percent of calcium. The saturated sandstone core was placed in the core holder and a NaCl/CaCl₂ salt solution was injected through the core at an average pore water velocity of 5 m/day. The inlet pH was in the range 7 while the pH of the effluent was found to vary between 7 and 8. As described earlier, the ionic strength of the salt solution was decreased in a step-wise manner to obtain a range for the CIS. The ionic strength (IS) and the calcium percentage (% Ca) are related to the molarities of Na⁺ and Ca²⁺ in the following manner:

$$IS = M_{Na} + 3M_{Ca}$$

$$Ca\% = 100 \left(\frac{2M_{Ca}}{M_{Na} + 2M_{Ca}} \right) \quad (3.2)$$

2.2.12 Effect of pH

The pH of water can vary depending on the presence of deferent chemicals in the water. Values of pH vary widely depending primarily on the type of aquifer sediment and composition of injection water and native groundwater. In acidic conditions the pH may be less than 5 whereas alkaline conditions can exist in limestone aquifers. A series of experiments were conducted to determine the effect of pH changes on the clay release and clogging behaviour. Core samples were equilibrated with a solution of 10 mM NaCl at pH 6. Then the same solution with various pH (from 6 to 9), representing the range of pH that may be possible for RO-permeate, RO-feed or groundwater, was injected for 10 pore volumes at a flow rate of 10 mL/min. Analysis of pressure and effluent data was carried out for permeability determination and clay analysis.

2.3 Mathematical modelling of clogging due to colloid release and transport

Mathematical modelling was conducted to quantitatively analyse the observed colloid release and clogging processes due to injection of water at various flow velocities and chemical conditions into the sandstone cores from Precipice aquifer. In this section, a mathematical model is presented for describing clogging caused by the release and transport of in situ colloids in porous media. This model is based on the mechanism of in situ colloid release from the sand grain surfaces of the aquifer sediments and the mechanism of re-deposition of the released colloids at the pore constrictions. The mechanisms are schematically illustrated in Figure 2.4 showing a pore body and two pore throats. At equilibrium or time zero, all the colloidal particles are attached to the pore wall. Upon a change in chemical or hydrodynamic conditions, a fraction of the colloids may be released due to changes in adhesion energies or hydrodynamic forces or by a combination of these factors. Following the detachment from the pore wall, the colloids become suspended in the pore body and are transported with the flow. During the transport in the porous media, a fraction of the suspended colloids may become retained at the pore throats (pore constrictions) resulting in a permeability reduction. Figure 2.4b illustrates the blockage of the pore throat due to entrapment of the released colloids. The model formulation incorporates three mass balance equations for the processes of colloid release, transport of suspended colloids, and retention at the pore constrictions. In addition, an equation for the permeability reduction caused by colloids retained at the pore constrictions is incorporated. It should be mentioned that we do not assume any re-

deposition on the pore wall of the pore body as the conditions are not favourable for re-attachment following the release.

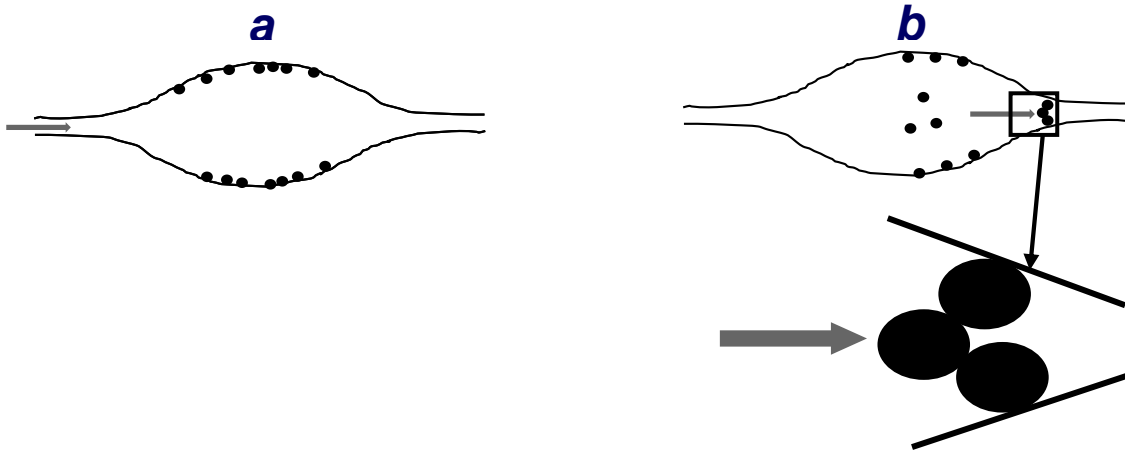


Figure 2.4. A conceptual illustration of pore body and throats in porous media. (a) shows that at equilibrium all the colloidal particles are attached to the pore surface. (b) shows that a fraction of the colloids are released and trapped at the pore constrictions following the release of colloids

2.3.1 Modelling the release process

A mass balance equation incorporating a first order kinetic release is used to describe the rate of colloid release from the grain surfaces into the aqueous phase:

$$\rho_b \frac{\partial S_1}{\partial t} = r_{rel} = -\kappa \rho_b \left(1 - \frac{IS}{IS_c}\right) (S_1 - (1 - f)S_i) \quad \text{for } IS < IS_c \quad (3.3)$$

$$\rho_b \frac{\partial S_1}{\partial t} = r_{rel} = 0 \quad \text{for } IS \geq IS_c$$

Where S_1 [Mc/Ms] is the colloid concentration on the sand surfaces, ρ_b [Ms L⁻³] is the sediment bulk density, IS [ML⁻³] is the ionic strength of the water, IS_c is the critical IS below which colloid release occurs, κ [T⁻¹] is the release rate constant, S_i [Mc/Ms] is the initial colloid concentration on sand surfaces. $f(-)$ denotes the fraction of colloid deposits on the grain surfaces that is released upon a chemical perturbation. It is noted that colloid release occurs only when the IS decreases below the critical IS. When the colloid release is induced by hydrodynamic forces where the flow velocity exceeds the critical flow velocity, the following equation is employed:

$$\rho_b \frac{\partial S_1}{\partial t} = r_{rel} = -\kappa \rho_b (S_1 - (1 - f)S_i) \quad \text{for } v > v_c \quad (3.4)$$

$$\rho_b \frac{\partial S_1}{\partial t} = r_{rel} = 0 \quad \text{for } v \leq v_c$$

Here, the v_c is the critical average pore water velocity above which the colloid release may occur. Typically, the release process can be simulated reasonable well using a single type release site incorporating a one-site kinetic equation. However, as it will be discussed later, a two-site first-order kinetic model, which consists of different release rate coefficients, was used to describe the release behaviour due to changes in the flow velocity. Two-site kinetic models have been previously used to model the colloid release process in natural sediments (Grolimund and Borkovec, 2006).

2.3.2 Transport of suspended clay

Colloids are transported in porous media with water flow as a result of advection, diffusion, and mechanical dispersion. Colloid transport is modelled based on the advection-dispersion equation, with terms for release from the matrix of the porous media and retention at the pore constriction (Bradford et al., 2013). Water flow is typically described using Darcy's equation. The following expression was employed for colloid transport in one dimension in the aqueous phase that includes the colloid release and retention at pore constrictions:

$$\frac{\partial C}{\partial t} = D \frac{\partial^2 C}{\partial x^2} - v \frac{\partial C}{\partial x} - \frac{r_{rel}}{n} - \frac{r_{ret}}{n} \quad (3.5)$$

Where x [L] is the distance in the direction of flow, and t [T] is the time, C [McL-3, where M is mass of colloids] is the colloid concentration in the aqueous phase, D [L²T⁻¹] is the hydrodynamic dispersion coefficient, v [LT⁻¹] is the average pore water velocity, n is the porosity] r_{rel} [ML⁻³T⁻¹] is the release rate from the pore wall, and r_{ret} [ML⁻³T⁻¹] is the retention rate at the pore constrictions. Note that it is assumed that the change in the porosity is small.

2.3.3 Clay retention at the pore constrictions

One possibility is that the retention of colloids at the pore constrictions occurs mainly due to hydrodynamic bridging or size exclusion. These retention processes results in closure of the pore constrictions causing permeability reduction, but does not considerably influence the porosity. First-order kinetic expressions are frequently used to account for the colloid retention. The solid-phase mass balance equation for colloids deposited at the pore constrictions is commonly given as

$$\rho_b \frac{\partial S_2}{\partial t} = -\lambda v C \left(1 - \frac{S_2}{S_{max2}}\right) \quad (3.6)$$

Where S_2 [McMs⁻¹] is the colloid concentration at the pore constriction. S_{max2} [McMs⁻¹] is the maximum concentration of retained colloids at the pore constrictions. Note that the initial value of S_2 is zero. λ [T⁻¹] is the retention coefficient which depends on various parameters such as size distribution of colloids and pore constrictions.

Equations 3.1 to 3.6 are solved simultaneously with the COMSOL software package to obtain $C(x,t)$ and $S_2(x,t)$. However, we need to know the release coefficient (κ) and its dependence on the system variables, the retention coefficients at the pore constrictions (λ) and its dependence on the system variables, such as the flow rate, etc.

2.3.4 Permeability reduction

If the released colloids are retained at the pore constrictions during their transport in the porous media, a decrease in the permeability occurs resulting in either lower flow rates when the inlet pressure is constant or higher pressure losses at a constant flow rate. The correlation between retained particles at the pore constrictions and associated permeability decline is imperative to describe the clogging process. We would take care to note that the extent to which these processes occur is highly sample dependent. For very clean coarse sandstones there are few colloids sized particles to mobilize and hence the effects of such colloid related processes may be negligible.

For deposition of colloids on the pore spaces causing a decrease in the porosity and subsequently a decrease in permeability, the Kozeny-Carman equation may be used to predict the permeability, k :

$$\kappa = \frac{d_m^2}{216} \frac{n^3}{(1-n)^2} \quad (3.7)$$

Where n is the effective porosity. In this model, the underlying assumption is when the colloids deposit in porous media, including pore bodies and throats, they reduce the porosity which causes

permeability reduction. However, when colloid entrapment at the pore constrictions is the primary process, the Kozeny-Carman equation is not successful in predicting the changes in permeability during colloid release and transport process as the porosity does not change a lot. One of the many empirical equations relating the permeability change during colloid release to the retained colloids at the pore constrictions is of the following form:

$$\frac{K}{K_0} = (1 - \alpha S_2)^b \quad (3.8)$$

where α and b are positive parameters. This equation is frequently expanded into a power series:

$$\frac{K}{K_0} = \frac{1}{\left(1 + n\alpha S_2 + \frac{n(n+1)}{2}\alpha^2 S_2^2 + \dots\right)} \quad (3.9)$$

By introducing β which is commonly referred to as formation damage (clogging) factor and when terms in S_2^2 and above are dropped, the permeability decreases linearly with the amount of colloid retained at the pore constrictions.

$$\frac{K}{K_0} = \frac{1}{1 + \beta S_2} \quad (3.10)$$

It should be mentioned that these equations contain adjustable parameters that must be determined for each specific experiment. Note that it is extremely difficult, if impossible, to measure the retained colloids over time at the pore constrictions.

The extent of clogging is dependent on the amount of deposited colloids at the pore constrictions. It is possible in the laboratory to measure the pressure drop across the core and determine the hydraulic conductivity using Darcy equation. Therefore, the amount of colloid retained at the pore constriction can be estimated by knowing the relationship between the hydraulic conductivity and the concentration of the entrapped colloids. There is no widely accepted correlation between the permeability and the amount of entrapped colloids in the pore constrictions (Fogler and Khielar, 1998).

The governing equations for the conservative tracer, colloid transport, release, retention, and permeability changes were implemented and solved using COMSOL Multiphysics software (COMSOL, Inc., Palo Alto, CA 94301). For the simulation discussed below, a zero flux boundary condition was used at the inlet, and a concentration gradient of zero was specified at the outlet. An initial condition of no suspended colloids in solution and a fixed uniform concentration of initially deposited colloids in the simulation domain were used. The Levenberg-Marquardt algorithm in the Optimization Module of COMSOL was employed to estimate the values of model parameters by fitting the measured colloid concentrations in the outlet of the core and average core permeability to the solution of the governing equations.

Values of porosity and dispersivity were estimated by fitting the tracer (NO_3^-) breakthrough concentrations to the solution of Eq. [3.6]. The value for dispersivity was found to be very low (~ 0.01 cm), confirming that the core was rather homogeneous. Note that the effect of clogging on the possible changes of dispersivity was not considered in this study.

The average pore water velocity (v) was calculated from the porosity and direct measurements of the flow rate. The initial value of S_{i1} of each core sample was estimated based on the XRD analysis of the clay content (see Table 2.4), whereas the initial value of S_{i2} was set to zero. Values of S_{i1} and S_{i2} for each subsequent release step (B1-B5) was obtained directly from the model output.

A critical parameter in modelling colloid release was to determine the fraction of colloid release as a result of temporal changes in solution IS and flow velocity. Experimental information on the initial clay content and mass balance of the effluent colloid concentration during each release step was used to constrain the optimization of f_{nr1} . This approach assumes that the amount of retained colloids at pore constrictions was much less than that of in the effluent.

The values of other parameters such as κ_1 , λ , β , S_{max2} , and κ_2 were determined by fitting the solution of Eqs. [2]-[5] to colloid release curves and permeability data. However, not all of these parameters were fitted during each release step. For example, only κ_1 , f_{nr1} , λ and S_{max2} were determined during Step A when colloid release was induced by lowering IS to that of RO water. It should be mentioned that potential effect of gravity force on the kinetics of colloid release and retention was not considered in the present study. This effect has recently been shown to be significant for colloid transport under different velocities and ionic strengths, especially for the larger and denser particles (Chrysikopoulos and Syngouna, 2014).

2.4 Results

2.4.1 Clogging potential of Precipice sandstone

In the first series of experiments, the clogging potential of the Precipice sandstone due to clay dispersion was evaluated by injecting RO-water into a core sample saturated with a 0.5 M NaCl solution. The core was placed in the core holder and the 0.5 M NaCl solution was flown through the core with a flow velocity of 5 m/day during which the initial hydraulic conductivity was determined. Note that negligible colloid release and permeability reduction were observed during this phase of the experiments. After a few pore volumes of injecting 0.5 M NaCl solution, the influent water was switched to RO water.

Figure 2.5 shows the typical results of four core samples from BSF illustrating that a step decrease in the salt concentration resulted in the release of in situ clay particles of the core. The released clay particles were transported through the porous media and appeared in the core effluent after about one pore volume. After one pore volume, the colloid concentration sharply increased and reached its maximum at approximately 2.5 pore volumes followed by a gradual decrease with time. It took more than 15 pore volumes until the colloid concentration dropped to 10% of the peak concentration.

Colloid release is expected to occur with a decrease in solution ionic strength due to the expansion of electrostatic double layer and an associated increase in the repulsive forces (Khilar and Fogler, 1998). It should be noted that in spite of a substantial colloid release, the pressure loss across the core plug did not increase during the course of the experiments. This implies that a very small (if any) colloid retention occurred at the pore constrictions upon the release of clay particles resulting in no reduction in the core hydraulic conductivity.

The initial hydraulic conductivity of these core samples from BSF formation in the presence of 0.5 M NaCl was about 2.3 m/d, indicating the core contains large pore sizes and relatively small amount of clay. Indeed, it was found that the total amount of clay release in each test was different which suggests that each core contained various amount of releasable clay. The concentration of clay and the pore size distribution of the porous media are expected to play an important role in colloid capture at pore constrictions.

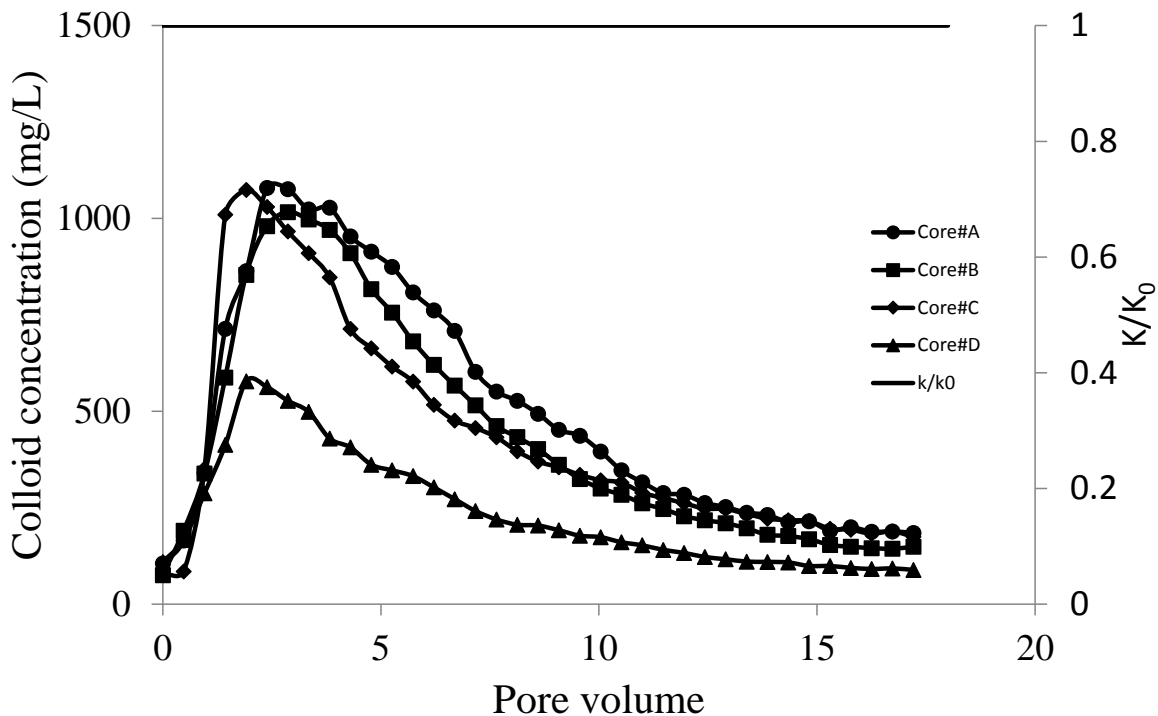


Figure 2.5. Observed breakthrough concentrations of colloids with changes of salt concentration. The core samples were initially preconditioned with 0.5M NaCl, then the IS of influent water was decreased to that of RO water at time zero. Note that one pore volume (PV) corresponds to ~20 mL

Figure 2.6 shows the measured (symbols) and simulated (solid lines) colloid release (effluent concentrations) and overall permeability reduction versus pore volumes for two representative core samples from the Precipice aquifer. In these experiments we specifically examined the effect of colloid release on the mean permeability of the core whose contained relatively larger amount of clay and smaller initial permeability compared with those of BSF cores (see Appendix A).

It is observed that considerable colloid release and permeability loss occurred when the water salinity decreased to that of RO-water. In general, the colloid release processes discussed earlier for the core samples from BSF are applicable and valid for these core samples, but a greater amount of colloids was released from these cores compared with those of BSF. The mean permeability (K) of the core was calculated based on the pressure head losses across the core plug.

Figure 2.6 shows the normalized permeability, which is the ratio of the average K of the core to that of the initial K during the injection of the 0.5 M NaCl solution, as a function of the number of pore volumes of water passed through the core. Note that prior to the injection of RO-water during which the core was equilibrated with the 0.5 m NaCl, the mean value of permeability was about 0.35 and 0.55 m/d for core plug E and F, respectively. It is observed that decreasing the solution ionic strength to that of RO-water led to a decline in the core permeability. Permeability declined in exponential fashion during the first few pore volumes and levelled off with further injection of RO-water. Note that similar to the core samples from BSF, the effluent colloid breakthrough pattern exhibited an exponential release process. One also observes that the change in the permeability occurred immediately after one pore volume following the corresponding change in the input solution. Much of the clogging occurred during the high effluent colloid concentration suggesting that the clogging process was due to colloid release and subsequent entrapment of a fraction of the released colloids at pore constrictions.

Comparing these observations with those of BSF cores suggests that the clogging potential depends on the amount of colloid release and the initial permeability of the core which is related to the distribution of the pore sizes. A series of core-flooding experiments with selected core samples from the Precipice aquifer showed reductions in hydraulic conductivity ranged from 50% to over 90% when RO-water was injected into the core, displacing the 0.5 M NaCl solution. It should be noted that these experiments were conducted using 5 cm core samples. It is logical to expect that the concentration of released clay would also depend on the length of the core sample. Therefore, clay release may have resulted in clogging if the length of core sample was larger than what was used in these experiments.

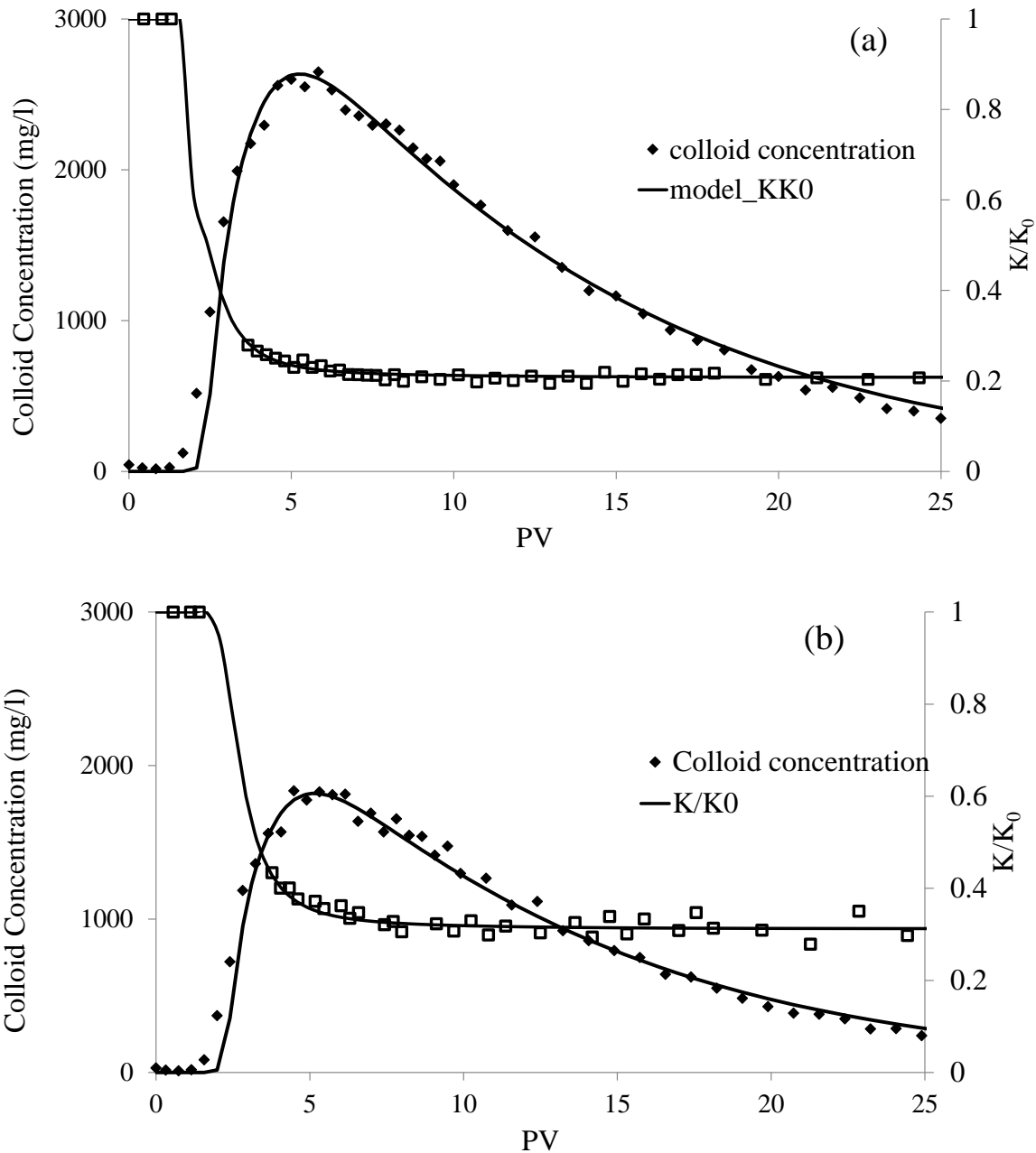


Figure 2.6. Experimental data (symbols) and model calculations (solid lines) of colloid release and permeability loss (K/K_0) upon RO water injection into core sample E (a) and F (b) from Precipice sandstone

In order to verify that the deterioration of the hydraulic conductivity of the aquifer materials was a result of clay dispersion and not in situ clay swelling, the flow direction was reversed following the completion of the core-flooding tests with cores from Precipice sandstones. After a few pore volumes of RO water injection into the core in the reversal mode, the flow direction was again switched back to the original direction and RO water was flown into the core for a number of pore volumes. It was observed that flow reversal process restored the hydraulic conductivity of the core by a factor of about 40%. These observations demonstrated that the observed clogging during the first phase of the experiment was due to clay release, transport, and subsequent entrapment in pore constrictions of the sandstone. Furthermore, these findings indicate that when flow is switched from a high salinity condition to a fresh water, clay particles may be released from the grain surfaces. The released particles then migrate in the direction of the flow and may become trapped at pore constrictions causing pore blockage and permeability loss. Results suggest that there exists a significant risk of clogging in case of injection of a source water whose solution chemistry is not compatible with the aquifer sandstone. Therefore, controlling the clogging process is essential to economical and effective operation of well injection.

It should be mentioned that the colloid size distribution of the effluent samples from previous experiments was analysed and the results showed that the average hydrodynamic radii of the colloids was about 1-5 μm and remained constant within experimental errors during the course of experiment. We therefore conclude that properties of the released colloids were almost constant in spite of the fact that their supply was finite in each core sample. The clay fraction was analysed by SEM_EDAX and the result revealed that the majority of the particles was Kaolinite and quartz (Figure 2.7).

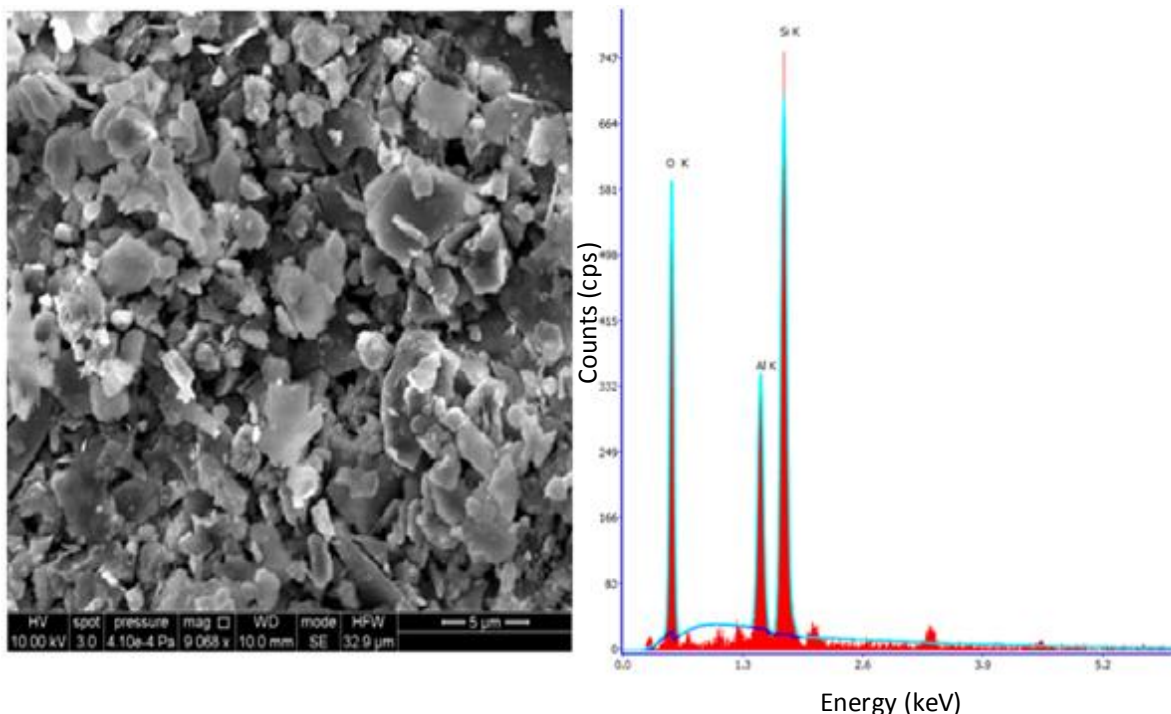


Figure 2.7. Typical SEM Micrograph and EDX spectrum of the released colloids from BSF core samples showing the majority of the released colloids was Kaolinite

2.4.2 Simulations

Figure 2.6 also shows the simulated colloid release and permeability changes for the two core samples from the Precipice sandstone. The fitted model parameters for each experiment are given in Table 2.4, along with the coefficient of linear regression (R^2). It is observed that the processes of colloid release and clogging induced by a transient in solution chemistry was satisfactorily modelled using a set of first-order kinetic equations (Eqs. [3.2]-[3.6]) by accounting for the releasable fraction of colloid mass on the grain surfaces. The value of S_{i1} reflects that initial amount of clay in the core and was therefore set equal to 50 g/kg consistent with XRD analysis. Consistent with mass balance information, only a very small fraction of the in situ colloids were released by reducing the IS to that of RO water (see the values of $(1 - f_{nr1})$ in Table 2.44). The value of κ_1 was low, ranging from 0.0004 to 0.0005 sec⁻¹, and is related to the mass transfer kinetics of the deposited clay particles from the collector surfaces. Hydrodynamic bridging in the model was accounted for using values of λ that ranged from 0.002-0.009, and a constant value of $\beta=2.5$. In agreement with other reported studies (e.g. Khilar and Fogler, 1984; Kia et al., 1998), we found in another set of experiments (to be shown later in the report) that there is a critical salt concentration below which colloid release begins in cores from these core materials. It is noted that the linear relationship given in Eq. [3.8] was adequate to describe the dependency of colloid release on the solution IS. As mentioned above, the value of S_{i1} was large and reflects the initial amount of clay in the core. Values of S_{max2} were optimized to determine the maximum amount of clay in the pore constrictions and ranged from 0.6 to 2 g/kg. The peak value of the BTCs was mainly controlled by the values of κ_2 and f_{nr2} .

Table 2.4. Summary of the values of the parameters of the best fit for modelling of the core samples a and b from the Precipice sandstone

Flow velocity (m/d)	$\kappa_1(\text{sec}^{-1})$	$1 - f_{nr1}$	$\lambda(\text{sec}^{-1})$	β	R^2 (%)
Core sample E: S_{i1} (g/kg)=50, S_{max2} (g/kg)=2					
5	0.0005	0.17	0.009	2.5	94
Core sample F: S_{i1} (g/kg)=50, S_{max2} (g/kg)=0.6					
5	0.0004	0.15	0.0021	2.5	96

2.4.3 Critical Salt Concentration (CSC) in a single salt system

Based on the previous experiments showing water sensitivity of Precipice sandstones, we conducted a series of experiments to determine the critical salt concentration (CSC), below which clay release may occur in Precipice sandstone. A series of experiments, employing core samples from Precipice sandstone at Reedy Creek and Condabri, was conducted in which the NaCl concentration of the injection water was decreased in stepwise manner and the effluent breakthrough concentrations of colloids and pressure difference were measured. It should be mentioned that the average pore water velocity was maintained at 5 m/day in these experiments. Figure 2.8 shows representative results of two core samples. The dashed vertical line in the figure indicates the pore volume at which the abrupt decrease in salinity concentration occurred. For example, after passing 10 pore volumes of 0.5 M NaCl through the core, the flow was switched to 0.3 M NaCl solution. We observed that there was negligible colloid release for a series of step decreases from 0.5 to 0.03 M NaCl. Only when the salt concentration was reduced to 0.02 M, the

clay release occurred resulting in an increase in the effluent turbidity. The samples collected from the effluent were analysed and it was found that the colloidal particles were virtually all kaolinite with some traces of silica and illite, as revealed by scanning electron microscope (SEM) analysis. Table 2.5 summaries the results of various core samples used in this series of experiments. It is observed that the CSC varies between 15 and 20 mM.

Colloid mass balance information for each step decrease in solution IS revealed that only a small fraction of the colloid deposit on grain surfaces was released upon each decrease in ionic strength. This fraction tended to exhaust over the course of the experimental phase associated with a specific IS. This behaviour can be attributed to alteration of the torque and force balances acting on colloids on grain surfaces upon each step decrease in IS. Colloid release is expected to increase with a decrease in IS due to an increase in the repulsive electrostatic force and the associated decrease in the resisting adhesive torque which can be overcome by the applied hydrodynamic torque (Torkzaban et al., 2007). It is evident that with further decrease of IS below the critical salt concentration, a fraction of the deposited colloids on sand grains were released. This can be attributed to the spatial variations in adhesive and hydrodynamic forces due to chemical heterogeneity and roughness, the location of deposited colloids on sand grains, and differences in the strength of adhesive interactions for deposited colloids.

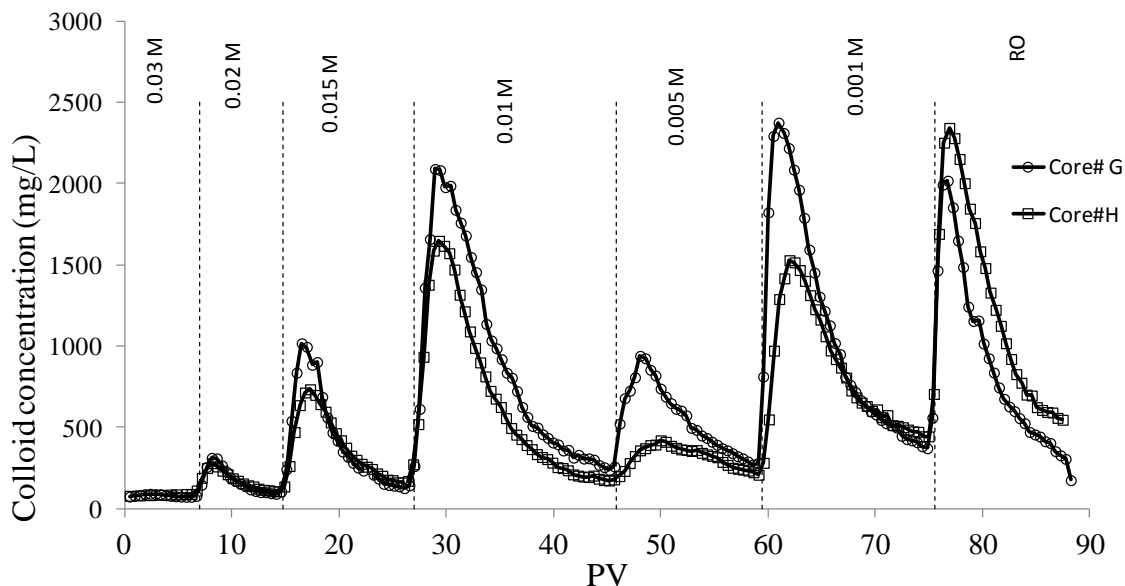


Figure 2.8. Representative plots of the effluent colloid concentration for two core samples from BSF as a function of pore volumes (PV) for transient ionic strength (IS) experiments. The sequence of the transient experiments was as follows: Preconditioning of the core with 0.5M NaCl solution and then influent solution IS was lowered in several steps indicated in the figure. Note that no noticeable permeability change was observed for these cores during the entire experiment.

It should be noted that we did not observe any noticeable decrease of the hydraulic conductivity for these core samples. This is expected to be due to the large pore sizes of BSF core samples and the fact that the core plugs were small (5 cm); resulting in a small amount and concentration of clay release which was not sufficient to plug the pore constrictions. Consequently, it is concluded that the clay particles present in the sandstone are not released until the salt concentration of the water in contact with the sandstone drops below a certain salt concentration. This salt concentration has been defined as the "critical salt concentration" (CSC). The CSC for NaCl solution at an average flow velocity of 5 m/day was determined to be between 15 and 20 mM (Table 2.55).

The CSC is a useful parameter in injection well processes since it should be attempted to avoid injection of water with a salt concentration below the CSC into the aquifer. To examine the effect of various physical and chemical factors on the CSC, additional series of experiments were undertaken to examine the effects of parameters such as the flow velocity (i.e. injection flow rate), ion type (e.g. CaCl₂), and pH on the CSC.

Table 2.5. Values of CSC for various core samples initially in equilibrium with 0.5 M NaCl. The average pore water velocity was maintained 5 m/day during the course of experiment

Plug ID	CSC (mM)	Initial K (m/day)	Final K (m/day)
RC_64_3	20	0.05	0.006
RC_64_4	20	0.13	0.01
RC_67_3	15	0.11	0.01
RC_67_4	20	0.06	0.007
RC_76_3 (G)	20	2.3	2.1
RC_76_4 (H)	20	2.1	2.1
C_69_3	15	0.14	0.01
C_69_4	20	0.07	0.005
C_71_3	15	0.17	0.01
C_71_4	20	0.09	0.004
C_74_3	20	0.08	0.005
C_74_4	20	0.12	0.01

2.4.4 Effect of flow velocity on the CSC

The effects of flow velocity on the CSC of sodium chloride solution were investigated over a range of velocity of 5 to 30 m/day. The highest velocity, 30 m/day corresponds to a high flow velocity realized in the vicinity of the injection well. It was found that the CSC is dependent on water velocity. Figure 2.9 shows the colloid release behaviour of two core samples from BSF formation as the salinity decreased sequentially at constant velocity of 10 and 30 m/day, respectively.

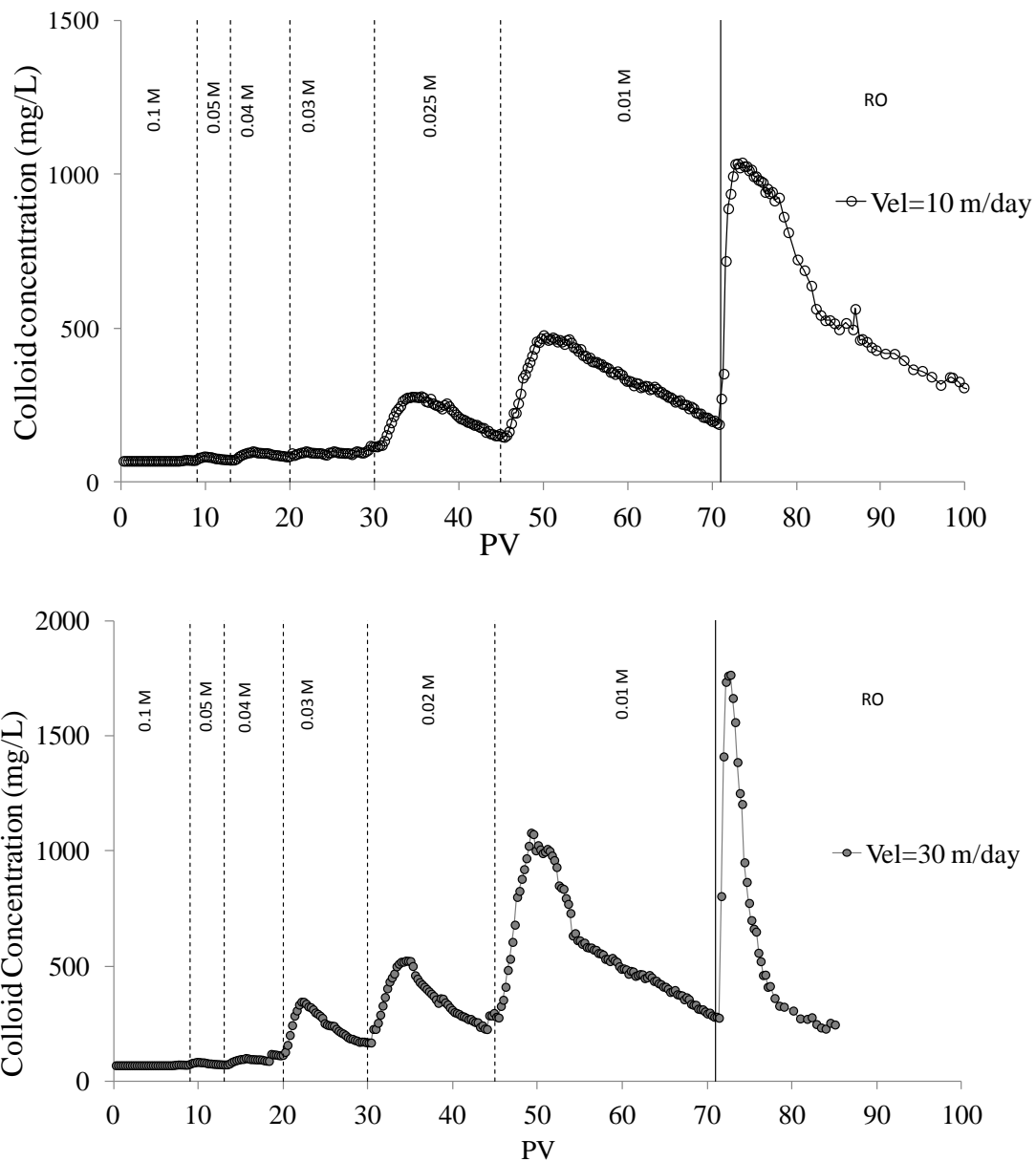


Figure 2.9. Representative plots of the effluent colloid concentration for two core samples from BSF as a function of pore volumes (PV) when the IS decreased in stepwise manner for two different flow velocity

Table 2.66 summarizes the values of CSC measured for various core samples at two different flow velocities. Colloid release is expected to increase with an increase in v due to an increase in the hydrodynamic shear force and the associated increase in the applied hydrodynamic torque which can overcome the resisting adhesive torque (Torkzaban et al., 2015). It is evident that the critical salt concentration is increased with increasing the flow velocity. This can be attributed to the fact that the drag force acting on a colloidal particle attached to the pore surface is proportional to the fluid velocity and the particle size. Therefore, it is expected that the CSC is dependent on the flow velocity. The detached particles induced by the hydrodynamic forces are transported down gradient with the fluid which may block narrow pore throats.

Table 2.6. Values of CSC for various core samples initially in equilibrium with 0.5 M NaCl. The average pore water velocity was maintained at 5 m/day during the course of experiment

Plug ID	Water velocity (m/day)	CSC (mM)	Initial K (m/day)	Final K (m/day)
RC_64_5	10	25	0.09	0.005
RC_64_6	30	30	0.11	0.01
RC_67_5	10	20	0.14	0.01
RC_67_6	30	25	0.1	0.007
RC_76_5	10	20	2.1	2.0
RC_76_6	30	25	2.4	2.2
C_69_5	10	20	0.13	0.01
C_69_6	30	30	0.09	0.008
C_71_5	10	20	0.16	0.02
C_71_6	30	30	0.13	0.01
C_74_5	10	20	0.11	0.01
C_74_6	30	25	0.15	0.01

2.4.5 CSC for a divalent cation solution

The critical salt concentration (CSC) of a solution with divalent cation (e.g. CaCl_2) was examined by stepwise decrease of the CaCl_2 concentration at an average pore water velocity of 5 m/day. The dashed vertical line in the Figure 2.10 indicates the pore volume at which the Ca^{2+} concentration decreased. The experiments were started with 0.1 M CaCl_2 and after a number of pore volumes the Ca^{2+} concentration was sequentially decreased. It was found that the valency of a cation have a significant effect on the CSC. In fact, we observed a negligible clogging for some of the core samples when calcium concentration decreased to zero. However, a gradual decrease in hydraulic conductivity was observed for some of core samples with a fine texture and initial lower permeability (Precipice cores) when the calcium concentration decreased to zero. The CSC for CaCl_2 solution at an average flow velocity of 5 m/day was determined to be less than 0.01 mM. Notice that the CSC for NaCl solution at the same flow velocity was found to be 20 mM. Table 2.7 summarizes the values of CSC measured for various core samples.

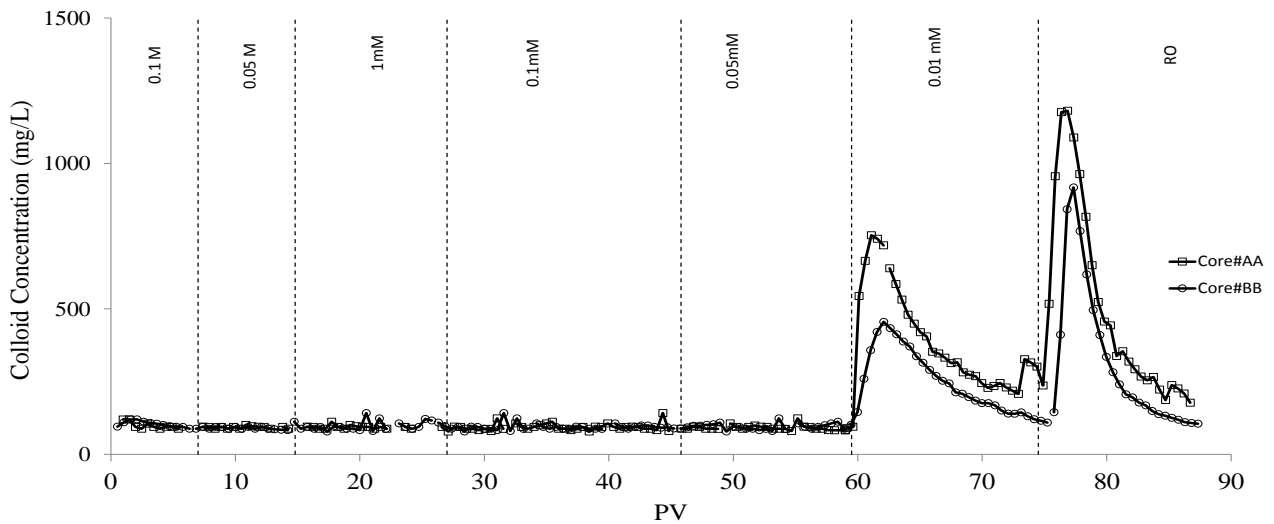


Figure 2.10. Representative plots of the effluent colloid concentration for two core samples from BSF as a function of pore volumes (PV) when the concentration of Ca^{2+} decreased in stepwise manner. The sequence of the transient experiments was as follows: Preconditioning of the core with 0.1M CaCl_2 solution and then influent solution IS was lowered in several steps.

Table 2.7. Values of CSC for various core samples initially in equilibrium with 0.1 M CaCl_2 . The average pore water velocity was maintained at 5 m/day during the course of experiment

Plug ID	CSC (mM)	Initial K (m/day)	Final K (m/day)
RC_64_7	0.01	0.1	0.08
RC_64_8	NE*	0.12	0.11
RC_67_7	NE	0.15	0.14
RC_67_8	0.01	0.11	0.1
RC_76_7 (AA)	0.01	2.4	2.3
RC_76_8 (BB)	0.01	2.2	2.2
C_69_7	NE	0.14	0.14
C_69_8	0.01	0.08	0.06
C_71_7	NE	0.14	0.14
C_71_8	NE	0.12	0.12
C_74_7	0.01	0.09	0.08
C_74_8	0.01	0.13	0.11

*NE indicates that no CSC existed for the core sample

In order to verify that the core samples employed in this series of experiments were water sensitive, select core samples was re-saturated and flushed with 0.5 M NaCl solution for about 10 pore volumes upon the completion of the test with CaCl_2 , followed by RO water injection. We observed that within 3 pore volumes of RO water injection the mean permeability of the core decreased by about 85%, indicating a significant clogging potential due to clay release and capture in the pore constrictions. These results indicate that when the exchangeable calcium cations were replaced by sodium cations, the core became water sensitive. In another test in which the core was

flushed with 0.05 M instead of 0.5 M NaCl, the reduction in hydraulic conductivity was not so severe when RO water was injected into the core. This suggests that the cation exchange did not occur completely when the concentration of monovalent cations in the aqueous phase was low. This is consistent with previous literature suggesting that the calcium ion is held more strongly on the mineral surfaces than the sodium ion (Sposito, 2001).

2.4.6 The Critical Ionic Strength (CIS) in a mixed solution

Additional core-flooding tests were undertaken to determine the critical solution IS in a mixed system. Note that the ionic strength at which the pressure drop across the core begins to increase and/or the clay particles appear in the effluent is referred to as the critical IS. In these experiment, selected Precipice sandstone cores was vacuum saturated with a solution of mixed NaCl/CaCl₂ and at a given mole percent of calcium (see Table 2.88 and Table 2.99).

Table 2.8. Summary of the values of the CIS for several core samples from Reedy Creek at various IS and calcium percentages

Plug ID	Ionic strength (mM)	% Ca	Critical IS (mM)	Initial K (m/day)	Final K (m/day)
RC_64_9		0	15	0.13	0.02
RC_64_10		5	10	0.13	0.06
RC_64_11		10	5	0.11	0.1
RC_64_12	20	15	0.1	0.14	0.1
RC_64_13		20	NE*	0.09	0.05
RC_67_9		0	15	0.15	0.02
RC_67_10		5	5	0.11	0.05
RC_67_11	15	10	1	0.18	0.15
RC_67_12		15	0.1	0.19	0.16
RC_67_13		20	NE	0.08	0.08
RC_76_9		0	10	2.1	2.1
RC_76_10		5	1	2.2	2.2
RC_76_11	10	10	0.1	2.3	2.3
RC_76_12		15	0.01	2.1	2.1
RC_76_13		20	NE	2.4	2.4
RC_64_14		0	5	0.19	0.04
RC_64_15		5	0.1	0.12	0.08
RC_67_14	5	10	NE	0.15	0.14
RC_67_15		15	NE	0.13	0.12
RC_76_14		20	NE	2.4	2.4

*NE indicates that no CSC existed for the core sample

The saturated sandstone core was placed in the core-holder and the mixed NaCl/CaCl₂ solution was injected into the core at an average water velocity of 5 m/day. The IS of the injectant was decreased in a stepwise fashion while the Calcium percentage was kept constant, the IS was first decreased by large steps and then it was decreased in small steps to accurately determine the CIS.

It was observed that no permeability decline and clay release occurred until the IS was higher than the CIS value. Table 2.88 and Table 2.99 summarize the values of CIS measured at various calcium percentages. As the concentration of Ca ions was increased at a given IS, the extent of permeability reduction of the sandstone during water flow was decreased. For example, pre-treatment of a core with a solution having with 20% calcium caused a negligible permeability decrease, compared with a drop of more than 50% for a core equilibrated with a solution having 5% calcium. It is observed that CIS decreases as the calcium percentage increases. Indeed, it appeared that there was no CIS when the calcium percentage was above 20% as we did not observe any clogging or clay release when the influent was switched to RO water. As discussed later, this reduction seems to be a result of incomplete ion exchange of sodium ions for calcium ions.

Table 2.9. Summary of the values of the CIS for several core samples from Condabri at various IS and calcium percentages

Plug ID	Ionic strength (mM)	% Ca	Critical IS (mM)	Initial K (m/day)	Final K (m/day)
C_69_9		0	20	0.12	0.03
C_69_10		5	15	0.2	0.1
C_69_11		10	5	0.14	0.12
C_69_12	20	15	0.5	0.06	0.05
C_69_13		20	NE*	0.13	0.12
C_71_9		0	10	0.13	0.03
C_71_10		5	5	0.17	0.1
C_71_11	15	10	0.5	0.11	0.09
C_71_12		15	0.2	0.15	0.14
C_71_13		20	NE	0.21	0.2
C_74_9		0	10	0.18	0.05
C_74_10		5	2	0.12	0.08
C_74_11	10	10	0.2	0.09	0.05
C_74_12		15	0.02	0.12	0.11
C_74_13		20	NE	0.31	0.26
C_69_14		0	5	0.13	0.05
C_69_15		5	0.2	0.17	0.12
C_71_14	5	10	NE	0.16	0.15
C_71_15		15	NE	0.05	0.05
C_74_14		20	NE	0.18	0.18

*NE indicates that no CSC existed for the core sample

The experimental results can be explained through a qualitative analysis, by comparing the zeta potentials of clay particles and the consequent variations in the double layer interactions. As briefly mentioned earlier, clay particles are typically negatively charged because of substitution of lower-valence cations in the clay lattice structure (e.g., Al^{3+} for Si^{4+} and Mg^{2+} for Al^{3+}). In aqueous phase (e.g. groundwater) in order to maintain electrical neutrality, the negative charge of

the clay lattice is balanced by positive cations located on and near the clay surface. The spatial distribution of cations is determined by the charge density on the negative clay surfaces and cation concentration in the bulk aqueous phase. The concentration distribution of cations around the clay particle is often referred to as the diffuse double layer. In water with a low ionic strength (salt concentration), diffusion forces are large and the double layer is thick. When the repulsion between double layers of two clay particles exceeds van der Waals attractive force, the particles disperse or detach from each other. Increasing ionic strength will cause the double layer thickness to contract. Critical salinity is the cation concentration above which the double layer thickness is sufficiently thin that van der Waals attractive forces cause clay particles to attach to each other or to pore walls.

Moreover, the zeta potential values of kaolinite exhibited to strongly depend on the extent of surface coverage of Ca^{2+} ions. Previous studies have shown that calcium surface coverage depends on the ion exchange equilibria between the colloids and the ionic condition (Bolt, 1955; Wilemsky, 1982). The ionic condition of the electrolyte can be described by two parameters: the calcium percentage and the total ionic strength. The reduction in zeta potential with increasing calcium percentage causes the double layer repulsive potential to decrease and therefore the probability of clay release will be small. Therefore, the total ionic strength must be reduced to increase the diffuse double layer and increase the probability of release. Consequently, increasing the calcium percentage lowers the CTIS.

The strength of different cations in preventing clay release varies with their valence. Within a given valence, the strength decreases with increasing hydrated ionic radii. Therefore, binding strength has been shown to decrease in the order $\text{Cs}^+ > \text{Rb}^+ > \text{NH}_4^+ > \text{K}^+ > \text{Na}^+ > \text{Li}^+$ for monovalent cations and $\text{Ba}^{2+} > \text{Sr}^{2+} > \text{Ca}^{2+} > \text{Mg}^{2+}$ for divalent cations (Sposito, 2001). Table 2.8 and Table 2.9 show that divalent cations like Ca^{2+} are 50 to 100 times more effective in stabilising clays than monovalent cations, and increasing Ca^{2+} concentration sharply reduces the clay release.

2.4.7 Effect of pH

Figure 2.11 shows the result of a typical experiment in which the pH of injection water into the core samples increased in several steps. In these experiments, the equilibrated core same with 0.5 M NaCl was first flushed with 30 mM NaCl solution at pH 5.8 for several pore volumes. Then the solution salinity was maintained constant, while the pH was increased in stepwise fashion. The pH of the solutions was adjusted with careful addition of 0.1M NaOH and HCl.

It was observed that a step increase in pH to 8, 9, and 10 reduced the core permeability gradually. Permeability reduction was coincided with a rise in clay concentration in the core effluent. After several pore volumes (e.g. 5 PV) under high pH conditions the core permeability stabilised at a lower steady state.

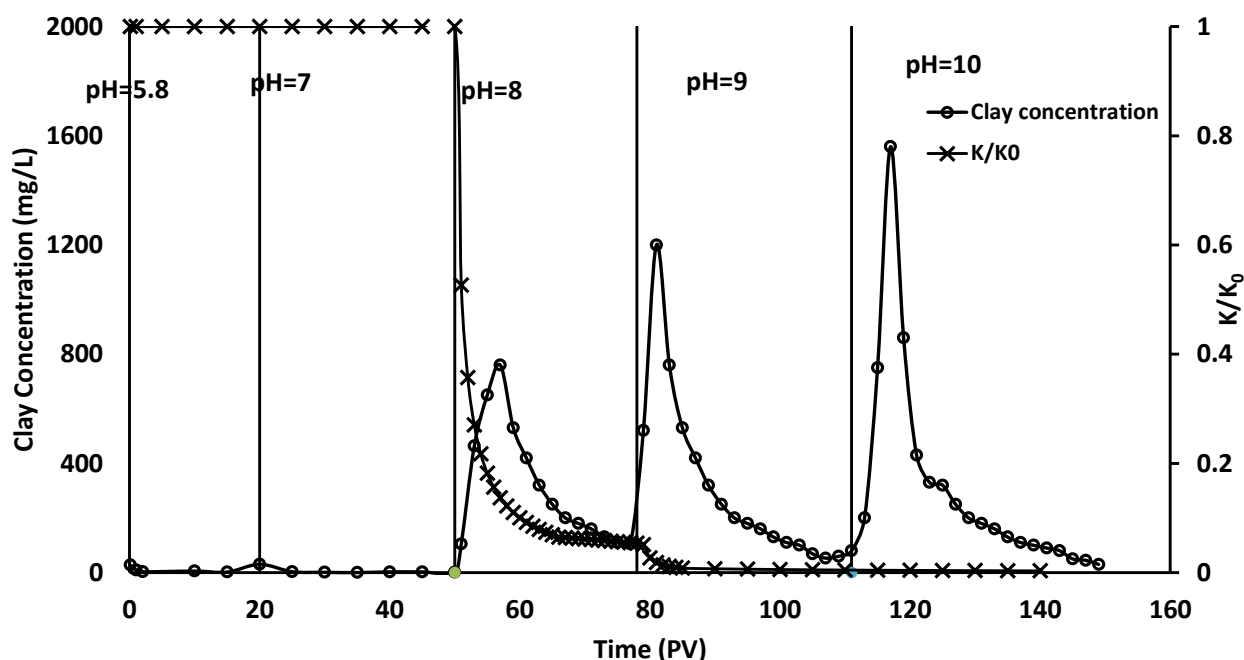


Figure 2.11. Representative plots of the effluent colloid concentration and relative permeability for a core sample from Reedy Creek (RC_64_15) as a function of pore volumes (PV) when the pH of the 30 mM Na⁺ solution increased in stepwise manner

2.4.8 Effect of flow reversal

In a series of experiments, the flow direction was changed following occurrence of clogging in the core sample due to clay release. In these experiments, the flow of the same original electrolyte solution was continued in the reverse direction in an attempt to examine the effect of backwashing on the clogging phenomenon. We observed that the core permeability was recovered to some extent (~20%) when the flow direction was reversed. However, the final permeability was always lower than the initial permeability. The interpretation which may be put forward here is that in the reverse flow mode some of the clay particles captured at the pore constrictions during the previous phase was mobilised resulting in a sudden permeability improvement.

2.5 Discussion

2.5.1 Clogging Mechanisms

Prior to injecting any freshwater into an aquifer, consideration should be given to the possibility of chemical reactions which might interfere with the injection process. For example, if freshwater is saturated with dissolved oxygen and the ambient groundwater contains none high concentrations of iron and manganese, precipitation of iron or manganese hydroxides may occur within the aquifer when the freshwater is injected, resulting in loss of hydraulic conductivity of the aquifer. However, chemical analysis of the native groundwater indicated that the iron and manganese concentration in the Precipice aquifer is too small (less than 0.1 mg/L) to account for significant loss in hydraulic conductivity because of precipitation. Another possible chemical reaction could be precipitation of calcium carbonate. However, chemical analysis indicated that the concentration of calcium in both the injection water and groundwater was below equilibrium (saturation) values, and no precipitation would occur when the two waters are mixed.

After examining the data, it was concluded that when injection occurs, the major chemical effect would be simple dilution; in which case, three chemical zones are formed around the injection well. These include, in order of decreasing distance from the well: (1) Undiluted groundwater; (2) mixed groundwater and freshwater; and (3) freshwater. In this study we have shown that the permeability of a near-well formation can be permanently reduced if the water and aquifer materials are incompatible. It was shown that water-clay interactions can result in clogging both near the injection wells but also deeper in the aquifer. The latter process will be evidenced by a gradual loss in the injectivity, and is very difficult to remediate. The compatibility of injection water and aquifer clays was shown to be significant during water re-injection operation. Indeed, these findings are in agreement with the field observations of injection trails during which no noticeable clogging due to clay release was observed when the salinity of injected water was maintained above 95% of the salinity of native groundwater and pH within 0.5 unit of the native groundwater.

There are, in principle, three mechanisms of clay related clogging as below:

- a) The effect of swelling clay in reducing the pore space.
- b) The mobilisation of clay and quartz particles resulting in clogging of the pore constrictions.
- c) A combination of clay swelling and mobilisation.

Clay particles are found intermixed with quartz and other colloidal particles in the pore spaces of aquifer porous structure. The forces keeping these particles to the pore surfaces and to each other in their aggregated form depend on physical and electrostatic interactions. The experimental work presented in the previous chapters shows that several factors may alter the equilibrium conditions and result in clay release and transport. For example, the region around a injecting well is susceptible to clogging by clay mobilisation and pore-blocking through the action of the high water velocities. High velocities may cause formation of low permeability cake-type deposits. In experiments in this project, water velocities ranging from 5-100 m/day were unable to detach clay particles when the water salinity was high. However, when the water salinity was in the range of critical release salinity, water velocity played a role in the mobilisation of clay particles and subsequent clogging of the core samples. In this condition any change in the hydrodynamic conditions in the aquifer is likely to affect the equilibrium state.

Clogging can also occur due to clay swelling as opposed to clay mobilisation effects. However there are distinctive differences in the way in which permeability reductions occur in each mechanism. In the case of clay swelling, permeability declines when the water salinity is reduced below a critical value. An indirect consequence of the swelling process is that clay particles may become mobilised. This would result in a combined swelling-mobilisation clogging. Swelling clay was not found to be present in the examined sandstones. Here, all core samples used in the experiments contained very small amounts of the swelling clays. Clogging caused by clay release, transport and retention in the pore constrictions occurred initially at fast rate and then stabilised. In core-flooding tests, a reversal of flow direction results in a temporary but small increase in permeability.

2.5.2 Salinity Effect

Rapid clogging was observed when RO water displaced high concentration of monovalent solutions in core-flooding experiments. The permeability loss was coincident with the release of large amount of clay particles from sand grain surfaces. Analysis showed that more than 90% of the clay mineral was kaolinite. Typical permeability reduction exhibited two distinct behaviours of an immediate permeability loss followed by a period of slow reduction toward stabilisation. The final permeability was less than 70% of initial. It was evident that colloids advancing through the

core in a high concentration had a marked effect on permeability. The more permanent reduction occurred in large core samples due to the recapture of clay within the core. These clay particles plugged the pore constrictions causing a decrease in the available cross-sectional area for flow. This reflected in the permanent permeability loss. Permeability reduction effects were minimised in experiments where water salinity was reduced in several steps as opposed to one step salinity reduction. It was observed that when the concentration of Na^+ in the formation water was low (e.g. 20 mM), the permeability loss was much less severe than those experiments in which the core was equilibrated with 0.5 M NaCl solution. When the core samples were in equilibrium with high concentration of Ca^{2+} , decreasing water salinity resulted in little permeability reduction and clay release.

Clay particles are typically negatively charged because of substitution of lower-valence cations in the clay lattice structure (e.g., Al^{3+} for Si^{4+} and Mg^{2+} for Al^{3+}). In aqueous phase (e.g. groundwater) in order to maintain electrical neutrality, the negative charge of the clay lattice is balanced by positive cations located on and near the clay surface. The spatial distribution of cations is determined by the charge density on the negative clay surfaces and cation concentration in the bulk aqueous phase. The concentration distribution of cations around the clay particle is often referred to as the diffuse double layer. In water with a low ionic strength (salt concentration), diffusion forces are large and the double layer is thick. When the repulsion between double layers of two clay particles exceeds van der Waals attractive force, the particles disperse or detach from each other. Increasing ionic strength will cause the double layer thickness to contract. Critical salinity is the cation concentration above which the double layer thickness is sufficiently thin that van der Waals attractive forces cause clay particles to attach to each other or to pore walls.

The results of experiments in which salinity was decreased in stepwise fashion indicated that there existed a critical level of salinity of about 20 mM NaCl at neutral pH conditions for the tested sandstone cores. We observed that when the core was flushed with a high sodium concentration at the start of experiment, divalent and other multivalent cations that effectively bind clay particles together and enable attachment to grain surfaces, were largely removed from the exchangeable sites. The extent to which these binding cations were removed depends on the concentration of the concentration of monovalent (Na^+) cation in the water in contact with clay minerals. It was shown that most of multivalent cations were removed from clay surfaces when a 0.5M NaCl solution was used in the pre-conditioning phase. Therefore, it is concluded that the concentration of monovalent cations in the native groundwater and recharge water would significantly affect the clay sensitivity to fresh water injection. The cation exchange properties of clay minerals have therefore a direct effect on the critical salinity level.

As the concentration of Na^+ cation is reduced in the injection water, repulsive double layer forces increase and exceed the attractive Van der Waals forces. A change in the total interaction potential energy occurs such that a fraction of the clay particles are released upon each reduction in the Na^+ concentration. It is likely that clay particles previously attached together in a primary energy minimum were detached from each other by lowering water salinity. Studies on the aggregation of clay particles have suggested that changes occur in the mode of clay-clay and clay-grain surface condition. It is well known that kaolinite platelets adopt very specific face-face and edge-face interactions under various ionic strength conditions (Elimilech et al., 1995). It is expected that clay attachment in the presence of divalent cations possess a stronger attractive forces compared to those with monovalent cations. Clays that are most susceptible to release can be assumed to be readily accessible to the monovalent cations in the bulk solutions. The released particle would be the discrete particles and small aggregates. It is likely that the expansion of the double-layer in the reducing salinity solutions causes the release of clay particles which are exposed to the sodium cations. Residual divalent cations present in the clay deposits prevent complete dispersion of all clays unless the rate of cation exchange is infinitely high when even these ions are extracted from tightly bound clays.

The reducing water salinity appears to yield a transition state which is typically referred to as water sensitivity of clays. Increases in water flow velocity adversely affected permeability under these conditions. During water injection into a well both the critical salinity and the flow rate are the determining parameters for clay release.

2.5.3 Effect of pH

The pH of injection water is an important factor in the clay mobilisation process. Kaolinite particles are hexagonal shaped plates from sub-micron to a few microns in their major dimensions. The thickness of each plate is usually less than 0.1 micron (Sposito, 2001). A kaolinite card-pack may be composed of tens of plates held together by strong Van der Waals forces operating when the electrolyte concentration is high. Under neutral pH conditions kaolinite particles are negatively charged. Low pH conditions favour the binding of clay particles due to the presence of hydrogen ions on the edges. This provides a net positive charge to some clay particles causing edge-face attraction. The transition between negative and positively charged kaolinite particles occurs around pH 5.5 (Sposito, 2001). Under alkaline and low electrolyte conditions, kaolinite particles detach from each other into discrete particles or small groups of platelets.

In the experiments with high pH, clay particles previously in equilibrium with neutral pH water will go through cation exchange reaction in which hydrogen and calcium cations are leached into the displacing high pH water. The consumption of divalent cations is a function of the amount and type of clay minerals, the concentration of divalent ions, salinity of water (Elimelich et al., 1995). We observed that core samples were clogged to varying degrees when the pH of injection water was increased. Core plugs suffered little permeability reduction when the injection water had a pH lowered than 7.5. It is likely that the observed permeability reduction was caused, by a combination of dissolution effects and rearrangement of the clay in the core. High pH conditions favour both face-face and edge-face detachment. With higher pH solutions (e.g. 9 and 10), significant amount of clay was released in the effluent and permeability loss was more severe. These results indicate that hydroxyl ions attacked the clay-clay aggregation, causing large clay masses to break up and disperse upon introduction of a high pH water.

2.5.4 Cation Exchange Effect

Our experimental results showed that while fresh water injection caused a severe clogging after the core had been equilibrated with high sodium concentration, the extent of clogging and clay release was decreased when calcium cations were added to water prior to freshwater injection. The conditioning solution can be thought of the native groundwater in the field condition. When the concentration of Ca cations in the native groundwater is high, the permeability decline is smaller upon freshwater (RO water) injection compared to when the native groundwater contains lower concentration of divalent cations. We observed when the conditioning solution mainly contained monovalent cations, clay release was very fast and the concentration was high during RO water injection. However, when the core samples were initially saturated with high concentration of divalent solution, clay release was negligible upon RO water injection.

Cation exchange leading to weakening of inter-particle and particle-surface interactions is the most probable cause of clay release. Under natural aquifer conditions, clays exist as aggregated materials which are deposited on the grain surfaces. Major cations such as calcium, magnesium, potassium and sodium are all present in considerable quantities in native groundwater and on clay surfaces in their natural conditions. It is believed that changes in the double layer around clay particles and their surface charge density are influenced by cation exchange process between clays and the electrolyte surrounding clays. The extent and rate of cation exchange determine the extent of double layer expansion or contraction and as a result the attractive and repulsive forces. Higher

valence cations like calcium and magnesium are preferentially adsorbed on clay particles when they are present in mixtures of monovalent and divalent solutions. These preferential cations may be removed from clay surfaces if the displacing water has high concentrations of monovalent ions.

As already mentioned, clay minerals exist as stacks of platelet particles due to their deposition history. Therefore, it is expected that only the outermost platelets of a clay stack are exposed and would undergo through cation exchange. Cation exchange occurs rapidly at these locations. Another question is whether it is the clay-clay or the clay-silica interactions which are affected upon the cation exchange and salinity reduction. Our batch and column experiments presented in Appendix 2 indicated that clay-silica forces are relatively strong compared to the clay-clay forces. Therefore, it is likely that the break-up of forces holding the clay aggregates causes clay release. These particles are then transported through pore spaces of the core with the flowing water.

The mechanism of cation exchange appears to be dependent on the salt concentration of the solution. Specifically, the relative concentration of divalent to monovalent cations in the solution appears to be an important factor in the inhibition of cation exchange processes between clays and water. A solution with a low monovalent percentage may not cause removal of divalent ions originally on clay surfaces. This is primarily due to the selectivity of clay minerals for divalent cations. However, in the case of high monovalent concentrations, the monovalent cations effectively replace the divalent cations on the clays. This process has a marked effect on the clay zeta-potentials which determine double layer effects. We have shown that the critical Na^+ concentration for ion exchange exists at a higher level than the minimum threshold salinity reported to prevent permeability reduction (Kia et al., 1998). There is a critical minimum salinity for each ion type. Above this critical value the clay particles remain attached. However, if monovalent cations are present at high concentrations, they will replace any stronger cations on the clays. We showed that even low concentrations of calcium in the injection water (e.g. 1 mg/L) can significantly reduce the rate and extent of clay release.

Our results show that the concentration of sodium ions should be at least 0.05 M for ion exchange to take place. Calcium ions or divalent ions have much higher charge densities than dictated by their increased valence compared to monovalent cations. This is due to the fact that there is little difference in ionic sizes in the alkali metal ions. For example, calcium has an ionic radius almost equal to that of sodium and smaller than that of potassium. Thus, in order to remove a calcium ion from a clay particle complexation or preferential adsorption site, five or six times as many monovalent ions are needed in close proximity (Vulava et al., 2002). Moreover, the divalent cations may be of such a size that it is tightly held on an adsorption site on the clay surface. This would explain why sodium chloride concentrations higher than the flocculation concentration would be required to replace such ions. These ions may be termed 'binding' ions as their location on clay surfaces determines the adhesion between clay particles or the adhesion between clays and grain surfaces. Thus the sodium ion concentration would need to be high before ion exchange can take place.

When a CaCl_2 solution was used to pre-flush the core samples (see Table 2.9), followed by RO water, very little reduction in hydraulic conductivity was observed. However, when the core was re-saturated with high concentration of NaCl followed by injection of RO water, clogging did occur and the effluent was highly turbid. These observations indicated that the exchange of sodium for calcium is a reversible reaction. We observed that if a low concentration of NaCl (e.g. 20 mM) was used to re-saturate the core, then the reduction in hydraulic conductivity was not very severe as in previous test. This result suggested that the cation exchange may not be as complete when the concentration of monovalent cations in water is low. This is to be expected, as the calcium ion is held more tightly on clay surfaces than the sodium ion.

The most significant factors causing clay release was found to be a change in the content and type of exchangeable cations in the double-layer thickness surrounding a clay particle. When the salt concentration of groundwater is large, as in the case of brackish groundwater, and is dominated

with monovalent cations (e.g. Na^+), the injection of fresh water with a low salt concentration, will cause expansion of the double and force the clay particles apart. This expansion will result in decrease in attractive van der Waals forces to the extent that Brownian and repulsive electrostatic forces promote disaggregation and clay release.

The effect of Ca cations in reducing the extent of clay release and subsequent clogging was observed for a variety of core samples. On the basis of our experimental study, we expect that 15 wt% of calcium, accompanied with the slow decrease of salinity, would be sufficient to prevent clay release and clogging (see Table 2.9). In experiments where the salinity was decreased drastically (high salinity difference, but with 15 wt% calcium), significant clay release and severe clogging were observed (see Table 2.9). We believe this observation can be attributed to the process of cation exchange. Our results suggest that the possibility of clogging depends on the competition between the two processes of cation exchange and clay dispersion. Clogging would occur only if the dispersion process occurs before the completion of the cation-exchange process. When the salinity is decreased gradually (in several steps), lowering of the ionic strength favours surface coverage of the clay minerals with Ca through cation exchange. Therefore, when the salinity of injection water is decreased in several steps, the exchangeable sites on clay surfaces are predominantly covered with Ca, and the dispersion of clays will not occur despite the low ionic strength. Table 2.9 shows that the critical calcium percentage below which clay release occurs is also dependent on the ionic strength of the native groundwater. For example, the critical calcium percentage is less than 10% when the IS of the native groundwater is 5 mM.

2.5.5 Hydrodynamic effect

Water may flow through an aquifer at a velocity of a few metres a day. Invariably the Reynolds number based on the superficial velocity in the aquifer will be very low, in the range of 0.01. Water shear forces are likely to be most important since values of Reynolds number less than one are sufficiently low so that the lift force is small. Moreover, the pore water velocities will vary widely because of the pore size distribution. We observed that the hydrodynamic forces acting on deposited clay particles may cause detachment due to frictional drag forces of the flowing water. Typically, the drag forces are negligible when compared with colloidal double layer and Van der Waals forces as calculated by Treumann et al. (2013) (see Appendix 2). In core samples saturated with high salinity solution (e.g. 0.1 M NaCl) there was virtually no increase in clay release in response to increases in flow velocity. Step increase in water flow rate in the range 10-50 mL/min corresponding to average pore water velocities of 20-400 m/day produced very small increase in clay concentration in the core effluent. These increases were insignificant when compared to the amount of clay produced in a salinity-shock tests.

However, water velocity was found to be an important factor in permeability reduction when the mobilisation of clay particles was already underway in water salinity shocks. In this condition, permeability reduction was dependent on water velocity. Typical results for core-flooding tests undergoing salinity shock showed that permeability decreased abruptly when the flowrate was increased during the experiment. The mechanism of release of clay particles from grain and pore surfaces is very much a chemical controlled process with water velocity playing a part only after the release process is about to occur.

2.5.6 Water-compatibility criteria for injection-water salinity

Our results revealed that there are two important parameters which determine whether injection water would cause well clogging. The first parameter is the total salt concentration, which should be higher than a minimum value to prevent clay release. The second one is the cation composition of injection water which determine the cation exchange process during injection. We found that in

order to minimize clay release and clogging the process of cation exchange should not result in a reduction in the concentration of exchangeable multivalent cations. In this section, we introduce a schematic criteria to employ for injection water quality to prevent clay mobilisation and minimize well clogging.

The critical concentration of divalent cations obtained from core-flooding experiments were combined into generalized stability diagram for various values of groundwater ionic strength (see Fig. 2.12). At any given IS of the native groundwater, when injection water chemistry (i.e. Total salinity and calcium percentage) is located above and to the right of the critical salinity line, it is compatible and clay release is unlikely to occur. Below and to the left of the critical line, injection water has insufficient total and/or divalent cation concentration to prevent clay release and the potential for clogging is high. The lower the ionic strength or divalent cation, the greater the clogging potential. It should be mentioned that the critical salinity line strongly depends on the cation composition of the native groundwater and clay type. Therefore, core-flooding experiments are the best option to determine the water compatibility with the aquifer sediments. Cation analyses of injection and native groundwater and XRD analysis of aquifer materials are important parameters in determining the water compatibility. When these data are not available, Figure 2.12 can be used to determine the composition of injection water.

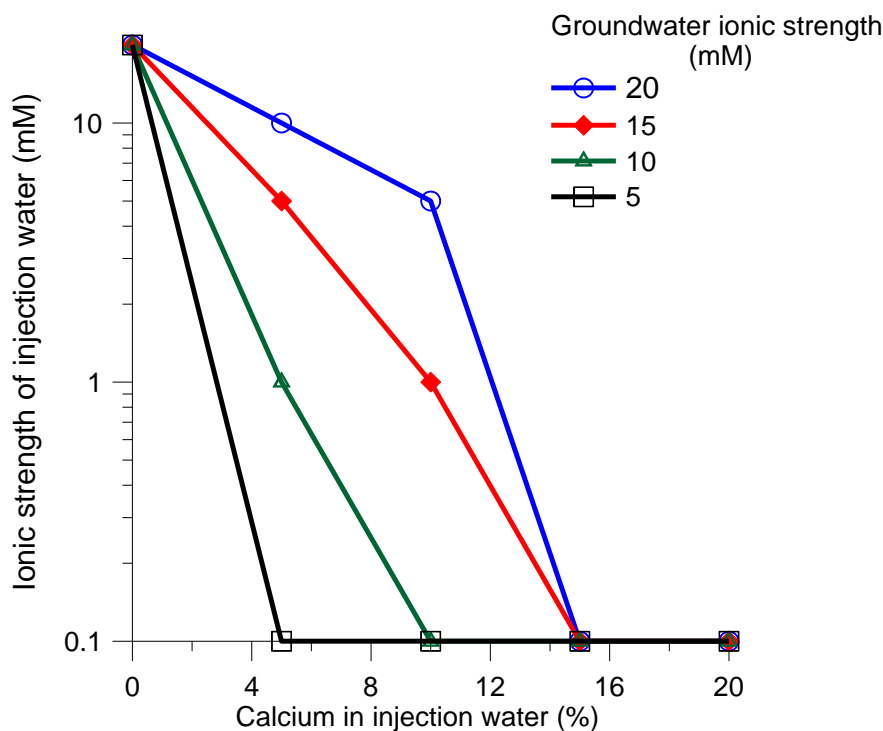


Figure 2.12. Salinity criteria for the injection water at various values of groundwater ionic strength

2.6 Conclusions

It was shown that the release and retention of clay particles in aquifers play an important role in the sustainable operation of reinjection of CSG associated water into surrounding aquifers. The processes of clay release, retention, and associated permeability changes in consolidated aquifer sediments were studied by injecting water with various chemical qualities at different flow velocities. Significant amounts of clay release occurred when: (i) the high salinity water was

displaced by RO-water with a low ionic strength (IS), and (ii) the flow velocity was increased in a stepwise manner.

The amount of colloid release and associated permeability reduction upon RO-water injection depended on the initial clay content of the core. The concentration of released colloids was relatively low and the permeability reduction was negligible for the core sample with a low clay content of about 2 to 3%. In contrast, core samples with about 5-8% clay content exhibited: (i) close to two orders of magnitude increase in effluent colloid concentration and (ii) more than 90% permeability reduction.

This dependence of colloid release and permeability changes on flow velocity and colloid concentration was consistent with colloid retention and release at pore constrictions due to the mechanism of hydrodynamic bridging. A mathematical model was formulated to describe the processes of colloid release, transport, retention at pore constrictions, and subsequent permeability changes. Our experimental and modelling results indicated that only a small fraction of the in-situ colloids was released for any given change in the IS or flow velocity. Comparison of the fitted and experimentally measured effluent colloid concentrations and associated changes in the core permeability showed good agreement, indicating that the essential physics were accurately captured by the model. However, we acknowledge that this model cannot be still used as a predictive tool in the field conditions as it has several empirical parameters which are obtained by a careful fit to experimental data.

It was confirmed that kaolinite was the predominant clay minerals among the colloidal particles deposited onto grain surfaces of sandstones from the Precipice sandstone aquifers. The mobilisation or release of clay particles was caused when the attractive force between the particles and grain surfaces weakened. Clay particles were found to rapidly detach from grain surfaces when core samples were flushed with high salinity water followed by RO water or low salinity water (<30 mM). This mobilisation resulted in a high concentration zone of clay which moves through the core. Concentrations of clay suspension greater than 2 g/L was observed under the experimental conditions of this work. Small amount of quartz particles was also found in the core effluent samples. Cation exchange processes between clay and bulk solution were found to be responsible for the weakening of the adhesive forces. The rate of cation exchange was found to be dependent on the salt concentration and pH of the water in contact with the clay. The treatment of sandstone with divalent cations or mixtures of monovalent and divalent cations can significantly minimise the clay release rate. However, these cations may be removed from the clay particle surfaces by any subsequent flow of sufficiently concentrated monovalent solution. We observed an effective reduction of clay mobilization with relatively low concentrations of divalent cations. When only 15% of the cations in the injection water were divalent (calcium or magnesium), the permeability of the core was unaffected.

The pH of the solution was a controlling parameter for cation-exchange between clays and flowing water. Low-pH conditions (pH<6) minimise clay release by inhibiting the exchange of the cations originally on clay surfaces with monovalent cations from the bulk solution. It is expected that the hydrogen ion interacts with clay surface charges to minimise the exchange process. High pH conditions (pH > 8) promote clay release and disaggregation processes. The hydroxide ion may interact with clay surfaces at high pH conditions resulting in double layer expansion. Hydrodynamic shear forces alone at typical groundwater conditions were not effective to induce the release of attached clay particles. A weakening of the adhesive forces between the colloids and colloid-grain was a precursor for the clay release. This weakening allows double layer expansion to occur when RO water or low ionic strength solution come into contact with clays. The hydrodynamic shear force then become strong enough to initiate the release and subsequent clogging. The underlying mechanism of permeability reduction (clogging) in sandstone cores where clay mobilisation occurred was found to be due to pore-plugging (hydrodynamic bridging)

in the cores. Clay particles bridged at pore constrictions and the bridging probability was a function of clay concentration. We observed that a fraction of the bridged clay particles could be released by flow reversal depending on their deposited condition.

It was also shown that the deliberate change in flow direction, as would occur during injection well rehabilitation procedures such as back-washing or air-development, may increase permeability to some extent. That is, appropriate and early rehabilitation strategies designed to alter the torque and forces acting on the colloids may prove effective in mitigating clogging induced by clay release resulted from introduction of low solute concentration water. For injection well in Precipice Sandstone aquifers, it appears that to avoid physical clogging within a few meters of the injection well, the well needs to be appropriately developed to remove colloidal particles in the near-well formation. For the aquifer material tested, maintaining salinity and divalent cation concentration above the salinity of the native groundwater appears sufficient to manage clogging issues.

3 Preventing Well Clogging Using Chitosan as a Clay Stabilizer

3.1 Introduction

Aquifer sediments always contain a certain amount of clay minerals deposited on the grain surfaces. Clay particles are usually immobile during native groundwater conditions. However, they may be released into water in response to perturbations of the native conditions, such as the injection of water with a low salinity or high pH (Grolimund et al., 2001; Rosenbrand et al., 2012). The released clay particles are transported with flowing water and may subsequently re-deposit down gradient (e.g., at pore constrictions), resulting in permeability reduction of porous media, commonly referred to as clogging, (e.g. Mays and Hunt, 2005; Ochi and Vernoux, 1998). Clogging has been recognized to be the most significant technical challenge in managed aquifer recharge (MAR) operations (Martin, 2013). Emerging large-scale applications of MAR in Australia involve well injection of low salinity water (e.g., domestic wastewater and industrial wastewater produced during coal seam gas recovery) into sandstone aquifers (Seibert et al., 2014). In addition, when well injection techniques are utilized for groundwater recharge, there can be considerable spatial and temporal variability in flow rate due to the applied injection pressure, periods of intermittent flow and periodic surging or back-washing to remediate near-well clogging.

Basically, surfaces of clay minerals are negatively charged at typical pH conditions of groundwater. These negative charges are responsible for the clay sensitivity to low-salinity water injection. The negative charges of clay minerals, which exist naturally in stacked or randomly arranged platelets on the grain surfaces, are neutralised by various cations present in the native groundwater. Usually Na^+ or Ca^{2+} comprise the major cations of groundwater. However, the introduction of a less saline water (e.g. freshwater) can dilute the native groundwater and reduce its ionic strength. As the cation cloud surrounding the clay surfaces becomes more diffuse, water molecules enter between the clay platelets, resulting in swelling (in case of smectite clays and some mixed-layer clays) or dispersion (for kaolinite, illite, and chlorite). Mobilization, transport, and deposition of clays can block the pore throats. This type of clogging is, for the most part, irreversible and requires acid stimulation for removal.

In the past thirty years, a great deal of effort has been made in the field of petroleum engineering to mitigate the clogging problems related to clay release and swelling. This has resulted in development of numerous chemicals often called clay stabilizers. Clay stabilizers have evolved from simple inorganic compounds, to inorganic polymers, and to complex organic polymers (Himes et al., 1991). They are typically used in drilling, completion, acidizing, fracturing, water flooding, and steam injection. The economic success in applying clay stabilizers depends on the choice of clay stabilizer(s). To efficiently use clay stabilizers, it is important to evaluate the applicability and limitation of a given clay stabilizer. Himes et al. (1991) describe the desirable features of an effective clay stabilizer as following: (i) the product should have a low, uniform molecular weight to prevent bridging and plugging of pore channels. (ii) the chemical should be non-wetting on sandstone surfaces to reduce water saturation. (iii) it should have a strong affinity for clay surfaces, (iv) the molecule must have a suitable cationic charge to neutralize the surface anionic charges of the clay effectively.

The efficient way to maintain the stability of clays and therefore prevent clogging is to ensure that the ionic strength and composition the injection water is equal to or greater than the critical value (see previous chapter). It is known that different cations provide more stability than others at the same salt concentration. For example, K^+ cations maintain a stable clay at much lower concentrations than Na^+ . Calcium ion is also an excellent stabilizer, but it is not widely used in high concentrations because of chemical incompatibility with most of groundwater aquifers (e.g. calcite precipitation). Divalent cations (e.g. Ca^{2+} and Mg^{2+}) have become popular clay stabilizers and are nearly always included in the recharge water. However, because these cations can easily displace the Na^+ cation during the injection, they can also be exchanged during recovery back to Na^+ ; therefore, their stabilization effect is not permanent.

Improvements in clay stabilization came with the development of "polymeric" inorganic cations such as hydroxyl aluminium and zirconium oxychloride (Reed, 1974). These chemicals consist of a complex structure of multiple cationic sites that are resistant to cation exchange by Na^+ and therefore are more permanent. Disadvantages of such treatments include the need to re-treat after acidizing and their restriction to non-carbonate-containing sandstone formations (Himes et al., 1991). Coppel et al. (1973) presented a field study with a hydroxyl-aluminium treatment. It was observed that some wells experienced a rapid clogging during productions after acid stimulations.

Cationic organic polymers (COP) have been shown to efficiently stabilize clay minerals upon exposure to freshwater (Himes et al., 1991). These organic polymers have the additional advantages of being acid-resistant (Himes et al., 1991). They are also unaffected by carbonate content in the formation and may be used to stabilize clays in carbonate formations. These compounds are typically composed of long-chain organic polymers with molecular weights from 5,000 to well over 1,000,000. Variations of these chemicals have been introduced to solve various clay-related production problems, such as clay dispersion. However, the size of these molecules has restricted their use to low concentration in low-permeable formations due to blocking of the small pore throats by the polymer mass. A commonly used COP has a molecular weight averaging - 500,000 and a calculated average size of 1.1 μm . Therefore, it is expected that the larger fractions of the COP create clogging in the porous media. In fact, flow studies conducted in a 30-md sandstone showed that clogging and permeability reduction occur when a 0.1 wt% active solution of a 500000 molecular weight COP in 2% NH_4Cl was injected in to the core (Himes et al., 1991). Similar study reported by Nasr-El-Din et al. (1999) proved that these stabilizers are ineffective in low-permeability porous media. Patel (2009) pointed out several environmental issues for previous inhibitors such as oligometric cationic amines, polymeric quarterly amines, and mono cationic amines.

Another factor that must be taken into consideration when selecting a clay stabilizer is the health effects. Intake of large amount of inorganic stabilizer may contribute to the development of neurodegenerative diseases, including Alzheimer's. The effect of aluminium salts have been reviewed and epidemiological evidence was found to link aluminium and Alzheimer's disease. It was observed that nine out of thirteen published cases have statistically significant positive relations (Gauthier et al., 2000). In this study, chitosan, which is a natural biodegradable and non-toxic polymer, was investigated as an alternative to the traditional clay stabilizers. Core-flooding experiments were conducted to (1) test its ability to mitigate clay release and associated clogging problems, (2) examine the effect of salt concentration, acidic and alkaline conditions on its performance, (3) find the optimum dosage, and (4) verify its effect in long cores.

3.2 Chitosan Chemistry

Chitosan is cellulose like copolymer of glucosamine and N-acetyl glucosamine of high molecular weight obtained from the deacetylation of chitin. Chitin itself is obtained by grinding the shell of shrimp and crabs. Chitosan contains two reactive hydroxyl groups and a very high reactive amino group, which give chitosan its powerful reactive capacity. Chitosan is a biodegradable, non-toxic, and linear cationic biopolymer with a strong positive charge allowing it to strongly bind to negatively charged surfaces (Kawamura, 1991). Chemically, chitosan is similar to cellulose, with the hydroxyl in the 2-position replaced with a primary amino acid group. The protonation of amine groups gives chitosan cationic properties that explain its affinity for anionic compounds (e.g. metal anions, organic compounds, dyes) (Roberts, 1992; Guibal et al., 2006).

The coagulation–flocculation capacity of chitosan depends largely on its amino acid group. The protonation of this group makes the chitosan positively charged which can bind to the negatively charged particles (e.g. clay and silica) (Divakaran and Pillai, 2002). Chatterjee et al. (2009) stated many mechanisms for coagulation of colloidal particles using chitosan, including electrostatic attraction, sorption (due to the protonation of the amino group), chelating capacity (due to the high content of OH group) and bridging (due to the high molecular weight of chitosan). It has been shown that chitosan has an excellent chelating property toward many toxic metals such as molybdenum, arsenic, cadmium, chromium, lead, and cobalt. So, such metals would be removed during coagulation of water (Chatterjee et al., 2009). Chitosan has many advantages over other cationic organic polymers. One main advantage is related to its non-toxic and biodegradable characteristic. Another advantage is non-existing residual metal contents.

Chitosan has been used as a coagulant and as a coagulant aid (Chatterjee et al., 2009). Divakaran and Pillai (2002) reported that chitosan as the primary coagulant at a dose of 0.5 mg/L achieved over 80% turbidity removal from initial raw water of 10 NTU. More recently, Guibault et al. (2006) demonstrated that the degree of acetylation and molecular weight could somewhat affect coagulation–flocculation performance. Specifically, molecular weight had more effect on bentonite suspensions and dye solutions than on kaolin and humic acid suspensions. When the pH of the suspension was less than 6.2 (the intrinsic pH of chitosan), very low doses of chitosan were required for the treatment of concentrated suspensions of bentonite (Chatterjee et al., 2009). Along with unique biological properties that include biocompatibility, biodegradability, and nontoxicity, chitosan may be produced at a low cost, which collectively offers an extraordinary potential in a broad spectrum of applications which are predicted to grow rapidly. Given the abovementioned properties, we hypothesized that chitosan could effectively stabilize the clay minerals present on the grain surfaces of aquifer materials and therefore prevent clogging.

3.3 Materials and methods

3.3.1 Sandstone cores

The core-flooding experiments were conducted using core plugs from various types of sandstones, including Precipice sandstone at Reedy Creek, Buff Berea, Castlegate, and Berea. The latter three sandstones were purchased from Kocurek industries (Houston, United states). The average initial permeability of sandstones ranged from 100 to 280 md. The composition and physical properties such as permeability of these sandstones were relatively uniform, and they were readily available in large quantities necessary to carry out a complete set of experiment. As it will be shown later, clay release and re-deposition was the principal clogging mechanism in these sandstones.

3.3.2 Chitosan solution

Low molecular weight chitosan (molecular weight: 5 kDa) was purchased from Sigma–Aldrich (Stenheim, Germany). Various chitosan concentrations ranging from 5 to 30 ppm was prepared by dissolving a required amount of chitosan powder in an acidified solution (1%, v/v acetic acid). Chitosan solutions were agitated for 2 hours with a shaker to achieve complete dissolution. To examine the effect of pH on the performance of chitosan stabilization, 0.1 M HCl and NaOH were used to adjust the pH of the chitosan solution to any desired value.

3.3.3 Core-flooding experiments

Extensive core-flooding experiments were conducted to examine the clay stabilizing effect and clogging mitigation of chitosan. Various variables were investigated including chitosan concentration, injection time, sandstone type, water salinity, and flow rate. A schematic of the core-flooding setup is shown in Fig 2.2. Briefly, it consisted of a positive displacement pump for water injection, a Hassle cell in which the core was contained, and pressure and effluent collection devices. For a constant injection rate, the pressure drop across the core was monitored continuously over the time span of the experiment. All the sandstone samples used in the experiment were from the same block, therefore had the same initial permeability. One-inch diameter cores were cut from a large block. The dry cores at 40°C were vacuum saturated with 0.5M NaCl, then were placed in the core holder with a confining pressure of 2000 psi. The core was then flushed with a 0.5M NaCl or 0.1 CaCl₂ solutions through the core at a flow rate of 10 mL/min to equilibrate the core with the solution. Then, the initial permeability was measured and used as the reference permeability. The porosity of the core samples was determined through weighing method in each experiment.

Following the equilibration step, a pulse of chitosan solution (pH=4) at a given concentration and ionic strength was introduced into the core for several pore volumes at the same flow velocity (Phase 1). In a series of experiments the pH of the chitosan solution was increased to 6 and then injected into the core sample during phase 1. The clay release and clogging was examined by systematically changing the solution chemistry or flow velocity in a series of experiments as follows: Following Phase 1, the influent was switched to DI water for several additional pore volumes (Phase 2), 0.5 M NaCl at pH 5.8 (Phase 3), DI water at pH 5.8 (Phase 4), and finally DI water at pH 10 (Phase 5). This is a severe test for water sensitivity, and also provides information about the exchangeability of chitosan adsorbed on the clay surfaces by Na⁺ cations.

In another set of experiments the average pore water velocity was sequentially increased during Phase 2 (DI water) with the following sequence: 5, 10, 20, 50, and 100 m/day. In a series of experiments, the cores were initially treated with 0.1M CaCl₂ to demonstrate the temporary stabilization effect of calcium. These cores, initially treated with 0.1 M CaCl₂, were flushed with DI water, 0.5M NaCl solution, DI water (pH=5.8), and DI water (pH=10). In selected experiments, the treated cores with chitosan were aged for a period of 3 months and then were flushed with DI water to examine the longevity effect of chitosan. Some cores were flushed with an additional 20 liters of 0.1M NaCl to determine if longer exposure and larger volumes would cause displacement of the chitosan polymers from surfaces and, in turn, greater permeability losses upon fresh water injection. In another series of experiment, the flow velocity was sequentially increased during Phase 4 (DI water) with the following sequence: 5, 10, 20, 50, and 100 m/day. To examine the influence of acid flushing on the stabilizing effect of chitosan, for a select core samples the flow was switched to 0.1 M HCl (pH =1) following phase 2 and the core was flushed for several pore volumes before changing the influent back to DI water at pH=5.8.

Effluent samples were continuously collected during the experiments at given intervals using a fraction collector. All solutions were injected at a constant rate of 10 mL/min. This rate was selected because it correspond to an average pore water velocity of 50 m/day to resemble flow velocity in the vicinity of a well.

3.3.4 Zeta potential

The mobility (converted to zeta potentials) of clay and chitosan–clay composites (0–0.3 g polymer/g clay) were measured using a Zetasizer Nanosystem (Malvern Instruments, MA). The clay and clay composites were measured in a dilute suspension (~0.05% clay).

3.4 Results and discussion

3.4.1 Water Sensitivity of Sandstones

A series of water sensitivity tests was performed by injecting DI water with a flow rate of 10 mL/min into the cores saturated and pre-conditioned with 0.5 M NaCl. As shown in Figure 3.1, the three types of sandstones are extremely water sensitive when the core was initially saturated with high concentration of sodium. This is manifested by the sharp permeability declines observed during RO water injection. The relative permeability declined sharply during the first few pore volumes and reached a value of 0.001mD, indicating a significant clogging potential due to clay release and capture in the pore constrictions. Consistent with the observed permeability reduction, Figure 3.2 shows that a significant clay release occurred when the core was flushed with RO water. This set of experiments demonstrates what can happen to the permeability of a severely water sensitive aquifer sediment when it is contacted by freshwater.

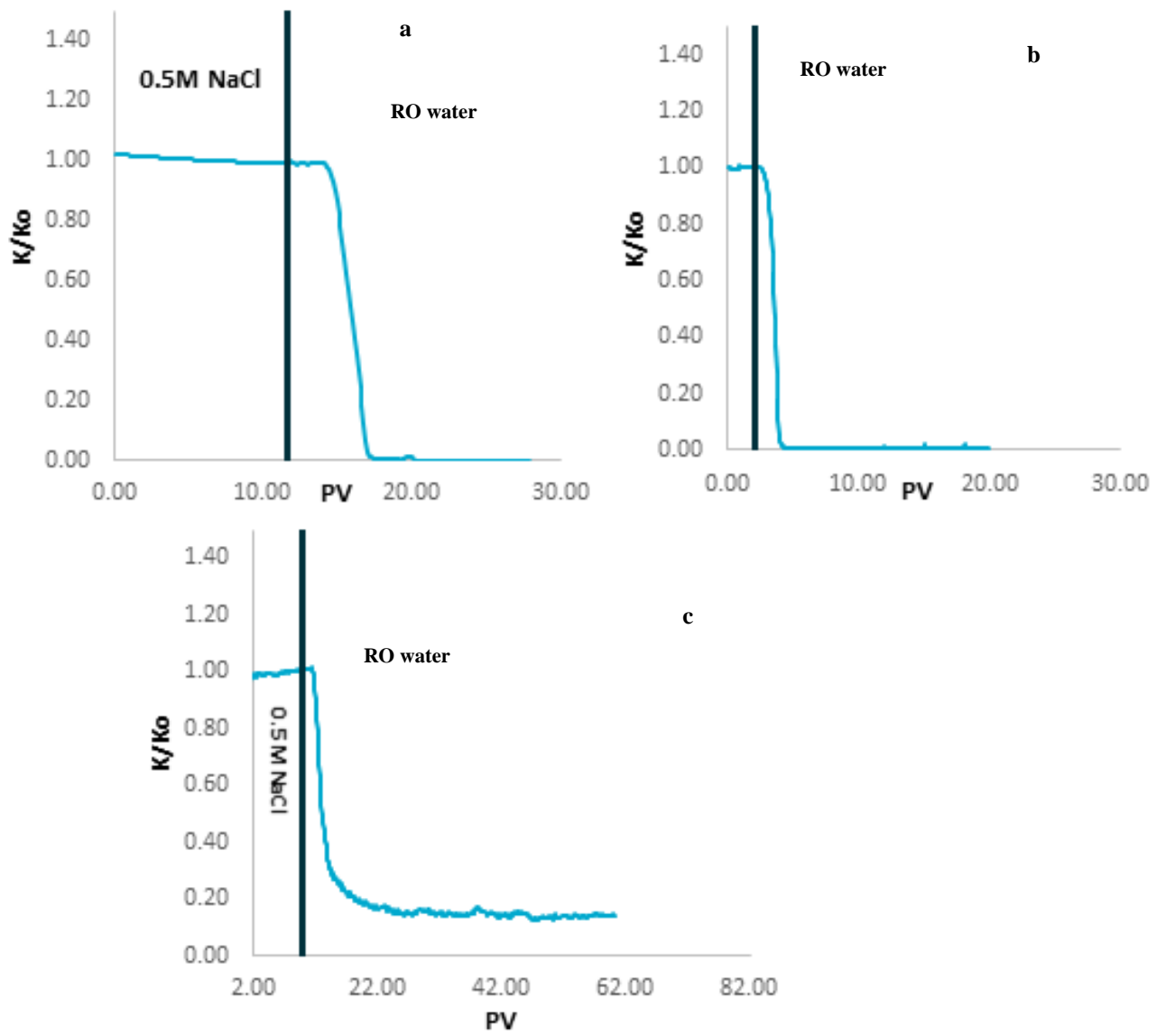


Figure 3.1. Permeability decline of core samples of Buff Berea (a), Berea (b), and Precipice (c) upon RO water injection

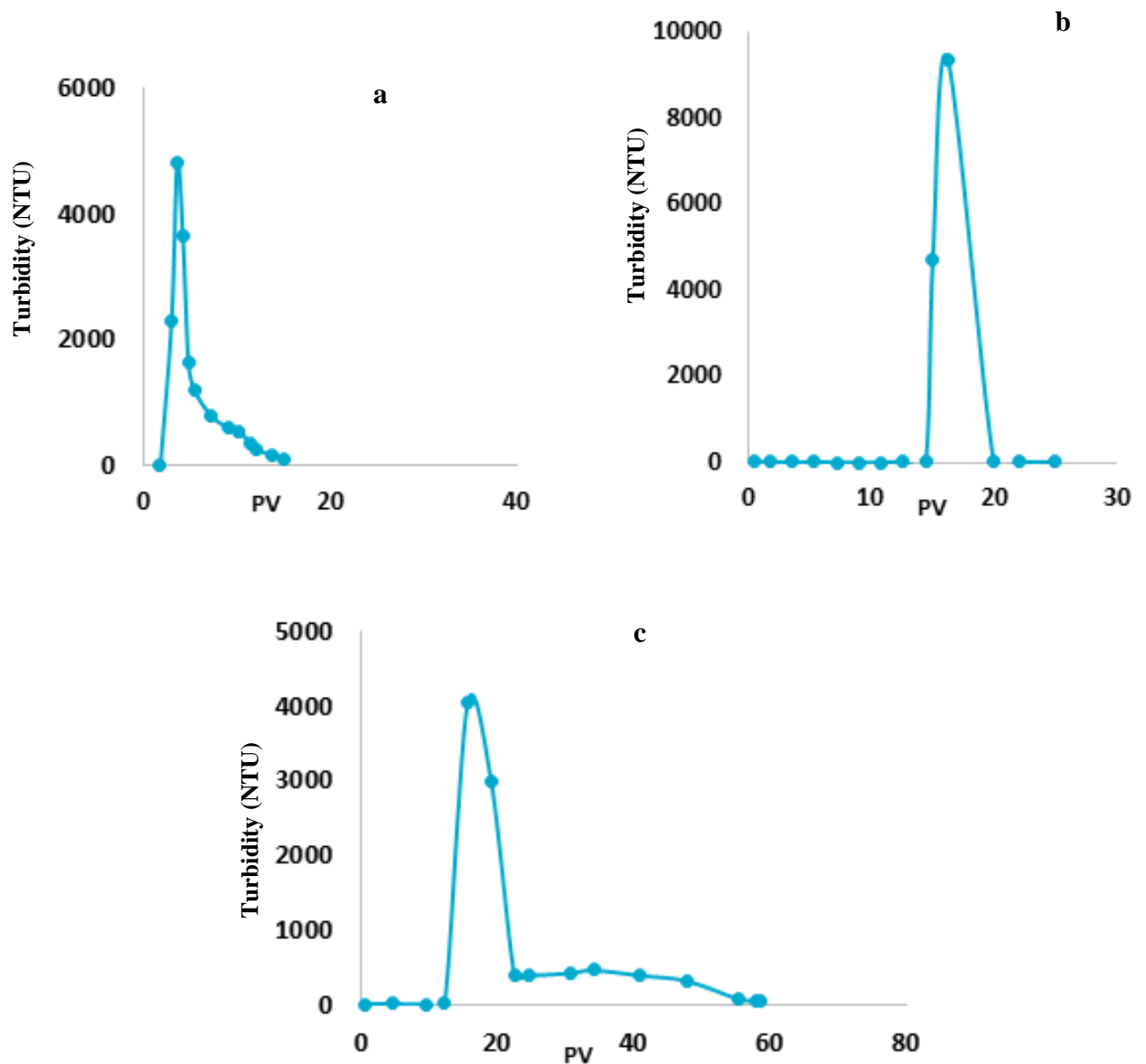


Figure 3.2. Clay release in Buff Berea (a), Berea (b), and Precipice (c) core samples upon RO water injection

In contrast, Figure 3.3 shows that when the core was initially saturated and flushed with CaCl_2 during the pre-equilibrium condition, RO water injection during Phase 2 resulted in a little permeability decline (~2% decrease). These observations suggest that divalent cations like Calcium can act as a strong clay stabilizer. However, it is expected that these cations can easily be displaced by the Na^+ cation and therefore they are not permanent. Indeed, Figure 3.3 shows that when the core was flushed with several pore volumes of 0.5 M NaCl during phase 3 followed by injection of RO water during phase 4, a severe clogging and clay release occurred. Therefore, it is concluded that injection of a higher concentration of calcium can significantly reduce clay release and clogging potential. A similar result was also reported by Read et al, (1976), who noted that exchangeable calcium or other divalent cations also reduce clogging potentials in Brea sandstones. It is important to note that the calcium effect would not necessarily be permanent. More notably, the benefit of calcium is short term. Calcium must be added continuously to the injection water.

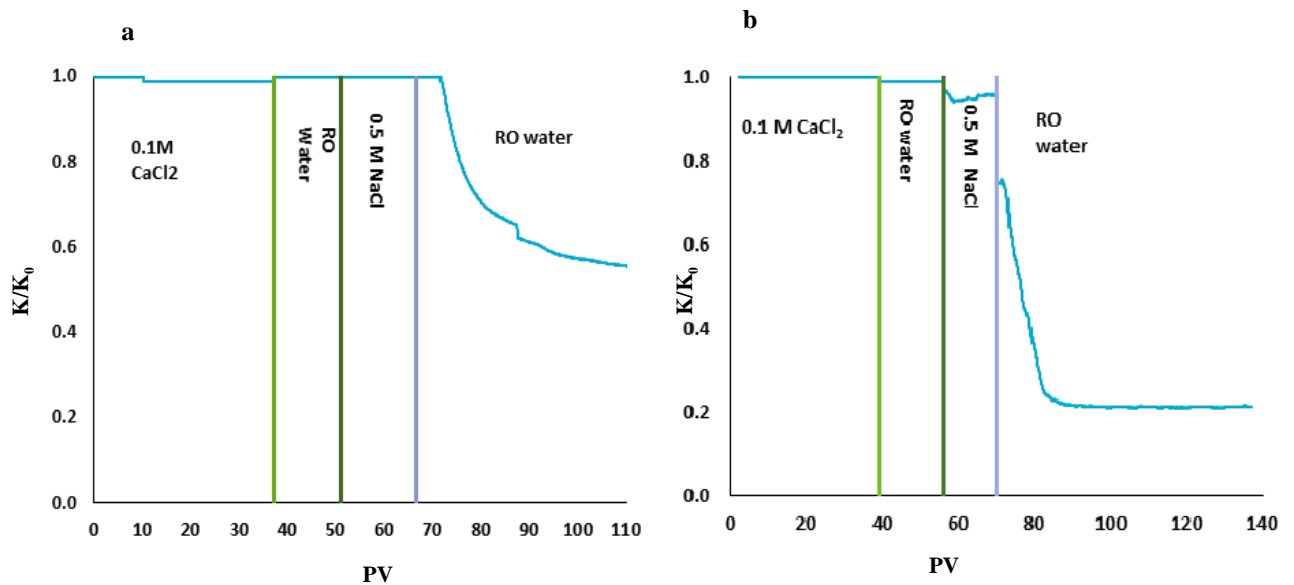


Figure 3.3. Permeability decline of core samples Buff Berea (a) and Precipice (b) initially saturated and flushed with 0.1 M CaCl₂

3.4.2 Effectiveness of Chitosan Treatment

In order to determine the effectiveness of chitosan as a clay stabilizer and clogging inhibitor, a solution containing 20 ppm chitosan prepared in RO water was injected into the sandstone core at a flow rate of 10 mL/min for several pore volumes. In a typical experiment, the influent was switched to RO water and continued for another 10 pore volumes. In contrast to previous experiments (see Figure 3.1), it was observed that chitosan treatment effectively stabilized clay particles since no clay release was detected in the core-effluent samples and negligible increase in the pressure across the core was noted during the injection of DI water (see Figure 3.4). Figure 3.4 shows representative graphs of relative permeability (K/K_0) of two core samples treated with chitosan solutions (20 ppm) before RO water injection. Comparison of results in Figure 3.4 and those in Figure 3.1 demonstrate that chitosan treatment provided an effective clay stabilization and as a result negligible clogging occurred upon RO water injection.

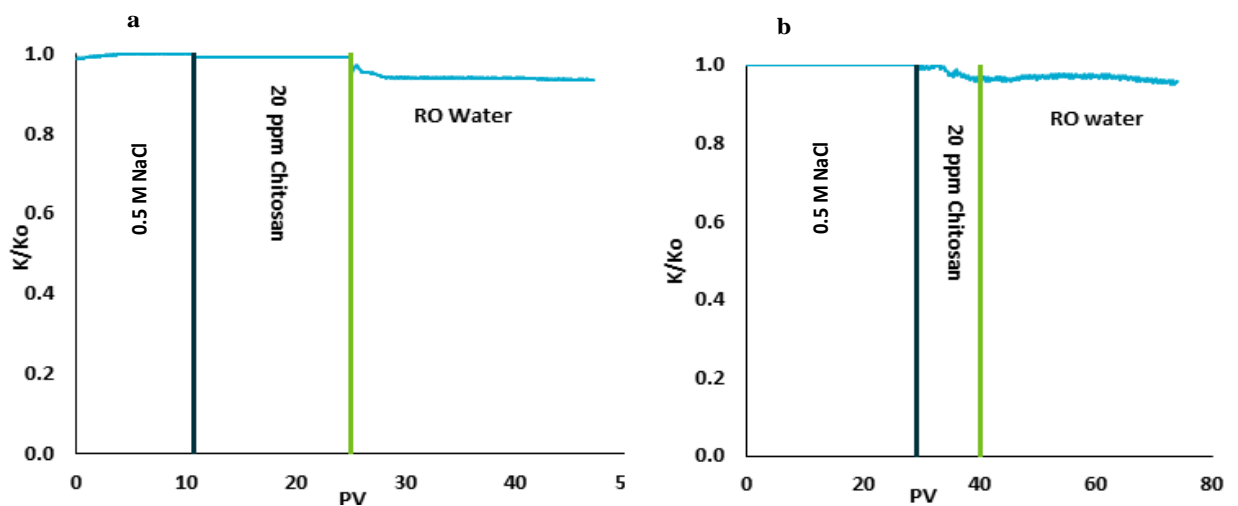


Figure 3.4. Representative plots of the relative permeability for two core sample from Buff Berea (a) and Precipice (b) as a function of pore volumes (PV) when the core was treated with chitosan at 20 ppm

3.4.3 Effect of Chitosan Concentration

Several experiments were performed at chitosan concentrations of 5, 10, and 20 ppm to determine the impact of chitosan concentration on clay release and permeability reduction of the core samples. In these experiments, chitosan solutions were prepared in acidified RO water (1% acetic acid). The procedure included 0.5 M NaCl injection for several pore volumes to measure the initial permeability, and then the injection of chitosan solutions at various concentration (5, 10, 20 ppm) during Phase 2 (5 PVs) followed by other phases as specified earlier. A significant drop in K/K_0 is an indication that the chitosan concentration was not sufficient to effectively stabilize the clay particles. It was observed that treating the cores with 5 ppm was not effective in preventing clogging as a significant decrease in the permeability was observed during Phase 3 (RO water). It should be mentioned that no measurable clay concentration in the core effluent was noted indicating that the chitosan was effective in stabilizing the majority of clay particles.

Reversing the flow direction improved the core permeability to some extent, but did not restore it completely. At chitosan concentrations of 10 and 20 ppm, there was slight decrease in the core permeability during the RO water injection, and no clay release was noted in the core effluent samples. Therefore, a chitosan concentration of 10 ppm would be the minimum concentration at which less than 5% permeability loss was observed when the core was flushed with RO water during Phase 3. As chitosan is both hydrophilic and cationic in acidic conditions, it should have a strong affinity to the negatively charged clay minerals. Chitosan chains may easily intercalate into the clay interlayer by means of cationic exchange.

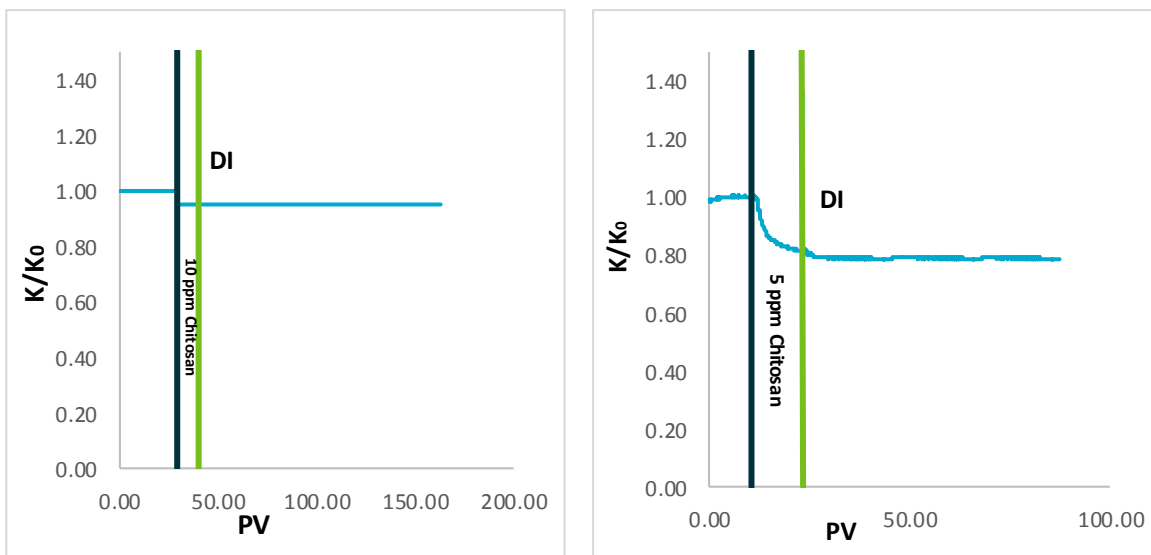


Figure 3.5. Representative plots of the relative permeability for two core samples from Precipice as a function of pore volume (PV) when the core was treated with chitosan at 10 ppm (a) and 5 ppm (b)

3.4.4 Effect of pH

The pH of the chitosan solution may affect the surface charge of the chitosan and subsequently its stabilization property. As depicted in Figure 3.4, chitosan demonstrated an excellent stability effect in the acidic conditions (pH=4). However, it was observed that this effectiveness was significantly dropped when the pH of the chitosan solution, injected into the core during phase 2, was increased to 6.5 (Figure 3.6). This decline of the stabilization effect can be attributed to the charge neutralization of the NH_2 group. The amino group in chitosan has a pKa value of about 6.5, which leads to a protonation in acidic solution with a charge density dependent on pH value.

Indeed, this makes chitosan water-soluble and it effectively binds to negatively charged surfaces such as in-situ clay particles on sand grains. It is therefore expected that chitosan adsorption onto clay minerals is limited when the pH of the chitosan solution is increased to near neutral or alkaline conditions. This limited adsorption in pH 6.5 may be responsible for the less effectiveness of chitosan in preventing clogging.

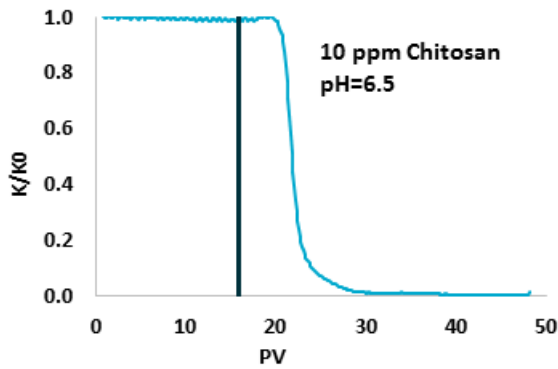


Figure 3.6 Representative plots of the relative permeability for a core sample from Precipice as a function of pore volumes (PV) when the core was treated with 10 ppm chitosan at pH=6.5

3.4.5 Effect of core length

Figure 3.7 illustrates the relative permeability data (K/K_0) obtained at different core lengths (5 and 10 cm) with a constant influent concentration of 10 ppm and flow rate of 10 mL/min. It is observed that chitosan treatment effectively prevent clogging of all core samples with various lengths when 10 minutes of chitosan was injected into the core samples.

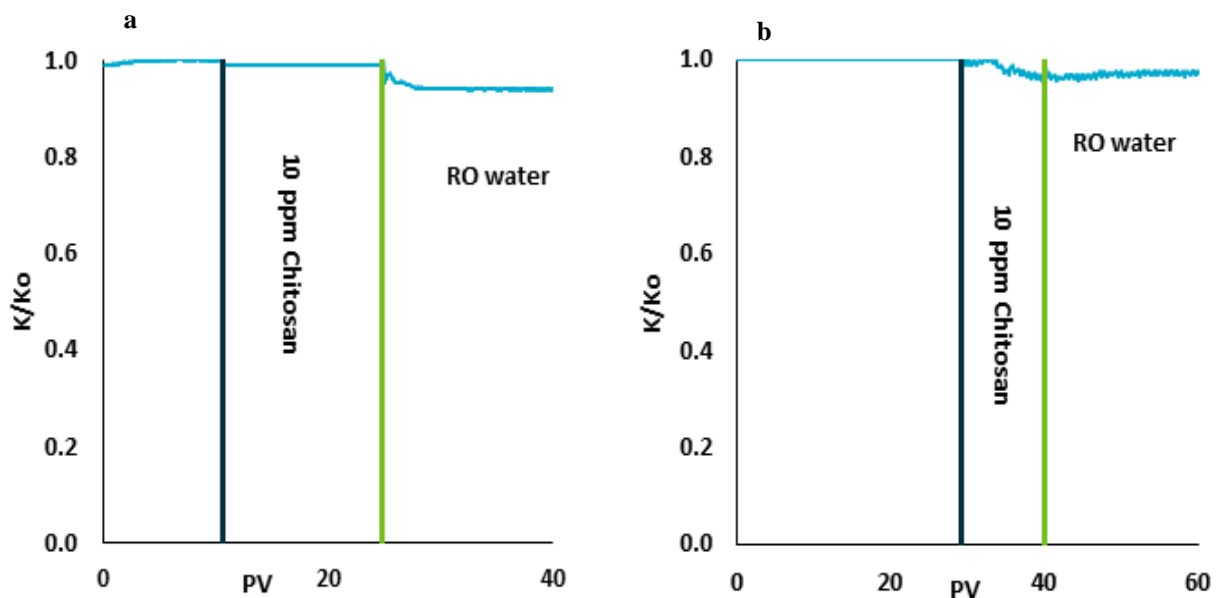


Figure 3.7. Representative plots of the relative permeability for two core samples with different length, 5 cm (a), and 10 cm (b) from Buff Berea sandstone when the core was treated with 10 ppm chitosan at pH=4

3.4.6 Effect of flow rate

To investigate the effect of flow rate (water velocity) on the clay release following chitosan treatment, a series of core-flooding tests were conducted in which the flow rate increased from 5 to 100 mL/min in several steps. It was observed that an increase in flow velocity caused negligible clay release or permeability change (data not shown). These results confirm the extremely high stabilizing effects of chitosan treatment may be attributed to the intercalation of more than one polymer layer on the clay particles.

3.4.7 Characterizing chitosan–clay composites

Zeta potential analysis was conducted to examine the charge characteristics of the clay particles treated with 10 ppm chitosan. It was observed that zeta potential values ranged from -35 mV for the bare clay to $+15$ mV upon adsorption of chitosan on clay particles (data not shown). The zeta potential of clay approached zero at 5 ppm chitosan concentration. Clay particles treated with a chitosan concentration higher than 10 ppm were positively charged indicating that clay aggregation may be promoted.

3.5 Conclusion

Experimental tests were performed to evaluate the chitosan ability as natural clay stabilizer for reducing clogging susceptibility of sandstone cores. It was shown that divalent cations (e.g. calcium) are effective to provide clay stabilization. However, the benefit of divalent ions is short term and these cations must be present continuously in the injection water. In contrast, chitosan can be added for a short period during an initial injection phase, which will provide a lasting effect for months without additional doses. The effect of several factors such as flow rate, chitosan concentration, and salt concentration on the stabilizing effect of the chitosan were examined. In conclusion, our laboratory tests demonstrated the effectiveness of chitosan, a natural bio-polymer, for preventing well clogging when freshwater is injected into a brackish groundwater.

4 Conclusions and Recommendations

An extensive series of laboratory experiments were conducted using selected core samples from the Precipice Sandstone aquifers to assess the impact of water re-injection on clay release and the associated clogging potential. The experiments provided data and insight into the reaction of the aquifer sediments to water chemistry and flow conditions. The main findings of this study are the following:

- 1) Kaolinite were found to be the predominant clay minerals among the colloidal particles deposited onto grain surfaces of sandstones from the Precipice Sandstone aquifers.
- 2) The mobilisation or release of clay particles is caused when the attractive force between the particles and grain surfaces is weakened. Clay particles were found to rapidly detach from grain surfaces when core samples were flushed with high salinity water followed by RO water or low salinity water (<30 mM). This mobilisation resulted in a high concentration zone of clay which moves through the core. Concentrations of clay suspension greater than 2 g/L was observed under the experimental conditions of this work. Small amount of quartz particles was also found in the core effluent samples.
- 3) Cation exchange processes between clay and bulk solution were found to be responsible for the weakening of the adhesive forces.
- 4) Kaolinite clay minerals were found to exhibit a strong cation exchange reaction when in contact with monovalent cation solutions. Conversely, these clay particles showed a very small rate of cation exchange when in contact with divalent cations.
- 5) The rate of cation exchange was found to be dependent on the salt concentration and pH of the water in contact with the clay.
- 6) The critical strength of NaCl solution which initiates rapid clay release in sandstone cores was found to be in the region of 30 mM at neutral pH.
- 7) The pH of the solution was a controlling parameter for cation-exchange between clays and flowing water. Low-pH conditions (pH<6) minimise clay release by inhibiting the exchange of the cations originally on clay surfaces with monovalent cations from the bulk solution. It is expected that the hydrogen ion interacts with clay surface charges to minimise the exchange process.
- 8) High pH conditions (pH > 8) promote colloid release and disaggregation processes. The hydroxide ion may interact with clay surfaces at high pH conditions resulting in double layer expansion.
- 9) Hydrodynamic shear forces alone at typical groundwater conditions are not effective to induce the release of attached clay particles. A weakening of the adhesive forces between the colloids and colloid-grain is a precursor for the clay release. This weakening allows double layer expansion to occur when RO water or low ionic strength solution come into contact with clays. The hydrodynamic shear force then become strong enough to initiate the release and subsequent clogging.
- 10) The underlying mechanism of permeability reduction (clogging) in sandstone cores where clay mobilisation occurred was found to be due to pore-plugging (hydrodynamic bridging) in the cores. Clay particles bridged at pore constrictions and the bridging probability was a function of clay concentration. We observed that the bridged clay particles could be released by flow reversal depending on their deposited condition.
- 11) We found lower values of zeta potential for the calcium form of clays compared to the sodium form. The charge density of the calcium clay was approximately half that of the sodium form. The observed permeability reduction in water sensitive aquifer materials was

attributed to fresh water invasion or water shock caused by osmotic effects as the salinity decreased.

12) The treatment of sandstone with divalent cations or mixtures of monovalent and divalent cations can significantly minimise the clay release rate. However, these cations may be removed from the clay particle surfaces by any subsequent flow of sufficiently concentrated monovalent solution. We observed an effective reduction of clay mobilization with relatively low concentrations of divalent cations. When only 10% of the cations in the injection water were divalent (calcium or magnesium), the permeability of the core was unaffected.

13) Chitosan was found to effectively prevent clay mobilisation and permeability. Negligible clay release and clogging was observed when core samples were subjected to RO water injection following chitosan treatment.

It was attempted to develop guidelines for injection water quality in order to minimize problems of compatibility between water and aquifer materials. It is proposed that the cation concentration, particularly divalent ions, of injection water should not be allowed to fall to levels below those dictated by the cation exchange capacities (CEC) of the clay minerals present in the aquifer formation. In core tests, kaolinite clays were shown to have a low exchange capacity of around 2 meq/L. Calcium potassium and ammonium ions are suggested as suitable candidates with treatment radii of 2-4 metres around the injection well.

For injection well in Precipice Sandstone aquifers, it appears that to avoid physical clogging within a few meters of the injection well, the well needs to be appropriately developed to remove colloidal particles in the near-well formation. For the aquifer material tested, maintaining salinity and divalent cation concentration above the salinity of the native groundwater appears sufficient to manage clogging issues.

5 References

- Australia Pacific LNG (2013) 2013 groundwater assessment.
- Allison, L.E. (1947) Effect of microorganisms on permeability of soil under prolonged submergence. *Soil Science*, 63: 439-450.
- Alvarez, A. C. (2005). Inverse problems for deep bed filtration in porous media. Ph.D., Instituto nacional de matematica pura e aplicada, Rio de Janeiro, Brasil.
- Appelo, C. A. J. and Postma, C. (1999). *Geochemistry, groundwater and pollution*. A.A. BalkemBaveye, P., Vandevivere, P. and De Lozada, D. (1992) Comment on “biofilm growth and the related changes in the physical properties of a porous medium. I. Experimental investigation” by S.W. Taylor and P.R. Jaffe. *Water Resources Research*. 28(5): 1481-1482.
- Bedrikovetsky, P., Marchesin, D., Shecaira, F., Souza, A. L., Milanez, P. V., and Rezende, E. (2001). Characterisation of deep bed filtration system from laboratory pressure drop measurements. *Journal of Petroleum Science and Engineering*, 32, 167-177.
- Bradford, S. A., S. R. Yates, M. Bettahar, and J. Simunek (2002). Physical factors affecting the transport and fate of colloids in saturated porous media. *Water Resour. Res.*, 38(12), 1327, doi:10.1029/2002WR001340.
- Bradford, S.A. and Torkzaban, S. (2008). Colloid Transport and Retention in Unsaturated Porous Media: A Review of Pore-Scale processes and Models. *Vadose Zone Journal*, 7:667- 681, DOI: 10.2136/vzj2007.0092.
- Civan, F. (2005). Applicability of the Vogel–Tammann–Fulcher Type Asymptotic Exponential Functions for Ice, Hydrates, and Polystyrene Latex. *Journal of Colloid and Interface Science*, 285, 429–432.
- Civan, F., (2007). *Reservoir Formation Damage, Fundamentals, Modeling, Assessment, and Mitigation*, Elsevier Inc.
- Clogging Issues Associated With Managed Aquifer Recharge Methods. IAH Commission on Managing Aquifer Recharge. In: Martin, R. (Ed.), (www.iah.org/recharge/clogging.htm).
- Derjaguin, B.V., Landau, L., (1941). *Acta Physicochim. U.R.S.S.*, 14, p. 633.
- de Zwart, A. H., (2007). Investigation of Clogging Processes in Unconsolidated Aquifers near Water Supply Wells. Ph.D., University of Technology Delft, Delft.
- Dillon, P., Pavelic, P., Massmann, G., Barry, K., Correll, R., 2001. Enhancement of the membrane filtration index (MFI) method for determining the clogging potential of turbid urban stormwater and reclaimed water used for aquifer storage and recovery. *Desalination* 140 (2), 153–165.
- Ehrlich, G.G. and Ku, H.F., Vecchioli, J; and Ehlke, T.A. (1979) Microbiological effects of recharging the Magogy aquifer, Bay Park, New York, with tertiary treated sewage. U.S. Geol. Surv. Prof. Pap. 751-E.
- Ehrlich, G.G., Ehlke, T.A., and Vecchioli, J. (1972) Microbiological aspects of ground water recharge injection of purified unchlorinated sewage effluent at Bay Park, Long Island, New York. *J. Res. U.S. Geol. Surv.* 1: 341-344.
- Ezeukwu, T., Thomas, R. L., and Gunnerod, T., (1998). Fines Migration Control in High-Water-Cut Nigerian Oil Wells,” *Journal of Petroleum Technology*, March, 88–89.
- Ford, H.W. (1982) Estimating the potential for ochre clogging before installing drains. *Trans.A.S.A.E.*, 25: 1597-1600.

- Forward P.D. (1994). Control of iron biofouling in submersible pumps in the Woolpunda Salt Interception Scheme in South Australia. Proc. of Water Down Under 94, The Institution of Engineers, Australia, Vol. 2, pp.169-174.
- Gdanski, R. D. and Shuchart, C. E., (1996). Newly Discovered Equilibrium Controls HF Stoichiometry. Journal of Petroleum Technology, February, 145–149.
- Goldenberg, L. C., Magaritz, M., Amiel, A. J., and Mandel, S.: 1984, Changes in hydraulic conductivity of laboratory sand-clay mixtures caused by a seawater-freshwater interface, J. Hydrol. 70, 329–336.
- Grolimund, D., Borkovec, M., 2006. Release of colloidal particles in natural porous media by monovalent and divalent cations. J. Contam. Hydrol. 87, 155–175
- Gregory, J., 1981. Approximate expression for retarded van der Waals interaction. J. Colloid Interface Sci. 83, 138–145.
- Gupta, R.P. and Swartzendruber, D. (1962) Flow associated reduction in the hydraulic conductivity of quartz sand. Soil Sci. Soc. Am. Proc. 26: 6-10.
- Gustafsson, T. K., Skrifvars, B. O., Sandstrom, K. V., and Waller, K. V., (1995). Modeling of pH for Control,” Industrial and Engineering Chemistry Research, 34, 820–827.
- Hayatdavoudi, A., (1998). Controlling Formation Damage Caused by Kaolinite Clay Minerals: Part II. SPE 39464 paper, SPE International Symposium on Formation Damage Control, Lafayette, Louisiana, February 18–19, 1998, 421–429.
- Hoyle, B.L. (1994) Biodegradation in saturated sand: Interactions between microbial population and sand matrix. PhD dissertation. University of California, Davis.
- Jackson, R., 1975. Some mathematical and physical aspects of continuum models for the motion of granular materials. In: Meyer, R.E. (Ed.), Theory of Dispersed Multiphase Flow. Academic Press, New York, NY.
- James-Smith, J., Shand, P., Hodgkin, T., Hill, T., Stadter, M. and Love, A. (2005) Aluminium hydroxide clogging of wells, Bookpurnong, South Australia: Conceptual model and Environmental risks. South Australia. Department of Water, Land and Biodiversity Conservation. DWLBC Report 2005/40.
- Herzig, J. P., Leclerc, D. M., and Le Goff, P. (1970). Flow of suspensions through porous media - application to deep filtration. Industrial and Engineering Chemistry, 65(5), 8-35.
- Hijnen, W.A.M. and van der Kooij, D., (1992). The effect of low concentrations of assimilable organic carbon (AOC) in water on biological clogging of sand beds. Water Research 26(7):963-972.
- Himes, R. E., Vinson, E. F., and Simon, D. E., (1991). Clay Stabilization in Low-Permeability Formations. SPE Production Engineering, August 1991, 252–258.
- Keelan, D. K. and Koepf, E. H., (1977). The Role of Cores and Core Analysis in Evaluation of Formation Damage. Journal of Petroleum Technology, May, 482–490.
- Khilar, K.C. and Fogler, H.S., (1998). Migration of Fines in Porous Media, Kluwer Academic, Dordrecht, Boston/London.
- Khilar, K.C. and Fogler, H.S.: "The Existence of a Critical Salt Concentration for Particle Release," J. Colloid Interface Sci. (1984) 101, 214.
- Khilar, K.C.: "The Water Sensitivity of Berea Sandstone," PhD thesis, U. of Michigan, Ann Arbor (1981).
- Kia, S.F., Fogler, H.S., Reed, M.G., Vaidya, R.N., 2001. Effect of salt composition on clay release in Berea sandstones. SPE Prod. Eng. 2, 277–283.

- Kretzschmar, R., Borkovec, M., Grolimund, D., and Elimelech, M. (1999). Mobile Subsurface Colloids and their Role in Contaminant Transport (Review Paper). *Advances in Agronomy*, 66, 121-194.
- Marsden, Z. (2001). Biochemical clogging processes during aquifer storage and recovery (ASR) with recycled water: laboratory experiment, South Australia. Flinders University of South Australia, School of Chemistry, Physics and Earth Sciences, Hons. Thesis.
- McCarthy, J. F. Z., J.M. (1989). Subsurface transport of contaminants. *Environ Sci Technol*, 23(5), 496-502.
- McDowell-Boyer, L. M., Hunt, J. R., and Sitar, N. (1986). Particle transport through porous media. *Water Resources Research*, 22(13), 1901-1921.
- Motta, E. P. D. and Santos, J. A. C. M. D. (1999). New Fluosilicic Acid System Removes Deep Clay Damage,” SPE 54729 paper, SPE European Formation Damage Conference, The Hague, The Netherlands, May 31–June 1, 239–245.
- Norman, C. A. and Smith, J. E. (2000). Experience Gained from 318 Injection Well KOH Clay Stabilization Treatments,” Paper SPE 60307, presented at the 2000 SPE Rocky Mountain Regional/Low Permeability Reservoirs Symposium and Exhibition held in Denver, CO, March 12–15.
- Pavelic, P., Dillon, P.J., Barry, K.E., Vanderzalm, J.L., Correll, R.L. and Rinck-Pfeiffer, S.M. (2007) Water quality effects on clogging rates during reclaimed water ASR in a carbonate aquifer. *Journal of Hydrology* 334:1-16.
- Prommer et al., 2015. Understanding and quantifying the geochemical response to re-injection of CSG water permeates, brines and blends. CSIRO, Australia (in preparation).
- Okubo, T. & Matsumoto, J. (1983) Biological clogging of sand and changes of organic constituents during artificial recharge. *Water Research*, 17 (7): 813-821.
- Olsthoorn T. N. (1982) The clogging of recharge wells, main subject. KIWA Communications-72, The Netherlands Testing and Research Institute, Rijswijk, The Netherlands
- Ouyang, Y., Shinde, D., Mansell, R. S., and Harris, W. (1996). Colloid-enhanced transport of chemicals in subsurface environments: a review. *Critical Reviews in Environmental Science and Technology*, 26(2), 189-204.
- Page, D, Vanderzalm, J, Miotlinski, K, Barry, K, Dillon, P, Lawrie, K and Brodie, RS (2014). Determining treatment requirements for turbid water to avoid clogging of aquifer storage and recovery wells in siliceous alluvium. *Water Research* 66, 99-110.
- Pavelic, P. and Dillon, P.J. (1997). Review of international experience in injecting natural and reclaimed waters into aquifers for storage and reuse. Centre for Groundwater Studies Report No. 74, May 1997.
- Pavelic, P., Vanderzalm, J., Dillon P., Herczeg, A., Barry, K., Levett, K., Mimoso, J., and Magarey, P. (2007). Assessment of the Potential for Well Clogging Associated with Salt Water Interception and Deep Injection at Chowilla, SA[R]. Final Report to Department of Water, Land, Biodiversity and Conservation.
- Penny, G. S. (1983). Enhanced Load Water-Recovery Technique Improves Stimulation Results,” SPE 12149 paper, SPE Annual Technical Conference and Exhibition, San Francisco, California, September 5–8.
- Pyne, R.D.G. (2005). Aquifer storage recovery; A Guide to groundwater recharge through wells. ASR Systems Publications, Gainesville, Florida, USA.
- Ragusa, S., de Zoysa, D.S. and Rengasamy, P. (1994) The effect of microorganisms, salinity and turbidity on hydraulic conductivity of irrigation channel soil. *Irrig. Sci.* 15: 159-166.

- Rajagopalan, R. a. T., C. (1976). Trajectory analysis of deep-bed filtration with the sphere-in-cell porous model." *AIChE Journal*, 22(3), 523-533.
- Ralph, D.E. and Stevenson, J.M. (1995) The role of bacteria in well clogging. *Water. Research.* 29(1): 365-369.
- Ramachandran, V., Fogler, S.H. (1999). Plugging by hydrodynamic bridging during flow of stable colloidal particles within cylindrical pores. *Journal of Fluid Mechanics*, 385, 29-156.
- Rebhun, M. and Schwarz, J. (1968) Clogging and contamination processes in recharge wells. *Wat. Res.*, 4: 1207-1217.
- Reed, M. G. (1974). Formation Permeability Maintenance with Hydroxy-Aluminum Solutions," U.S. Patent No. 3,827,500, August 6, 1974.
- Rinck-Pfeiffer, S.; S. Ragusa; P. Sztajn bok; & T. Vandevelde. (2000) Interrelationships between biological, chemical and physical processes at an analog in aquifer storage and recovery (ASR) wells. *Water Research*, 34(7): 2110-2118.
- Ryan, J. N., and Elimelech, M. (1996). Review Colloid mobilisation and transport in groundwater. *Colloids and surfaces A: Physicochemical and Engineering Aspects*, 107, 1-56.
- Sen, T. K., and Khilar, K. C. (2006). Review on subsurface colloids and colloid-associated contaminant transport in saturated porous media. *Advances in Colloid and Interface Science*, 119(2-3), 71-96.
- Shaw, J.C., Bramhill, B., Wardlaw, N.C. and Costerton, J.W. (1985) Bacterial fouling in a model core system. *Appl. Environ. Microbiol.*, 49: 693-701.
- Sharma, M. M., Y. C. Yortsos, and L.L. Handy, "Release and Deposition of Clays in Sandstones", *SPE Symposium on Oilfield and Geothermal Chemistry*, 04/1985.
- Sposito, G. 2001. *Geochemistry in Soil Science*. In W. Chesworth (ed.), *Encyclopedia of Soil Science*, pp. 283-289. Springer, New York.
- Sposito, G. (2008). *The Chemistry of Soils*. 2nd Ed. Oxford University Press, New York.
- Sreekanth, J. and Moore, C. (2015). CSG water injection impacts: Modelling, uncertainty and risk analysis; Groundwater flow and transport modelling and uncertainty analysis to quantify the water quantity and quality impacts of a coal seam gas produced water injection scheme in the Surat Basin, Queensland. CSIRO, Australia.
- Tchistiakov, A. A. (2000). Colloid Chemistry of In-Situ Clay-Induced Formation Damage. *SPE*, 58747.
- Thomas, R. L. and Crowe, C. W. (1978). Matrix Treatment Employs New Acid System for Stimulation and Control of Fines Migration in Sandstone Formations, 1978.
- Thomas, R. L., Saxon, A., and Milne, A. W. (1998). The Use of Coiled Tubing During Matrix Acidizing of Carbonate Reservoirs Completed in Horizontal, Deviated, and Vertical Wells," *SPE Production & Facilities*, August, 147-162.
- Torkzaban, S., S.A. Bradford, S.L. Walker. (2007) Resolving the Coupled Effects of Hydrodynamics and DLVO Forces on Colloid Attachment to Collector Surfaces. *Langmuir*, 23(19); 9652-9660.
- Tufenkji, N. a. E. (2004). Correlation Equation for Predicting Single-Collector Efficiency in Physicochemical Filtration in Saturated Porous Media. *Environ Sci Technol*, 38(2), 529-536.
- Van Beek, C.G.E.M and van der Kooij, D. (1982) Sulfate-reducing bacteria in groundwater from clogging and non-clogging shallow wells in the Netherlands river region. *Ground Water*, 20: 298-302.
- Vecchioli, J. (1970) A note on bacterial growth around a recharge well at Bay Park, Long Island, New York. *Wat. Res.*, 6 : 1415-1419.

- Vandevivere, P. and Baveye, P. (1992a) Saturated hydraulic conductivity reduction caused by aerobic bacteria in sand columns. *Soil Sci. Soc. Am. J.*, 56 (1) : 1-13.
- Verwey, E.J.W., Overbeek, J.T.G. (1948) *Theory of the Stability of Lyophobic Colloids* Elsevier, Amsterdam.
- Wennberg, K. E., and Sharma, M. M. (1997). Determination of the Filtration Coefficient and the Transition Time for Water Injection Wells. SPE, 38181.
- Yao, K. M., Habibian, T., and O'Melia, C.R. (1971). Water and Waste Water Filtration: Concepts and Applications. *Environmental Science and Technology*, 5(11), 1105-1112.
- Zaitoun, A. and Berton, N. (1996). Stabilization of Montmorillonite Clay in Porous Media by Polyacrylamides, SPE 31109 paper, SPE Formation Damage Control Symposium, Lafayette, Louisiana, February 14–15, 1996, 423–428.
- Zhou, Z., 1995. Construction and application of clay-swelling diagrams by use of XRD methods. *J. Pet. Technol.* 306.

Appendix A

Core Samples from Reedy Creek

Core Tube	Plug ID	Porosity (%)	Length (cm)	Saturated with	Hydraulic conductivity (m/day)
MB3H_064	RC_64_1	18	8	0.5M NaCl	0.16
	RC_64_2	17		0.5M NaCl	0.11
	RC_64_3	21		0.5M NaCl	0.05
	RC_64_4	19	5	0.5M NaCl	0.13
	RC_64_5	20		0.5M NaCl	0.09
	RC_64_6	21		0.5M NaCl	0.11
	RC_64_7	19		0.1M CaCl ₂	0.1
	RC_64_8	18		0.1M CaCl ₂	0.12
	RC_64_9	14		Mixed salt	0.13
	RC_64_10			Mixed salt	0.13
	RC_64_11			Mixed salt	0.11
	RC_64_12			Mixed salt	0.14
	RC_64_13			Mixed salt	0.09
	RC_64_14			Mixed salt	0.19
	RC_64_15			Mixed salt	0.12
MB3H_067	RC_67_1	19	5	0.5M NaCl	0.13
	RC_67_2	18		0.5M NaCl	0.09
	RC_67_3	15		0.5M NaCl	0.11
	RC_67_4			0.5M NaCl	0.06
	RC_67_5			0.5M NaCl	0.14
	RC_67_6		0.5M NaCl	0.1	
	RC_67_7		8	0.1M CaCl ₂	0.15
	RC_67_8			0.1M CaCl ₂	0.11
	RC_67_9			Mixed salt	0.15
	RC_67_10		5	Mixed salt	0.11
	RC_67_11	19		Mixed salt	0.18
	RC_67_12			Mixed salt	0.19
	RC_67_13			Mixed salt	0.08
	RC_67_14			Mixed salt	0.14
	RC_67_15		Mixed salt	0.12	

MB3H_076	RC_76_1	20	8	0.5M NaCl	2.2
	RC_76_2	22		0.5M NaCl	2.3
	RC_76_3	22		0.5M NaCl	2.2
	RC_76_4	23	5	0.5M NaCl	2.3
	RC_76_5	23		0.5M NaCl	2.1
	RC_76_6			0.5M NaCl	2.4
	RC_76_7			0.1M CaCl ₂	2.4
	RC_76_8			0.1M CaCl ₂	2.2
	RC_76_9			Mixed salt	2.1
	RC_76_10			Mixed salt	2.2
	RC_76_11			Mixed salt	2.3
	RC_76_12			Mixed salt	2.1
	RC_76_13			Mixed salt	2.4
	RC_76_14			Mixed salt	2.4
	RC_76_15				

Core samples from Condabri

Core Tube	Plug ID	Porosity (%)	Length (cm)	Saturated with	Hydraulic conductivity (m/day)
MB94_A69	C_69_1	20	5	0.5M NaCl	0.08
	C_69_2			0.5M NaCl	0.09
	C_69_3			0.5M NaCl	0.14
	C_69_4			0.5M NaCl	0.07
	C_69_5			0.5M NaCl	0.13
	C_69_6			0.5M NaCl	0.09
	C_69_7			0.1M CaCl ₂	0.14
	C_69_8			0.1M CaCl ₂	0.08
	C_69_9			Mixed salt	0.12
	C_69_10			Mixed salt	0.2
	C_69_11			Mixed salt	0.14
	C_69_12			Mixed salt	0.06
	C_69_13			Mixed salt	0.13
	C_69_14			Mixed salt	0.13
	C_69_15			Mixed salt	0.17

MB9H_71	C_71_1	23	8	0.5M NaCl	0.08
	C_71_2			0.5M NaCl	0.09
	C_71_3			0.5M NaCl	0.17
	C_71_4		5	0.5M NaCl	0.09
	C_71_5			0.5M NaCl	0.16
	C_71_6			0.5M NaCl	0.13
	C_71_7			0.1M CaCl ₂	0.14
	C_71_8			0.1M CaCl ₂	0.12
	C_71_9			Mixed salt	0.13
	C_71_10			Mixed salt	0.17
	C_71_11			Mixed salt	0.11
	C_71_12			Mixed salt	0.15
	C_71_13			Mixed salt	0.21
	C_71_14			Mixed salt	0.16
	C_71_15			Mixed salt	0.05
MB9H_74	C_74_1	22	5	0.5M NaCl	0.08
	C_74_2			0.5M NaCl	0.13
	C_74_3			0.5M NaCl	0.08
	C_74_4			0.5M NaCl	0.11
	C_74_5			0.5M NaCl	0.15
	C_74_6			0.5M NaCl	0.12
	C_74_7			0.1M CaCl ₂	0.09
	C_74_8			0.1M CaCl ₂	0.13
	C_74_9			Mixed salt	0.18
	C_74_10			Mixed salt	0.12
	C_74_11			Mixed salt	0.09
	C_74_12		8	Mixed salt	0.12
	C_74_13			Mixed salt	0.31
	C_74_14			Mixed salt	0.18

Appendix B

Understanding the transport process of colloidal particles to establish potential physical clogging during water re-injection- laboratory batch and column studies

1. Introduction

An understanding and ability to predict the transport and fate of colloids such as viruses, bacteria, protozoa, clay minerals, and engineered nanoparticles in porous media is essential for a wide variety of environmental and engineering applications (Bradford et al., 2014; Schijven and Hassanizadeh, 2000; Torkzaban et al., 2013; Mondal and Sleep, 2013). Colloid transport and fate are strongly influenced by retention in porous media (Ryan and Elimelech, 1996; Shen et al., 2008). Extensive theoretical and experimental studies have therefore been devoted to understanding and quantifying colloid retention in porous media (reviews are given by Bradford et al., 2014; Ginn et al., 2002; Harvey et al., 2002; Jin and Flury, 2002). It has been shown that colloid retention depends on a range of physicochemical and hydrodynamic conditions (Torkzaban et al., 2008; Li and Johnson, 2005; Li et al., 2004; Tufenkji and Elimelech, 2004; Pensini et al., 2012). Batch and column experiments are the most common methods to study colloid retention in saturated porous media. These experimental techniques offer the advantage that retention can be examined under well-defined conditions. However, numerous discrepancies between batch and column results have been reported in the literature (e.g. Bales et al., 1991; Sadeghi et al., 2013; Zhao et al., 2008).

Packed-column experiments are commonly utilized to study colloid transport and retention processes over a range of physical and chemical conditions. Analysis of colloid breakthrough curves (BTCs), and sometimes retention profiles (RPs) following completion of the experiment, are used to determine values of attachment and detachment rate constants (Harvey and Garabedian, 1991; Johnson et al., 2007; Schijven et al., 2000; Tong et al., 2005). These retention parameters are determined by fitting the solution of a mass balance transport model to experimental BTCs and/or RPs (Kim et al., 2009). The bulk of existing literature from column studies considers colloid transport to be controlled by attachment and detachment processes (Bradford et al., 2014; Schijven et al., 2000). These studies have demonstrated that the diffusion-controlled detachment rate is very slow during steady-state flow and chemical conditions (Torkzaban et al., 2013; Ryan and Elimelech, 1996). In addition to attachment, colloid straining (retention in grain-grain contacts and surface roughness) may also play a significant role in colloid retention (Bradford et al., 2013b; Ma et al., 2011). However, determination of the relative contribution of attachment and straining to retention is difficult, if not impossible, from only BTC and RP information (Bradford et al., 2009). Microscopic observations have been employed to identify specific mechanisms of colloid retention, but quantitative determination of the relative contributions of these mechanisms is still not possible. Moreover, recent studies have pointed out that colloid retention in packed-bed columns is limited to only a small fraction of the solid surfaces, and blocking-type behavior is typically observed if the input colloid concentration is high and/or the colloid injection continues for a relatively long time (Brown and Abramson, 2006).

Batch experiments are carried out by adding a quantity of solid (e.g. sand) into a solution containing a known concentration of colloids. The mixture is subsequently shaken for a sufficient period of time to reach a steady-state (equilibrium) condition. The final concentration of colloids in solution is measured and the amount of attached colloids is calculated from mass balance calculations. The apparent steady-state concentrations are used to construct equilibrium isotherms

using linear, Langmuir, or Freundlich models (Yates et al., 1987). The attachment process is typically considered to be linear and reversible (Schijven and Hassanizadeh, 2000). In this case, a distribution coefficient (K_D) is calculated and converted to a retardation factor (R) that may be used in transport studies. Colloid attachment and detachment rate coefficients can also be determined from batch studies provided that the colloid concentration in the aqueous phase is measured at various times before the steady-state concentration is reached (Sadeghi et al., 2013). However, attachment and detachment rates from batch experiments have not always been consistent and reproducible due to some yet-unknown factors (Chrysikopoulos and Aravantinou, 2012; Sadeghi et al., 2013; Syngouna and Chrysikopoulos, 2010; Thompson et al., 1998; Thompson and Yates, 1999; Zhao et al., 2008). Such factors may include the type and size of the container, the presence or absence of the air-water interface in the system, the method of shaking to achieve complete mixing, and the ratio of solid and liquid phases in the container.

A potential advantage of batch experiments is that they involve less space and labor than column studies. However, results of batch studies have not been consistent with those of column or field experiments (Sadeghi et al., 2013; Schijven and Hassanizadeh, 2000). Column experiments usually show no retardation in the BTCs, suggesting that a kinetic attachment process should be considered and that the rates of attachment and detachment are slow (Bales et al., 1991; Johnson and Elimelech, 1995; Kim et al., 2009). Batch experiments have been found to either overestimate (Sadeghi et al., 2013; Schijven et al., 2000; Zhao et al., 2008) or underestimate colloid attachment compared with that observed in column studies (Schijven et al., 2000; Torkzaban et al., 2008). This discrepancy has been attributed to the time duration of batch experiments and the selected solid/solution ratios (Sadeghi et al., 2013). Alternatively, differences in batch and column experiments may also be related to the hydrodynamic conditions, surface roughness, and pore structure. In particular, the solid phase is continuously mixed and the flow direction changes during batch experiments. This facilitates the collision of colloids to the solid phase, and possibly higher attachment rates, but also eliminates the pore structure and continuously changes the applied hydrodynamic (T_H) and resisting adhesive (T_A) torques that act on the colloids retained at roughness locations on the solid phase. Conversely, the solid phase in column experiments is stationary, and the colloids retained at surface roughness locations and grain-grain contacts will always experience a lower applied hydrodynamic torque and greater resisting adhesive torque (Bergendahl and Grasso, 2000; Bradford et al., 2009; Ma et al., 2011; Torkzaban et al., 2010). The solid surface area associated with colloid retention is therefore expected to be greater in column than batch systems. Furthermore, the potential influence of blocking on the kinetic of colloid attachment has not been investigated in batch studies.

This study has been explicitly designed to provide a critical and systematic comparison between batch and column experiments. The aim was to investigate the underlying factors causing the commonly observed discrepancies in colloid adsorption in column and batch experiments. We examined the adsorption behavior of four different sizes of carboxylate-modified latex (CML) microspheres in batch and column experiments. The advantage of using CML microspheres is that the influence of confounding factors on retention data can be minimized; e.g, particle aggregation for engineered nanoparticles, and inactivation and growth for microbes. Our results show that colloid adsorption in batch systems should be considered as an irreversible attachment process with a blocking behavior. The rate of attachment and the fraction of the surface area contributing to colloid immobilization (S_f) were much smaller in batch than column experiments due to differences in the hydrodynamics, and the role of surface roughness and pore structure. Results from column and batch experiments were generally not comparable, especially for larger colloids ($\geq 0.5 \mu\text{m}$). We believe this study is the first to systematically compare differences in colloid retention in batch and column studies.

2. Material and Methods

2.1. Colloids, Sand, and Electrolyte Solutions

Ultra pure quartz sand (Charles B. Chrystal Co., Inc., NY) was employed as the porous media for the column and batch experiments. The median grain diameter of the sand was 250 μm , and the coefficient of uniformity was 1.4 ($U = d_{60}/d_{10}$), where $x\%$ of the mass is finer than d_x). Prior to use the quartz was cleaned thoroughly to remove impurities. The cleaning steps included soaking the sand in 37 % HCl (Fisher) for 24 hours, washing in deionised water and drying at 105 $^{\circ}\text{C}$.

Various electrolyte solutions were made using Milli-Q water as the aqueous solution. The pH was unbuffered and ranged from 5.6 to 5.8. The solution IS was adjusted by adding NaCl to achieve IS ranging from 0-800 mM (Merck Pty Ltd., Product 10241J, AnalaR).

Fluoresbrite®Yellow-Green CML microspheres (Polysciences, Inc.) were used as model colloids in batch and column experiments due to their spherical shape, well-defined size and surface charge, and ease in detection at low concentration. Four sizes (2, 1, 0.5 and 0.1 μm) of CML microspheres were used in batch experiments, whereas only three sizes (2, 0.5 and 0.1 μm) were employed in column experiments. The colloid concentration was determined using a fluorometer (Synergy Mx F Monochromator-Based Fluorescence Microplate Reader, Biotec) at an excitation wavelength of 441 nm and an emission wavelength of 486 nm. Stock suspensions from the manufacturer were diluted in selected electrolyte solutions to achieve an initial concentration (C_0) for batch experiments of 1.4×10^6 , 1.1×10^7 , 9.1×10^7 , and 2.8×10^{10} N_cmL^{-1} for the 2, 1, 0.5, and 0.1 μm colloids, respectively. Several batch experiments with the 0.1 and 0.5 μm colloids were also conducted at a higher initial concentration of 2.0×10^8 and 9.1×10^8 N_cmL^{-1} for the 0.5 μm and 6.3×10^{10} and 2.8×10^{11} N_cmL^{-1} for the 0.1, μm colloids. For the column experiment influent concentrations of 1.1×10^6 , 7.3×10^7 and 2.3×10^{10} N_cmL^{-1} for the 2, 0.5 and 0.1 μm colloids, respectively were used.

2.2. Electrokinetic Characterization and DLVO Calculations

The electrophoretic mobility of the colloids and crushed sand grains was measured in various NaCl electrolyte solutions using a Zetasizer (Malvern, Zetasizer Nano Series, Nano-ZS). The Smoluchowski equation was used to convert the measured electrophoretic mobility values to zeta potentials. The measurements were repeated five times for each colloid suspension. Average zeta potential values are reported in Table B.1. Classical DLVO theory (Derjaguin and Landau, 1941) was used to calculate the total interaction energy (the sum of London-van der Waals attraction and electrostatic double-layer repulsion) for the colloids upon close approach to quartz surfaces (assuming sphere-plate interactions) for the various IS solutions used in our experiments. Retarded London-van der Waals attractive interaction force was determined from the expression of Gregory (1981) utilizing a value of 4.04×10^{-21} J for the Hamaker constant (Bergendahl and Grasso, 1999) to represent the latex-water-quartz system. In these calculations, constant-potential electrostatic double layer interactions were quantified using the expression of Hogg et al., (1966), with zeta potentials in place of surface potentials.

2.3. Batch Experiments

Batch experiments were conducted to determine the attachment behavior of the CML colloids to quartz sand in the absence of pore structure, where the entire system is in motion. These experiments were conducted by placing 31 g of sand and 31 mL of a known initial concentration of the colloid suspension into 42 mL glass tubes with the temperature kept at approximately 20 $^{\circ}\text{C}$. All tubes were completely filled with the colloid suspension to eliminate any presence of air, which might influence colloidal attachment in the system (Lazouskaya and Jin, 2008; Thompson et al., 1998; Thompson and Yates, 1999). Various solution IS were considered in the batch studies, as indicated in Table B.1. To provide complete mixture of the system during the experiment, the

tubes were rotated on a 45 degree angle with a tube rotator (Scilogex, Mx-Rd-Pro LCD) at a speed of 10 rpm. The colloid concentration was determined in the batch system at time intervals of 0, 10, 20, 30, 60, 120 and 180 minutes (total of 3 hours). Following the completion of the attachment phase (i.e., 3 hr of continuous shaking), some of the batch tubes underwent additional experimental phase to examine the reversibility of colloid attachment in the batch system. In this case, the colloid suspension in the batch tubes was removed and replaced with colloid-free electrolyte solution of the same chemical composition. The tubes were subsequently shaken for another 2 hours, and the initial and final colloid concentration of the aqueous phase was measured. Duplicates were carried out for all experiments to ensure repeatability. Additionally, a set of control tubes with only colloid suspension was prepared to ensure the stability of the colloids over the course of the experiments. Control tubes of sand and electrolyte solutions without colloids were also performed to measure the background colloid concentration originating from the sand. It was confirmed that the fluorometer did not detect any background colloid concentration originating from the sand over the range of tested IS.

The decrease in colloid concentration with time in the batch systems was attributed to attachment to the sand surface. The governing equations describing first-order attachment and detachment processes are given as:

$$V_w \frac{\partial C}{\partial t} = -V_w k_{att} \psi C + M_s k_{det} S \quad [1]$$

$$M_s \frac{\partial S}{\partial t} = V_w k_{att} \psi C - M_s k_{det} S \quad [2]$$

where C [$N_c L^{-3}$; where N_c and L denote the number of colloids and units of length, respectively] is the colloid concentration in the aqueous phase, t [T ; T denotes units of time] is time, M_s [M ; M denotes units of mass] is the dry mass of sand, S [$N_c M^{-1}$] is the solid phase concentration of attached colloids, V_w [L^3] is the volume of water, k_{att} [T^{-1}] is the colloid attachment coefficient, k_{det} [T^{-1}] is the colloid detachment coefficient, and ψ [-] is a dimensionless function that is used to account for a reduction in the attachment rate due to blocking (filling up) of favorable attachment sites. A Langmuirian model is used to describe ψ as (Adamczyk et al., 1994):

$$\psi = \frac{S_{max} - S}{S_{max}} = 1 - \frac{S}{S_{max}} \quad [3]$$

where S_{max} [$N_c M^{-1}$] is the maximum solid phase concentration of attached colloids. Equations [1]-[3] were numerically solved using the COMSOL software package (COMSOL, Inc., Palo Alto, California), subject to the initial conditions ($t=0$) of $C=C_0$ and $S=0$. The model parameters C_0 , M_s , and V_w were obtained directly from experimental measurements, whereas the values of k_{att} and S_{max} were determined by fitting of Eqs. [1]-[3] to observed batch concentration data. In all cases, the k_{det} value was set to zero as discussed later in the paper.

The fraction of the solid surface area that is available for attachment (S_f) may be determined from fitted S_{max} values using the following equation:

$$S_f = \frac{A_c \rho_b S_{max}}{(1-\gamma) A_s} \quad [4]$$

where A_c [$L^2 N_c^{-1}$] is the cross section area per colloid, A_s [L^{-1}] is the solid surface area per unit volume, i.e. the collector surface area per unit volume of porous media, and γ [-] is the porosity of a monolayer packing of colloids on the solid surface. In this work we assume a value of $\gamma = 0.5$ in all simulations based on information presented by Johnson and Elimelech, (1995).

2.4. Column Experiments

The column experiments were performed using acrylic columns with a length of 11 cm and a radius of 1 cm. The columns were wet packed, where the water level was always kept above the sand surface, with ~45 g of quartz sand. The average grain diameter of the sand was 255 μm , and the grain size ranged between 106-300 μm . The porosity was calculated gravimetrically to be 0.4, and the volume associated with one pore volume (PV) was 13.8 cm^3 . A syringe pump (Harvard Apparatus 22) was used to pump the solutions into the column at a steady rate. A fraction

collector (Spectra/Chrom® CF-1 Fraction Collector) was used to continuously collect the effluent samples. The average pore water velocity was maintained at 5 m/d for all experiments. A pulse of colloid suspension was injected for three pore volumes (PV), followed by a colloid-free electrolyte solution. Colloid transport experiments were conducted in duplicate at each solution IS. Sodium Nitrate (NaNO₃) was used as a conservative tracer to determine the pore water velocity and the dispersivity. Two pore volumes of 1 mM NaNO₃ was pumped into the column and the breakthrough of NO₃⁻ was monitored by measuring the absorbance of the effluent at 210 nm using a spectrophotometer.

The HYDRUS-1D code (Simunek et al., 2005) was used to simulate the colloid transport and retention in the columns. Relevant aspects of this code are described below. The code numerically solves the advection-dispersion equation that accounts for colloid retention in the column as given below:

$$\frac{\partial C}{\partial t} = \lambda v \frac{\partial^2 C}{\partial z^2} - v \frac{\partial C}{\partial z} - r_d \quad [5]$$

where λ [L] is the dispersivity, v [LT⁻¹] is the average pore-water velocity, and r_d [N_cL⁻³T⁻¹] is the retention rate of colloids on the solid phase. The value of r_d is given by:

$$r_d = \rho_b \frac{\partial S}{\partial t} = nk_{att} \left(1 - \frac{S}{S_{max}}\right) C - \rho_b k_{det} S \quad [6]$$

where ρ_b [ML³] is the sand bulk density and n [-] is the porosity. HYDRUS-1D is coupled to a non-linear least squares optimization routine based on the Levenberg-Marquardt algorithm (Marquardt, 1963) to fit model parameters (i.e. S_{max} , k_{att}) to breakthrough curves.

3. Results and Discussion

3.1. DLVO Calculations

Table B.1 shows that the zeta potential of the colloids and sand became less negative as the IS increased due to compression of the electrostatic double layer thickness (Bhattacharjee et al., 1998). This data was used in DLVO calculations to estimate the total interaction energy between colloids (2, 1, 0.5 and 0.1 μm) and the quartz collectors for the various IS levels. The energy barrier heights, and depths and separation distances for the secondary minima are listed in Table B.1. These DLVO calculations predict the absence of a repulsive energy barrier to colloid attachment to the sand surface and the existence of primary minimum interactions when IS ≥ 100 mM. Conversely, a substantial energy barrier is predicted to occur for all of these colloids when the IS ≤ 50 mM. The energy barriers increase with an increase in colloid size and a decrease in IS, ranging from 3.2 kT at IS = 100 mM for 0.1 μm colloids to over 4000 kT at IS = 1 mM for 2 μm colloids. These energy barriers suggest that it is unlikely for the colloids to attach in the primary energy minimum when the IS ≤ 100 mM. Furthermore, macroscale chemical heterogeneities that may produce primary minimum interactions are expected to be negligible for the ultra-pure quartz sand. However, colloid retention in a secondary minimum is possible when the depth of the secondary minimum is greater than the thermal energy of diffusing colloids (Shen et al., 2007; Simoni et al., 1998). This occurs when the absolute magnitude of the secondary energy minimum is greater than around 1.5 kT. The depth of the secondary minimum tends to increase with colloid size and IS as shown in Table B.1.

3.2. Batch Experiments

Batch experiments were conducted over a wide range of solution IS in order to systematically examine the attachment and detachment behavior of the various colloid sizes (2, 1, 0.5, and 0.1 μm). Figure B.1 presents plots of the normalized colloid concentrations (C/C_0 ; where C_0 is the initial colloid concentration) as function of time for the various IS and colloid sizes in the batch systems. We did not observe any colloid attachment to the sand surfaces at IS = 1 or 10 mM for all colloid sizes. However, the concentration of colloids in the solution began to decrease with further increases in the IS as a result of attachment. In general, values of C/C_0 rapidly decreased with time and then eventually approached a quasi-steady state concentration level. The amount

and dynamics of the colloid attachment process were strong functions of the solution IS and the colloid size; increasing with IS and decreasing with colloid size. Each of these observations will be examined in detail below.

Table B.1. The average of zeta potentials of colloids and quartz sand as well as calculated DLVO interaction parameters in the indicated solution chemistries

D _c (μm)	IS (mM)	Zeta potential (mV)		Energy barrier (kT)	Secondary min. depth (kT)	Secondary min. separation (nm)
		Colloid	Sand			
2	1	-68	-40	4403	-0.65	149
2	10	-48	-22	1543	-3.5	35.5
2	50	-37	-15	556	-10.6	12
2	100	-21	-11	73	-20.4	6
2	300	-16	-10	ND ^a	ND	ND
2	500	-12	-9	ND	ND	ND
1	1	-65	-40	2121	-0.24	151
1	10	-59	-22	949	-1.5	37
1	50	-34	-15	245	-5.1	12
1	100	-27	-11	69	-9.2	6.5
1	300	-21	-10	ND	ND	ND
1	500	-17	-9	ND	ND	ND
0.5	1	-60	-40	993	0.08	154
0.5	10	-51	-22	411	-0.6	36.5
0.5	30	-49	-19	300	-1.5	18.5
0.5	50	-34	-15	123	-2.4	12
0.5	100	-22	-11	22	-4.6	6
0.5	300	-17	-10	ND	ND	ND
0.1	1	-58	-40	194	-0.002	178
0.1	10	-52	-22	85	-0.05	39.5
0.1	30	-43	-19	52	-0.16	19
0.1	50	-32	-15	23	-0.3	12.5
0.1	100	-19	-11	3.2	-0.7	6
0.1	300	-15	-10	ND	ND	ND

^a Not determined

A first-order kinetic attachment and detachment model (Eq. [1] and [2] with $\psi=1$) is commonly used to simulate the kinetic of colloid attachment in batch systems (Schijven and Hassanizadeh, 2000). In this case, the value of C/C_0 is assumed to approach equilibrium conditions as time increases. If colloid attachment is consistent with a linear and equilibrium adsorption process, then an equilibrium partition coefficient between colloids in the aqueous and solid phases (K_D) can be defined in terms of k_{att} and k_{det} as $K_D = \frac{V_w k_{att}}{M_s k_{det}}$ (Schijven and Hassanizadeh, 2000). The value of K_D can be related to a retardation coefficient for breakthrough concentrations (BTCs) obtained in transport studies. Alternatively, the trend of decreasing C/C_0 with time can also be explained by irreversible attachment and blocking (filling up) of available attachment sites (Eq. [1] and [2] with $k_{det} = 0$). The ability of these two model descriptions to describe colloid attachment in the batch systems will be discussed below.

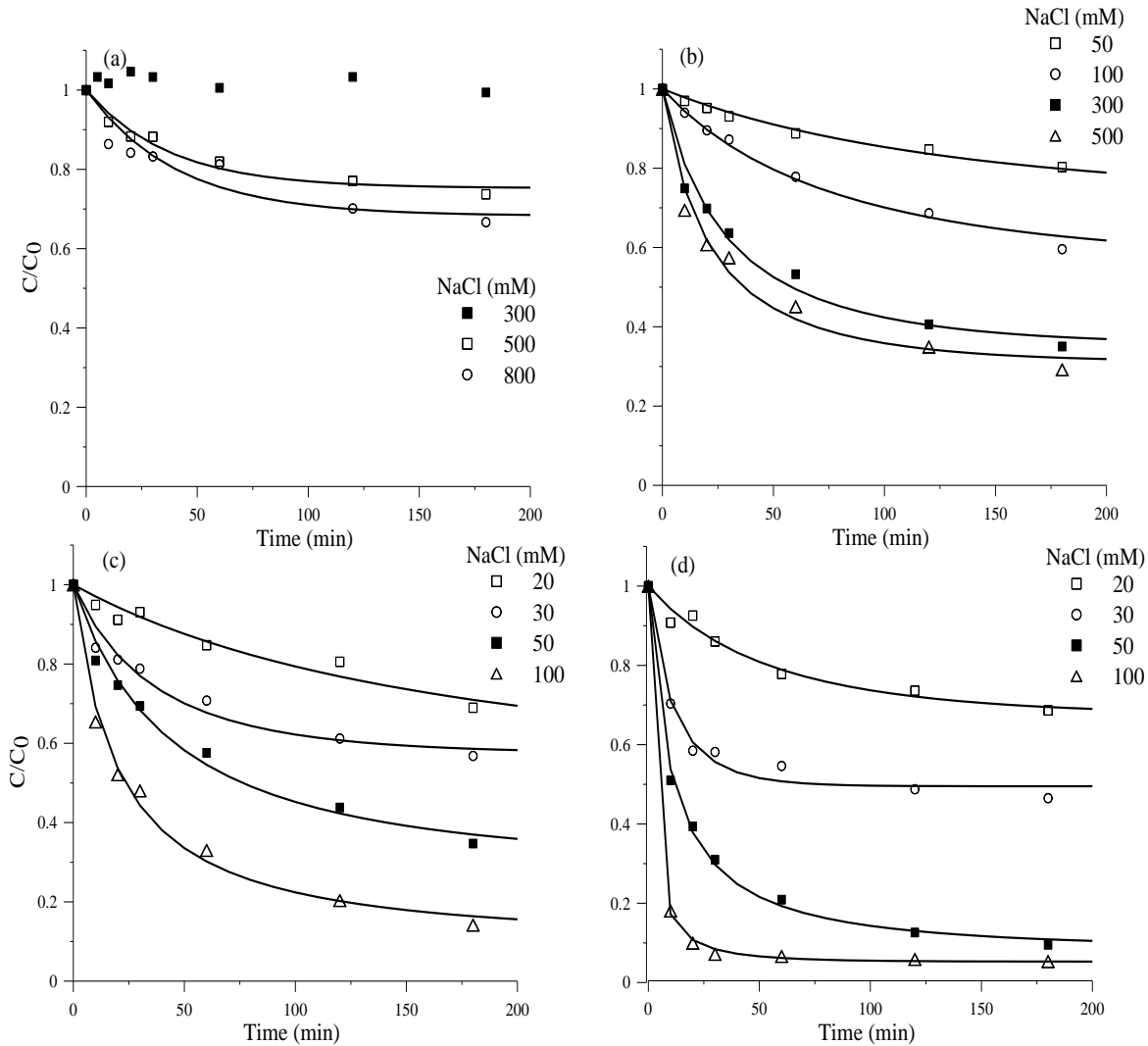


Figure B.1. Plots of observed (symbols) and simulated (lines) colloid concentrations in the batch experiments for various IS of (a) 2 μm , (b) 1 μm , (c) 0.5 μm and (d) 0.1 μm colloids. Simulations considered an irreversible attachment with a blocking behavior. Table B.2 provides the fitted values of k_{att} and S_{max} .

As it was mentioned earlier, to further examine the reversibility of attachment, and to determine the correct model formation to describe the batch experiments, after completion of the attachment phase shown in Figure B.1, the colloid suspension in the batch tubes was removed and replaced with colloid-free electrolyte solution of the same chemical composition. The tubes were subsequently shaken for another 2 hours, and the aqueous colloid concentration was measured. The colloid concentration was found to be negligible (data not shown), demonstrating that the detachment rate was very slow. Moreover, the attachment/detachment model predicts that batch results will be independent of the initial colloid concentration (C_0) assuming a linear equilibrium isotherm, whereas the attachment/blocking model predicts a strong sensitivity to C_0 . As it was mentioned earlier, additional batch experiments were conducted using different C_0 values for 0.5 and 0.1 μm colloids in 50 mM solution. Figure B.2 presents plots of C/C_0 as a function of time when different C_0 values were used. It is observed that the batch results were found to be highly sensitive to C_0 . However, it was found out that the fitted values of k_{att} and S_{max} determined from the experiments with the lower C_0 (i.e. 9.1×10^7 , and $2.8 \times 10^{10} \text{ N}_c\text{mL}^{-1}$ for the 0.5, and 0.1 μm colloids, respectively) simulated the observed colloid concentrations of the other experiments with

higher C_0 (see Figure B.2). Consequently, results from the above experiments were consistent with the attachment/blocking model, but not with the attachment/detachment model. Similarly, Jin et al., (1997) demonstrated that attachment sites for viruses were limited and interpreted their batch results using an irreversible attachment process. Therefore, the attachment/blocking model was used to describe the batch data shown in Figure B.1 and the simulation results are shown in this figure.

Table B.2 provides a summary of fitted values of k_{att} and S_{max} determined through inverse modeling and also calculated values of S_f (Eq. [6]). The irreversible attachment and blocking

Table B.2. Experimental conditions and fitted model parameters for column and batch experiments.

	IS (mM)	Size (μm)	k_{att} (min^{-1})	S_{max}/C_0 cm^2/g	S_{max} (No/g)	S_f (%)
Batch	20	0.1	0.01	0.32	9.1×10^9	0.67
	30	0.1	0.05	0.50	1.4×10^{10}	1.06
	50	0.1	0.09	0.91	2.6×10^{10}	1.92
	100	0.1	0.56	0.95	2.7×10^{10}	1.99
	20	0.5	0.00	0.46	4.2×10^7	0.08
	30	0.5	0.01	0.42	3.9×10^7	0.07
	50	0.5	0.02	0.70	6.4×10^7	0.12
	100	0.5	0.05	0.89	8.1×10^7	0.15
	300	0.5	0.32	0.94	8.5×10^7	0.16
	30	1	0.00	0.28	3.2×10^6	0.02
	50	1	0.01	0.44	5.0×10^6	0.04
	100	1	0.03	0.65	7.4×10^6	0.06
	300	1	0.04	0.69	7.9×10^6	0.06
	500	2	0.01	0.25	3.6×10^5	0.01
	800	2	0.07	0.31	4.4×10^5	0.01
	Column	10	0.1	0.01	0.20	4.5×10^9
30		0.1	0.14	0.82	1.9×10^{10}	1.39
50		0.1	0.35	0.81	1.9×10^{10}	1.37
5		0.5	0.04	2.66	1.6×10^8	0.30
10		0.5	0.07	5.00	3.1×10^8	0.57
50		0.5	0.13	ND ^a	ND	ND
5		2	0.04	ND	ND	ND
10		2	0.09	ND	ND	ND
50	2	0.12	ND	ND	ND	

^a Not determined

model provided an excellent description of the batch data ($R^2 > 0.95$). Inspection of Table B.2 reveals that higher values of k_{att} and S_{max} occurred when the IS was increased and the colloid size was decreased. Higher values of k_{att} and S_{max} with high IS are expected because of compression of the double layer thickness that produces a lower energy barrier and greater depth in the secondary minima (Table B.1), and an increase in the influence of nanoscale heterogeneities (Bradford and Torkzaban, 2012; Duffadar and Davis, 2008). Smaller colloids are more susceptible to the influence of nanoscale heterogeneities (Bradford and Torkzaban, 2013; Bradford et al., 2013b; Darbha et al., 2010), and the diffusion coefficient is also larger. Both of these factors will produce larger values of k_{att} for smaller colloids, whereas the influence of nanoscale heterogeneities will contribute to larger values of S_{max} .

Table B.2 indicates that calculated values of S_f were very small (<2%), especially for larger colloid sizes. The entire collector surface is expected to contribute to colloid attachment ($S_f=100\%$) under fully favorable attachment conditions. However, these S_f values suggest that highly unfavorable attachment conditions prevailed, even when the IS was very high and standard DLVO calculations predicted favorable attachment conditions (Table B.1). This information suggests that other factors were contributing to the reduction in colloid attachment in the batch systems.

Numerous deviations from standard DLVO predictions have been reported, especially in the presence of net repulsive electrostatic interactions (Bhattacharjee et al., 1998; Duffadar and Davis, 2007; Duffadar and Davis, 2008; Ma et al., 2011; Shen et al., 2010; Shen et al., 2012; Suresh and Walz, 1996). DLVO theory assumes that the colloid and collector surfaces are geometrically smooth (Hoek and Agarwal, 2006; Shen et al., 2012). Conversely, natural solid surfaces and colloids always exhibit some degree of surface roughness (Morales et al., 2009; Shellenberger and Logan, 2002; Suresh and Walz, 1996). For example, Figure B.3 presents SEM images of our quartz sand that demonstrate various degrees of surface roughness (number and size). DLVO theory has been extended to incorporate the influence of nanoscale roughness on interaction energies (Bradford and Torkzaban, 2013; Hoek and Agarwal, 2006; Shen et al., 2012). Results indicate that colloid interactions are strongly dependent on surface roughness properties (e.g., height, cross-sectional area, and number), as well as the colloid size and solution IS. The magnitudes of the energy barrier and depth of the secondary minima are reduced on rough surfaces in comparison with smooth surfaces (Bradford and Torkzaban, 2013; Shen et al., 2012). This decrease in interaction energy on rough surfaces has been attributed to increased van der Waals attraction at smaller separation distances and increased electrostatic repulsion at larger separation distances (Bradford and Torkzaban, 2013). Primary minimum interactions are therefore expected to increase on surfaces with nanoscale roughness, whereas secondary minimum interactions will decrease.

DLVO theory predicts an infinite depth of the primary minimum and therefore irreversible attachment on smooth surfaces. Conversely, the depth of primary minimum is finite on rough surfaces, and can even be eliminated when Born repulsion is considered (Bradford and Torkzaban, 2013; Shen et al., 2012). A weak primary minimum interaction on rough surfaces will be susceptible to removal by hydrodynamic forces (Bergendahl and Grasso, 2000; Shen et al., 2012). The hydrodynamic force that acts on colloids near collector surfaces increases with the cube of the colloid radius (Bergendahl and Grasso, 1999; Bradford et al., 2011; Shen et al., 2010; Torkzaban et al., 2007). Consequently, low values of S_f (<2%) in our batch systems, especially for larger colloids, are consistent with weak secondary ($IS \leq 50$ mM) and primary ($IS \geq 100$ mM) minimum interactions on rough surfaces that could have been overcome by hydrodynamic forces. The SEM images of sand grains in the batch experiments shown in Figure B.3 further reveal colloid attachment in depression regions where drag forces are negligible. If colloids can access these low velocity regions, then these locations will be hydrodynamically favorable for colloid retention. Indeed, S_f values increased in the order of 2, 1, 0.5 and 0.1 μm colloids. This observation suggests that the greater attachment of smaller colloids (0.5 and 0.1 μm) primarily occurred on rough locations composed of ridges and valleys because of negligible hydrodynamic forces associated with these regions.

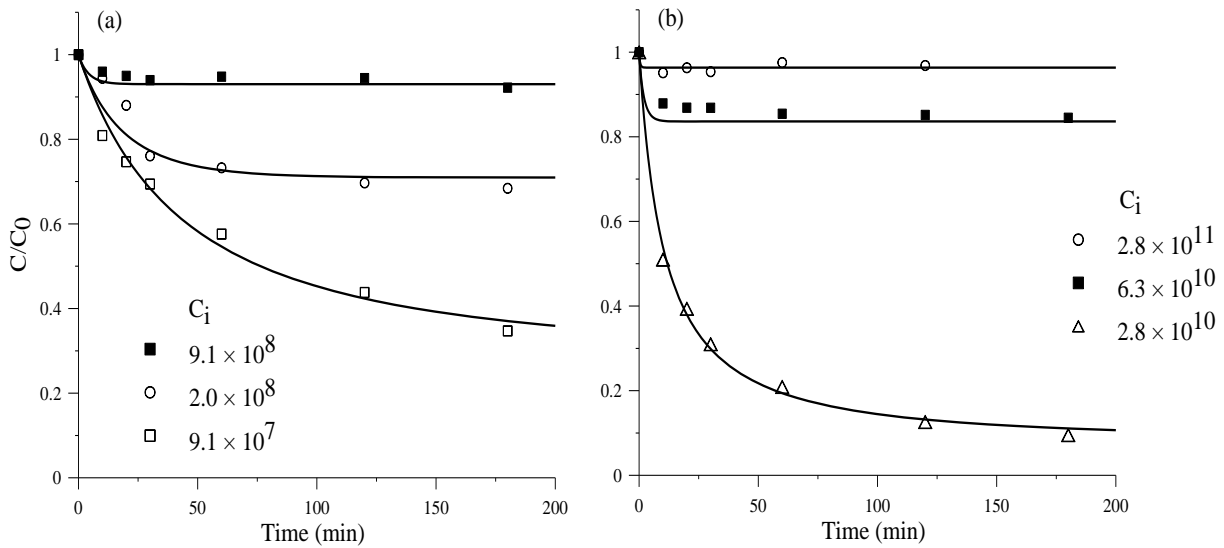


Figure B.2. Plots of observed (symbols) and simulated (lines) colloid concentrations in the batch attachments at 50 mM of (a) 0.5 μm and (b) 0.1 μm colloids when different initial colloid concentrations were used. Simulations considered an irreversible attachment with a blocking behavior.

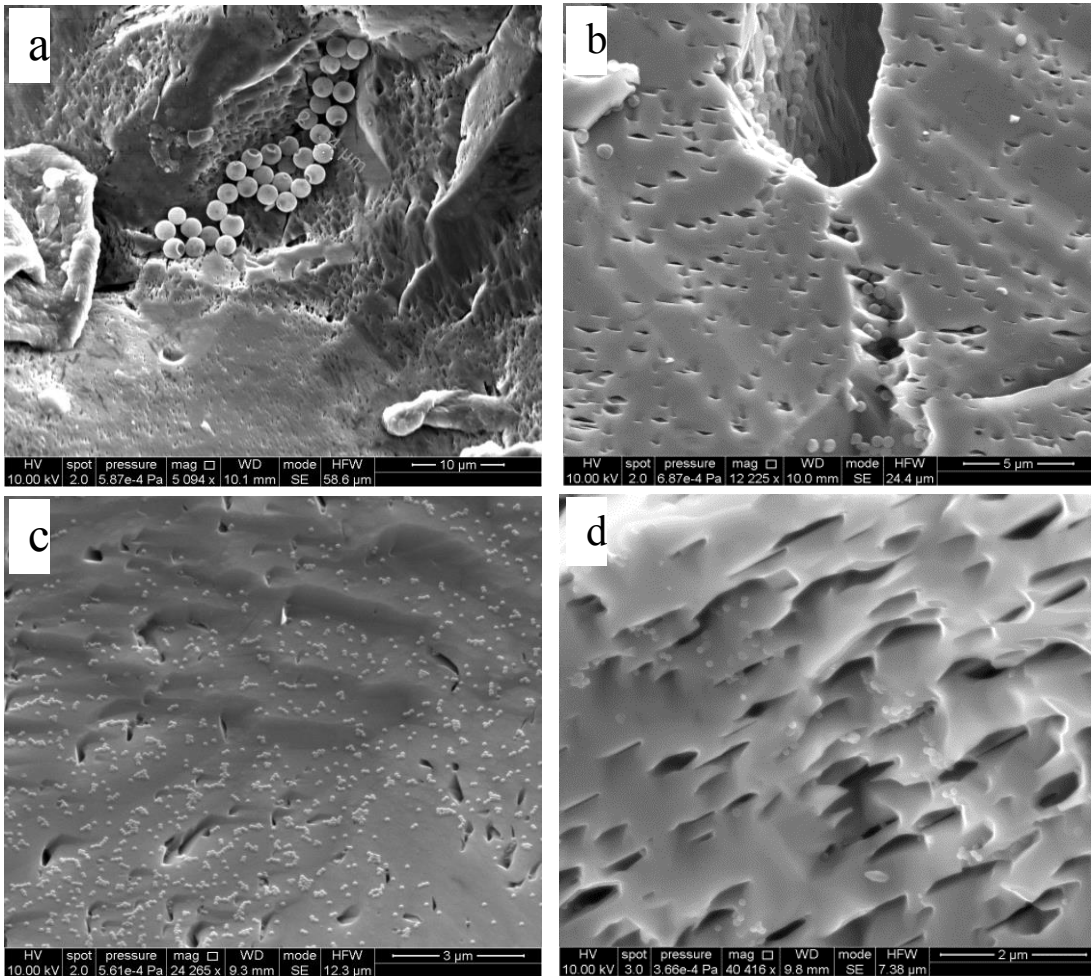


Figure B.3. Representative SEM images of colloids attached on sand grains in the batch experiments (a) 2 μm colloid at IS of 800 mM, (b) 0.5 μm colloid at IS of 300 mM, and (c & d) 0.1 μm colloid at IS of 100 mM.

3.3. Column Experiments

Figure B.4 presents observed and simulated BTCs for 2 (Fig. B.4a), 0.5 (Fig. B.4b), and 0.1 μm (Fig. 4c) colloids in the various IS solutions. Here normalized effluent concentrations (C/C_0) are plotted against the number of pore volumes. The simulations were obtained from the solution of Eqs. [4] and [5] using fitted values of k_{att} , S_{max} and λ . The value of k_{det} in these simulations was set to zero because we observed negligible tailing in the BTCs. The dispersivity coefficient (λ) was estimated by fitting the solution of Eq. [4] to the conservative tracer (NaNO_3) breakthrough data (data not shown). This value of λ was low (0.04 cm) as expected for an 11 cm column. The overall agreement between modeled and measured BTCs was excellent, with R^2 values ranging from 0.96 to 0.99. Table B.2 summarizes experimental conditions, fitted values of k_{att} and S_{max} , and calculated values of S_f (Eq. [6]) for the column experiments. It should be mentioned that the slope of the rising limb of the BTC was sometimes negligible (e.g., 2 μm), and in this cases a unique determination of S_{max} was not possible.

Very little colloid retention occurred when deionized water ($\text{IS} \sim 0$) was used as the background solution. Conversely, the amount of colloid retention and corresponding values of k_{att} and S_{max} , increased with IS. For example, more than 95% of the injected colloids (2, 0.5, and 0.1 μm) were retained in the sand when the IS was 50 mM. An increase in colloid retention with IS occurs because of compression of the double layer thickness that produces a lower energy barrier and greater depths in the primary and secondary minima, and an increase in the influence of nanoscale heterogeneities (Bradford and Torkzaban, 2012; Duffadar and Davis, 2008). The BTCs also exhibited blocking behavior (a decreasing rate of retention) as available retention sites were filled. This trend can be seen in BTCs for 0.1 μm colloids when $\text{IS} \geq 10$ mM, as well as to a lesser extent for 0.5 μm colloids when the $\text{IS} = 5$ and 10 mM. Blocking also produces a delay in the arrival of the BTCs for 0.1 μm colloids when the $\text{IS} \geq 10$ mM because of the high value of k_{att} for these smaller colloids (Torkzaban et al., 2010; Torkzaban et al., 2012). A linear, equilibrium retardation model cannot describe this delay, because detachment was not observed in the tailing of the BTCs.

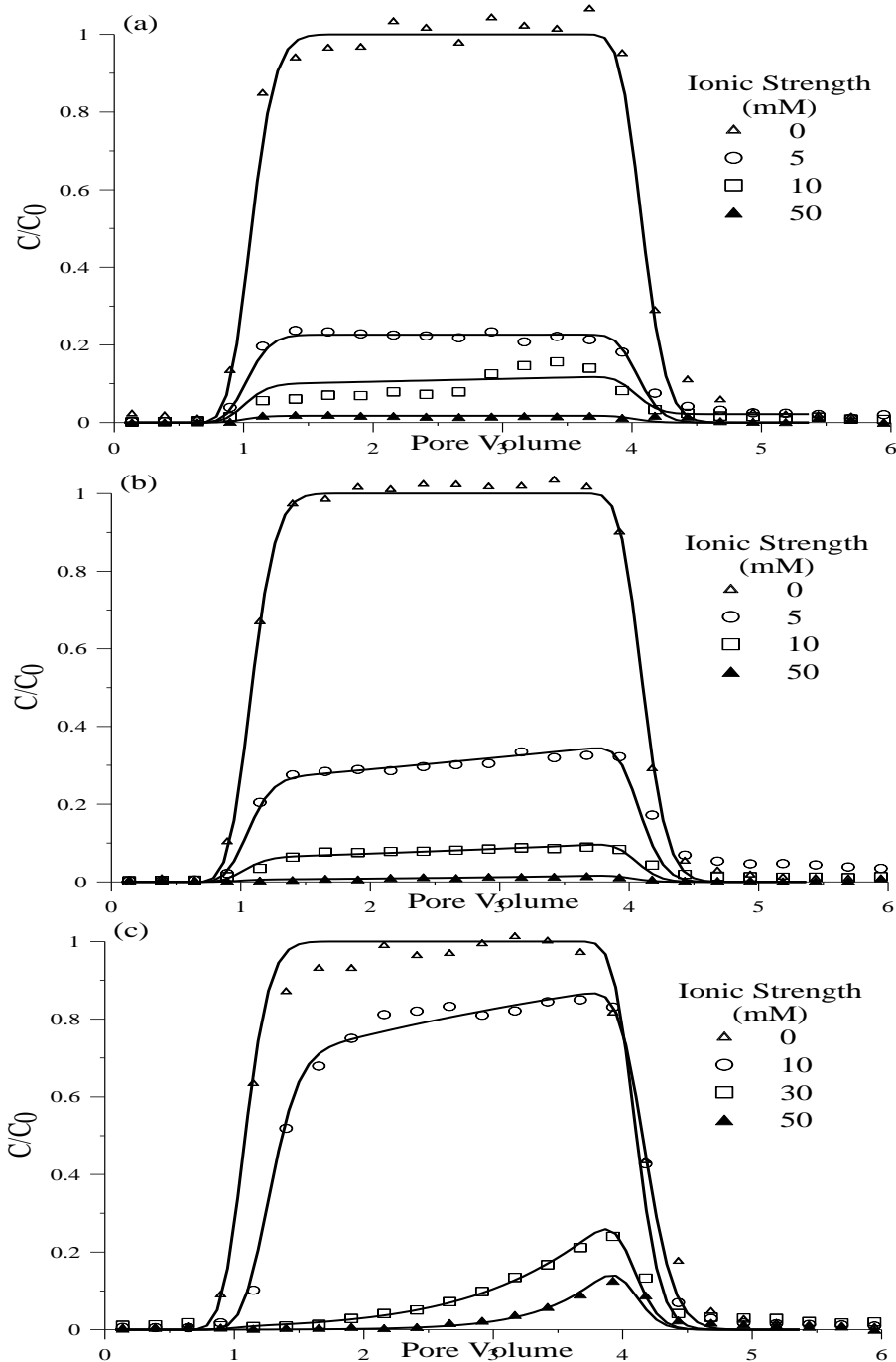


Figure B.4. Plots of observed (symbols) and simulated (lines) column breakthrough concentrations for various IS of (a) 2 μm , (b) 0.5 μm and (c) 0.1 μm colloids. Simulations considered attachment and blocking. Table B.2 provides information about predicted k_{att} and S_{max} .

3.4. Comparison of Batch and Column Results

The detachment rates were found to be very slow in both batch and column experiments. The amount of colloid retention, k_{att} , and S_f were higher in column than batch experiments (Table B.2) especially for larger colloids. Discrepancies between batch and column studies have been found by others (Jin et al., 1997; Powelson and Gerba, 1994; Torkzaban et al., 2008). The greater colloid retention, k_{att} , and S_f in column compared to batch studies cannot be attributed to stronger adhesive

forces because the batch experiments were conducted over a much wider range of IS that should have provided even stronger adhesive forces (Table B.2B.2). Our batch results (especially with 2 and 1 μm colloids) clearly demonstrate that the adhesive interaction energy between the colloids and sand surfaces was not strong enough to produce colloid attachment, even at an IS that was as high as 500 or 800 mM. Furthermore, rates of colloid mass transfer from the aqueous to the solid phase are expected to be greater for continuously mixed batch than those of column studies (Sadeghi et al., 2013). Consequently, it is logical to anticipate that differences in the amount of colloid retention, values of k_{att} and S_f in column and batch studies reflect the influence of hydrodynamics, pore structure, and sand surface morphology (to be discussed below).

Previous column studies have shown that majority retained colloids can be released and recovered when the sand was excavated and suspended in electrolyte solutions of the same IS as used in the transport experiment (Bradford et al., 2009; Li et al., 2004; Tong et al., 2005; Torkzaban et al., 2008). We also observed that retained 2 μm colloids in IS=50 mM solution were completely recovered from the column after the sand was excavated and the pore structure eliminated (data not shown). This finding is consistent with the results of our batch experiments (Figure B.1) and demonstrated that the 2 μm colloids were weakly attached onto the quartz sand surface. Colloid retention is well-known to depend on both the solution and solid phase chemical conditions (Ryan and Elimelech, 1996) and the system hydrodynamics (Duffadar and Davis, 2007; Torkzaban et al., 2007). Rolling has been demonstrated to be the dominant mechanism of colloid detachment from solid surfaces under laminar flow conditions (Duffadar and Davis, 2008; Torkzaban et al., 2007). A balance of applied hydrodynamic (T_H) and resisting adhesive (T_A) torques therefore determines conditions for colloid immobilization and rolling (Bradford et al., 2011). Colloid immobilization occurs when $T_H \leq T_A$, whereas rolling occurs when $T_H > T_A$. It should be noted that some researchers have neglected the effect of T_A altogether and implicitly assumed that colloid immobilization only occurs in an infinite primary minimum (Johnson et al., 2007b; Yang et al., 1998). However, this approach does not allow for colloid immobilization due to a secondary energy minimum in the presence of fluid flow (Torkzaban et al., 2008). Furthermore, this paradigm is not consistent with our batch results demonstrating a limited colloid attachment ($S_f < 2\%$) under unfavorable attachment conditions.

The sand surface morphology, which consists of large number of depressions, protrusions, nano- to micro-scale roughness, is known to influence the values of T_H and T_A because of their influence on the lever arms (Bradford et al., 2013; Shen et al., 2010). In particular, roughness will decrease the lever arm for T_H , and dramatically increase the lever arm for T_A . When the roughness height is greater than the colloid radius (r_c) the lever arms for T_H and T_A equal 0 and r_c , respectively. Grain-grain contacts will similarly influence the values of T_H and T_A . Consequently, greater amounts of colloid immobilization occur on microscopically rough than on smooth surfaces, and at grain-grain contact points. Bradford et al., (2013) conducted a balance of T_H and T_A over a porous medium surface that contained random roughness of a given height to determine the value of S_f under unfavorable attachment conditions. The S_f values depended on the solution IS, r_c , roughness height and fraction, and Darcy velocity (q_w). Colloid immobilization was demonstrated to occur on a rough surface in the absence of attachment, and may therefore be considered as a surface straining process.

The direction and magnitude of T_H and T_A are relatively constant with time at a particular location on the sand surface in a steady-state column experiment. Consequently, colloid retention on the collector surface may occur at locations where $T_H \leq T_A$. Conversely, the direction and magnitude of T_H and T_A will dramatically change with time at a particular location in continuously mixed batch systems. Conditions for colloid immobilization in the batch system will therefore constantly change with the direction of the hydrodynamic forces, even if the magnitude of the hydrodynamic force is small. The overall value of S_f and the amount of colloid retention is therefore expected to be much smaller in a batch than that of a column system. These observations suggest that it is not possible to adopt a protocol (like the solid/water ratio, speed and direction of shaking) to obtain

comparable results between batch and column systems. Consistent with other studies (Bales et al., 1991; Sadeghi et al., 2013; Schijven et al., 2000; Zhao et al., 2008), it appears that saturated column experiments provides a better approach for studying colloid (e.g. viruses, bacteria, engineered nanoparticles) transport and retention than batch techniques.

4. Conclusions

The bulk of existing colloid literature considers colloid deposition in porous media to be primarily controlled by interaction energies of colloids with grain surfaces. If this was the controlling mechanism, then batch results would have been reliable and comparable with those of column experiments. However, once a colloid collides with the SWI, attachment depends on a combination of forces and torques that act on the colloid at this location. These forces and torques include hydrodynamic drag and lift, electrical double-layer repulsion (or attraction), London–van der Waals interaction, and applied hydrodynamic and resisting adhesive torques. Of particular interest is the lever arm incorporated in the hydrodynamic and adhesive torques which depends on size and fraction of surface roughness. Colloid retention in flow systems (e.g. column) and to some extent in batch system for small colloids likely occurs in the regions on the grain surfaces where the roughness provides a favourable location for retention due to lever arm considerations. These locations on grain surfaces provide optimum locations for colloids that are likely associated with the solid phase either via secondary energy minimum or shallow primary minimum, to be retained due to reduced hydrodynamic forces and enhanced adhesive torque.

Our results indicate that in the presence of an energy barrier (unfavourable attachment conditions), the deposition behaviour of colloids in batch system is inconsistent with those of column experiments. Specifically, the fraction of surface area available for attachment is significantly lower than that of column experiments. Deviation between batch and column results is increasingly significant for larger colloids. Predictions based on classical DLVO theory were found to inadequately describe interaction energies between colloids and natural surfaces which are always rough ranging from nano- to micro- scale. This implies that surface roughness plays an important role in determining the interaction energies and torque balances between the colloids and collector surfaces. Indeed, it is expected that the surface roughness will be more important, if not overriding, than chemical heterogeneities. Based on information shown in this study, it is clear that the hydrodynamic forces and surface roughness are the dominant factors controlling colloid deposition in batch and column experiments.

References

- Adamczyk, Z., Siwek, B., Zembala, M. and Belouschek, P., 1994. Kinetics of Localized Adsorption of Colloid Particles. *Advances in Colloid and Interface Science*, 48: 151-280.
- Bales, R.C., Hinkle, S.R., Kroeger, T.W., Stocking, K. and Gerba, C.P., 1991. Bacteriophage Adsorption during Transport through Porous-Media - Chemical Perturbations and Reversibility. *Environmental Science & Technology*, 25(12): 2088-2095.
- Bergendahl, J. and Grasso, D., 1999. Prediction of colloid detachment in a model porous media: Thermodynamics. *Aiche Journal*, 45(3): 475-484.
- Bergendahl, J. and Grasso, D., 2000. Prediction of colloid detachment in a model porous media: hydrodynamics. *Chemical Engineering Science*, 55(9): 1523-1532.
- Bhattacharjee, S., Ko, C.H. and Elimelech, M., 1998. DLVO interaction between rough surfaces. *Langmuir*, 14(12): 3365-3375.
- Bradford, S.A., Kim, H.N., Haznedaroglu, B.Z., Torkzaban, S. and Walker, S.L., 2009. Coupled factors influencing concentration-dependent colloid transport and retention in saturated porous media. *Environmental Science & Technology*, 43(18): 6996-7002.
- Bradford, S.A. and Torkzaban, S., 2012. Colloid Adhesive Parameters for Chemically Heterogeneous Porous Media. *Langmuir*, 28(38): 13643-13651.
- Bradford, S.A. and Torkzaban, S., 2013. Colloid interaction energies for physically and chemically heterogeneous porous media. *Langmuir*, 29(11): 3668-76.
- Bradford, S.A., Torkzaban, S. and Wiegmann, A., 2011. Pore-Scale Simulations to Determine the Applied Hydrodynamic Torque and Colloid Immobilization. *Vadose Zone Journal*, 10(1): 252-261.
- Bradford, S.A., Torkzaban, S., Kim, H., Simunek, J., 2012. Modeling colloid and microorganism transport and release with transients in solution ionic strength. *Water Resources Research* 48 (9).
- Bradford, S.A., Torkzaban, S., Shapiro, A., 2013. A theoretical analysis of colloid attachment and straining in chemically heterogeneous porous media. *Langmuir* 29 (23), 6944-6952.
- Bradford, S.A., Wang, Y., Kim, H., Torkzaban, S. Šimunek, J., 2014. Modeling Microorganism Transport and Survival in the Subsurface. *Journal of Environmental Quality*, 43 (2), 421-440.
- Brown, D.G. and Abramson, A., 2006. Collision efficiency distribution of a bacterial suspension flowing through porous media and implications for field-scale transport. *Water Research*, 40(8): 1591-1598.
- Chrysikopoulos, C.V. and Aravantinou, A.F., 2012. Virus inactivation in the presence of quartz sand under static and dynamic batch conditions at different temperatures. *Journal of Hazardous Materials*, 233: 148-157.
- Darbha, G.K., Schaefer, T., Heberling, F., Luettge, A. and Fischer, C., 2010. Retention of Latex Colloids on Calcite as a Function of Surface Roughness and Topography. *Langmuir*, 26(7): 4743-4752.
- Derjaguin, B. and Landau, L., 1941. Theory of the stability of strongly charged lyophobic sols and of the adhesion of strongly charged particles in solutions of electrolytes. *Acta Physicochimica U.R.S.S.*, 14: 633-662.
- Duffadar, R.D. and Davis, J.M., 2007. Interaction of micrometer-scale particles with nanotextured surfaces in shear flow. *Journal of Colloid and Interface Science*, 308(1): 20-29.
- Duffadar, R.D. and Davis, J.M., 2008. Dynamic adhesion behavior of micrometer-scale particles flowing over patchy surfaces with nanoscale electrostatic heterogeneity. *Journal of Colloid and Interface Science*, 326(1): 18-27.
- Ginn, T. R., B. D. Wood, K. E. Nelson, T. D. Scheibe, E. M. Murphy, and T. P. Clement, 2002. Processes in microbial transport in the natural subsurface. *Advances in Water Resources*, 25(8-12): 1017-1042.

- Gregory, J., 1981. Approximate Expressions for Retarded Van der Waals Interaction. *Journal of Colloid and Interface Science*, 83(1): 138-145.
- Harvey, R.W. and Garabedian, S.P., 1991. Use of Colloid Filtration Theory in Modeling Movement of Bacteria through a Contaminated Sandy Aquifer. *Environmental Science & Technology*, 25(1): 178-185.
- Harvey, R.W., Harms, H. and Landkammer, L., 2002. Transport of microorganism in the terrestrial subsurface: In situ and laboratory methods. *Manual of Environmental Microbiology*.
- Hoek, E.M.V. and Agarwal, G.K., 2006. Extended DLVO interactions between spherical particles and rough surfaces. *Journal of Colloid and Interface Science*, 298(1): 50-58.
- Hogg, R., Healy, T.W. and Fuersten.Dw, 1966. Mutual Coagulation of Colloidal Dispersions. *Transactions of the Faraday Society*, 62(522P): 1638-&.
- Jin, Y. and Flury, M., 2002. Fate and transport of viruses in porous media. *Advances in Agronomy*, Vol 77, 77: 39-+.
- Jin, Y., Yates, M.V., Thompson, S.S. and Jury, W.A., 1997. Sorption of viruses during flow through saturated sand columns. *Environmental Science & Technology*, 31(2): 548-555.
- Johnson, P.R. and Elimelech, M., 1995. Dynamics of Colloid Deposition in Porous-Media - Blocking Based on Random Sequential Adsorption. *Langmuir*, 11(3): 801-812.
- Johnson, W.P., Li, X. and Assemi, S., 2007. Deposition and re-entrainment dynamics of microbes and non-biological colloids during non-perturbed transport in porous media in the presence of an energy barrier to deposition. *Advances in Water Resources*, 30(6-7): 1432-1454.
- Kim, H.N., Bradford, S.A. and Walker, S.L., 2009. Escherichia coli O157:H7 Transport in Saturated Porous Media: Role of Solution Chemistry and Surface Macromolecules. *Environmental Science & Technology*, 43(12): 4340-4347.
- Lazouskaya, V. and Jin, Y., 2008. Colloid retention at air-water interface in a capillary channel. *Colloids and Surfaces a-Physicochemical and Engineering Aspects*, 325(3): 141-151.
- Li, X.Q. and Johnson, W.P., 2005. Nonmonotonic variations in deposition rate coefficients of microspheres in porous media under unfavorable deposition conditions. *Environmental Science & Technology*, 39(6): 1658-1665.
- Li, X.Q., Scheibe, T.D. and Johnson, W.P., 2004. Apparent decreases in colloid deposition rate coefficients with distance of transport under unfavorable deposition conditions: A general phenomenon. *Environmental Science & Technology*, 38(21): 5616-5625.
- Ma, H., Pazmino, E. and Johnson, W.P., 2011. Surface Heterogeneity on Hemispheres-in-Cell Model Yields All Experimentally-Observed Non-Straining Colloid Retention Mechanisms in Porous Media in the Presence of Energy Barriers. *Langmuir*, 27(24): 14982-14994.
- Marquardt, D.W., 1963. An Algorithm For Least-Squares Estimation Of Nonlinear Parameters. *Journal of the Society for Industrial and Applied Mathematics*, 11(2): 431-441.
- Mondal, P.K., Sleep, B.E., 2013. Virus and virus-sized microsphere transport in a dolomite rock fracture. *Water Resources Research* 49 (2), 808-824.
- Morales, V.L., Gao, B. and Steenhuis, T.S., 2009. Grain Surface-Roughness Effects on Colloidal Retention in the Vadose Zone. *Vadose Zone Journal*, 8(1): 11-20.
- Pensini, E., Sleep, B.E., Yip, C.M., O'Carroll, D., 2012. Forces of interactions between bare and polymer-coated iron and silica: Effect of ph, ionic strength, and humic acids. *Environmental science & technology* 46 (24), 13401-13408.
- Powelson, D.K. and Gerba, C.P., 1994. Virus Removal from Sewage Effluents during Saturated and Unsaturated Flow-Through Soil Columns. *Water Research*, 28(10): 2175-2181.
- Ryan, J.N. and Elimelech, M., 1996. Colloid mobilization and transport in groundwater. *Colloids and Surfaces a-Physicochemical and Engineering Aspects*, 107: 1-56.
- Sadeghi, G., Schijven, J.F., Behrends, T., Hassanizadeh, S.M. and van Genuchten, M.T., 2013. Bacteriophage PRD1 batch experiments to study attachment, detachment and inactivation processes. *J Contam Hydrol*, 152: 12-7.

- Schijven, J.F. and Hassanizadeh, S.M., 2000. Removal of viruses by soil passage: Overview of modeling, processes, and parameters. *Critical Reviews in Environmental Science and Technology*, 30(1): 49-127.
- Schijven, J.F., Hassanizadeh, S.M., Dowd, S.E. and Pillai, S.D., 2000. Modeling Virus Adsorption in Batch and Column Experiments. *Quantitative Microbiology*, 2(1): 5-20.
- Shellenberger, K. and Logan, B.E., 2002. Effect of molecular scale roughness of glass beads on colloidal and bacterial deposition. *Environmental Science & Technology*, 36(2): 184-189.
- Shen, C., Huang, Y., Li, B. and Jin, Y., 2008. Effects of solution chemistry on straining of colloids in porous media under unfavorable conditions. *Water Resources Research*, 44(5).
- Shen, C., Huang, Y., Li, B. and Jin, Y., 2010. Predicting attachment efficiency of colloid deposition under unfavorable attachment conditions. *Water Resources Research*, 46.
- Shen, C., Li, B., Huang, Y. and Jin, Y., 2007. Kinetics of coupled primary- and secondary-minimum deposition of colloids under unfavorable chemical conditions. *Environmental Science & Technology*, 41(20): 6976-6982.
- Shen, C., Wang, L.-P., Li, B., Huang, Y. and Jin, Y., 2012. Role of Surface Roughness in Chemical Detachment of Colloids Deposited at Primary Energy Minima. *Vadose Zone Journal*, 11(1).
- Simoni, S.F., Harms, H., Bosma, T.N.P. and Zehnder, A.J.B., 1998. Population heterogeneity affects transport of bacteria through sand columns at low flow rates. *Environmental Science & Technology*, 32(14): 2100-2105.
- Simunek, J., van Genuchten, M.T. and Sejna, M., 2005. The HYDRUS-1D software package for simulating the one-dimensional movement of water, heat, and multiple solutes in variably-saturated media — version 3.0, HYDRUS software series 1. Department of Environmental Sciences, University of California Riverside, Riverside, CA.
- Suresh, L. and Walz, J.Y., 1996. Effect of surface roughness on the interaction energy between a colloidal sphere and a flat plate. *Journal of Colloid and Interface Science*, 183(1): 199-213.
- Syngouna, V.I. and Chrysikopoulos, C.V., 2010. Interaction between Viruses and Clays in Static and Dynamic Batch Systems. *Environmental Science & Technology*, 44(12): 4539-4544.
- Thompson, S.S., Flury, M., Yates, M.V. and Jury, W.A., 1998. Role of the air-water-solid interface in bacteriophage sorption experiments. *Applied and Environmental Microbiology*, 64(1): 304-309.
- Thompson, S.S. and Yates, M.V., 1999. Bacteriophage inactivation at the air-water-solid interface in dynamic batch systems. *Applied and Environmental Microbiology*, 65(3): 1186-1190.
- Tong, M.P., Li, X.Q., Brow, C.N. and Johnson, W.P., 2005. Detachment-influenced transport of an adhesion-deficient bacterial strain within water-reactive porous media. *Environmental Science & Technology*, 39(8): 2500-2508.
- Torkzaban, S., Bradford, S.A., van Genuchten, M.T. and Walker, S.L., 2008. Colloid transport in unsaturated porous media: the role of water content and ionic strength on particle straining. *J Contam Hydrol*, 96(1-4): 113-27.
- Torkzaban, S., Bradford, S.A. and Walker, S.L., 2007. Resolving the coupled effects of hydrodynamics and DLVO forces on colloid attachment in porous media. *Langmuir*, 23(19): 9652-9660.
- Torkzaban, S., Bradford, S.A., Wan, J., Tokunaga, T. and Masoudih, A., 2013. Release of Quantum Dot Nanoparticles in Porous Media: Role of Cation Exchange and Aging Time. *Environmental Science & Technology*, 47(20): 11528-11536.
- Torkzaban, S., Kim, H.N., Simunek, J. and Bradford, S.A., 2010. Hysteresis of Colloid Retention and Release in Saturated Porous Media During Transients in Solution Chemistry. *Environmental Science & Technology*, 44(5): 1662-1669.
- Torkzaban, S., Kim, Y., Mulvihill, M., Wan, J., Tokunaga, T.K., 2010. Transport and deposition of functionalized CdTe nanoparticles in saturated porous media. *Journal of contaminant hydrology* 118 (3), 208-217.

- Torkzaban, S., Wan, J., Tokunaga, T.K. and Bradford, S.A., 2012. Impacts of bridging complexation on the transport of surface-modified nanoparticles in saturated sand. *Journal of Contaminant Hydrology*, 136: 86-95.
- Tufenkji, N. and Elimelech, M., 2004. Correlation equation for predicting single-collector efficiency in physicochemical filtration in saturated porous media. *Environmental Science & Technology*, 38(2): 529-536.
- Yang, C., Dabros, T., Li, D.Q., Czarnecki, J. and Masliyah, J.H., 1998. Kinetics of particle transport to a solid surface from an impinging jet under surface and external force fields. *Journal of Colloid and Interface Science*, 208(1): 226-240.
- Yates, M.V., Yates, S.R., Wagner, J. and Gerba, C.P., 1987. Modeling virus survival and transport in the subsurface. *Journal of Contaminant Hydrology*, 1(3): 329 -345.
- Zhao, B., Zhang, H., Zhang, J. and Jin, Y., 2008. Virus adsorption and inactivation in soil as influenced by autochthonous microorganisms and water content. *Soil Biology & Biochemistry*, 40(3): 649-659.

CONTACT US

t 1300 363 400
+61 3 9545 2176
e enquiries@csiro.au
w www.csiro.au

YOUR CSIRO

Australia is founding its future on science and innovation. Its national science agency, CSIRO, is a powerhouse of ideas, technologies and skills for building prosperity, growth, health and sustainability. It serves governments, industries, business and communities across the nation.